

Preliminary Investigations in the Potential Use of Dye-Ligands to Bind Biological Macromolecules

by

Stefana Aprotosoaei

Canterbury Christ Church University

Thesis submitted for the Degree of MSc by Research

2022

Table of contents

Acknowledgements	5
Abstract	6
List of abbreviations	7
1. Introduction	9
1.1 <i>Foreword</i>	9
1.2 <i>Dyes and pigments: past and present</i>	9
1.3 <i>Procion dyes – chemical structure and uses</i>	10
1.4 <i>Principles of affinity chromatography</i>	13
1.5 <i>Applications of the Procion dyes in protein chromatography</i>	15
1.6 <i>Emerging infectious diseases</i>	17
1.7 <i>Virus biology and bacteriophage T4</i>	19
1.8 <i>Molecules bearing the ability to bind pathogens</i>	19
1.9 <i>Existing mechanisms to prevent transmission of infections</i>	21
1.10 <i>Aims and objectives of the present study</i>	23
2. General materials and methods	25
2.1 <i>Materials</i>	25
2.2 <i>Growth of Escherichia coli β-10 stocks</i>	25
2.3 <i>Bacterial protein extraction</i>	26
2.4 <i>Bacterial genomic DNA extraction</i>	26
2.5 <i>Bacterial RNA extraction</i>	27
2.6 <i>Bacteriophage stock preparation and storage</i>	27
2.7 <i>The phage plaque assay</i>	28
2.8 <i>Preparation of clear and dye-polysaccharide matrices</i>	28
2.9 <i>Traditional method for preparing chromatography columns</i>	29
2.10 <i>Dyeing of natural fabrics with Procion dyes</i>	30
2.11 <i>Statistical analyses and figures</i>	31
3. Testing the binding affinity of bacterial proteins to the Procion dyes	32
3.1 <i>Methods</i>	32
3.1.1 <i>Testing the affinity of bacterial proteins for the Reactive Blue 4 dye</i>	32

3.1.2	<i>Testing the affinity of bacterial proteins for the Procion dyes by SDS-PAGE gel electrophoresis</i>	33
3.2	<i>Results</i>	37
3.2.1	<i>Testing the affinity of bacterial proteins for the Reactive Blue 4 dye</i>	37
3.2.2	<i>Testing the affinity of bacterial proteins for the Procion dyes by SDS-PAGE gel electrophoresis</i>	38
3.3	<i>Discussion</i>	46
4.	Testing the binding ability of nucleic acids to the Procion dyes	53
4.1	<i>Methods</i>	53
4.1.1	<i>Testing the binding of bacterial nucleic acids to the Reactive Blue 4 dye</i>	53
4.1.2	<i>DNA binding to clear and dye-tagged DEAE-Sephadex A-50 in columns</i>	54
4.2	<i>Results</i>	54
4.2.1	<i>Testing the binding of bacterial nucleic acids to the Reactive Blue 4 dye</i>	54
4.2.2	<i>DNA binding to clear and dye-tagged DEAE-Sephadex A-50 in columns</i>	57
4.3	<i>Discussion</i>	59
4.3.1	<i>Testing the binding of bacterial nucleic acids to the Reactive Blue 4 dye</i>	59
4.3.2	<i>DNA binding to clear and dye-tagged DEAE-Sephadex A-50 in columns</i>	60
5.	Testing the binding of phage to the Procion dyes	63
5.1	<i>Methods</i>	63
5.1.1	<i>E. coli growth curves</i>	63
5.1.2	<i>Testing the effect of sodium chloride on phage survival</i>	64
5.1.3	<i>Testing the binding of phage to polysaccharide matrices</i>	64
5.1.4	<i>Phage elution from the polysaccharide matrices</i>	65
5.1.5	<i>Testing the binding of phage to natural fabrics</i>	66
5.1.6	<i>Testing the binding of phage to pre-wetted silk and cotton and dry dark-RB4 silk</i>	68
5.1.7	<i>Analysis of fabrics using Scanning Electron Microscopy</i>	68
5.2	<i>Results</i>	69
5.2.1	<i>E coli growth curves</i>	69
5.2.2	<i>Testing the effect of sodium chloride on phage survival</i>	70
5.2.3	<i>Testing the binding of phage to polysaccharide matrices</i>	71
5.2.4	<i>Phage elution from the polysaccharide matrices</i>	73
5.2.5	<i>Testing the binding of phage to natural fabrics</i>	73
5.2.6	<i>Testing the binding of phage to pre-wetted silk and cotton and dry dark-RB4 silk</i>	75
5.2.7	<i>Analysis of fabrics using Scanning Electron Microscopy</i>	76

Acknowledgements

With gratefulness, I would like to acknowledge Comax Life Sciences Co. Ltd. for providing the concept and financial resources for the present study. Without their support the conduction of the project would not have been possible. Namely, I would also like to thank Jason Comer and Dr. Michael Comer for their ideas, guidance, patience, encouragement, and the time they regularly invested in providing strategic and scientific advice throughout the period of the project.

Many thanks to Dr. Cornelia Wilson and Dr. Lee Byrne for their supervision, creative ideas and instructions. Particularly, I would like to thank Dr Cornelia Wilson for producing great electron microscopy images of my samples, included in my thesis. Thank you, Dr Lee Byrne, for taking the time to spend Mondays in the lab with me.

I would like to acknowledge the University of Liverpool for providing us with the T4 bacteriophage and *E. coli* K-12 host strain, and Calico Laine Ltd. for offering us silk and cotton fabrics. Last but not least, my appreciations go to Miss Minnatallah Al-Yozbaki for her constant help and valued suggestions she provided throughout the year.

Abstract

The uses in vastly diverse fields of dyes and pigments and the myths created around them throughout history have helped to shape the evolution of humanity. So called “Procion” dyes constitute an important class of reactive dyes, which are being used in many industries today, including textile, printing, cosmetics, and science. Applications of these dyes in the affinity chromatography of proteins has been extensively studied for over five decades. Their ability to bind a large array of proteins could make them a suitable candidate to bind other macromolecules biospecifically and in a differentiated manner. Nucleic acids or entities such as viral particles, encapsulated in a protein coating, may also demonstrate an affinity to particular dyes. Covering various surfaces with such dyes, including PPE, could provide a novel and inexpensive method to limit the spread of viral diseases by capturing viruses. In this study, a selection of five Procion dyes, including Blue MX-R, Red MX-5B, Yellow MX-4R, Red H-3BN and Orange MX-G, were bound to DEAE Sephadex A-50 slurry, and to cotton and silk textile fibres. A wide range of bacterial proteins, bacterial genomic DNA and RNA were found to bind differentially to the undyed and Procion dye-tagged resin. Double stranded DNA showed promising interaction with the dyes when passed through an improvised syringe column, containing Procion dye-ligand resin, especially with Blue MX-R and Orange MX-G. Interaction with Red MX-5B and Yellow MX-4R reduced bacteriophage titre substantially in a T4 sample, upon exposure to dyed cotton. However, it is still unclear whether these dyes may have the potential to control disease transmission. Additional research, involving larger sample sizes and alteration of some parameters, like pH and temperature, should be conducted to validate the current results.

List of abbreviations

APS – ammonium persulphate

AU – 1. absorbance units 2. arbitrary units

BPB – bromophenol blue

CFU – colony-forming units

CV – column volumes

Da – Dalton(s)

DEAE – diethylaminoethyl

DNA – deoxyribonucleic acid

DTT - dithiothreitol

EDTA – ethylenediamine tetra-acetic acid

gDNA – genomic DNA

HCl – hydrochloric acid

LB – Luria Bertani broth

M - molar

mV – millivolts

Na₂CO₃ – sodium carbonate

NaCl – sodium chloride

OD – optical density

PAGE – polyacrylamide gel electrophoresis

PBS – phosphate buffered saline

PFU – plaque-forming units

RB4 – Procion Blue MX-R/ Reactive Blue 4 dye

RNA – ribonucleic acid

RO1 – Procion Orange MX-G/ Reactive Orange 1

RPM – rotations per minute

RR2 – Procion Red MX-5B/ Reactive Brilliant Red 2

RR29 – Procion Red H-3BN/ Brilliant Red 29

RT – room temperature

RY14 – Procion Yellow MX-4R/ Reactive Yellow 14

SDS – sodium dodecyl sulphate

SEM – scanning electron microscope

TE – Tris-EDTA buffer

TEMED – N, N, N', N' – tetramethylethane – 1, 2 – diamine

Tris – Tris(hydroxymethyl)aminoethane

TRIzol – total RNA isolation reagent

TY 2× – 2× tryptone yeast medium

TYGPN – tryptone, yeast, glycerol, potassium nitrate, disodium phosphate medium

1. Introduction

1.1 Foreword

The potential use of synthetic dyes to preferentially bind macromolecules would seem intriguing, especially if this interaction demonstrated a capacity or was, in some way, biospecifically related, or occurred in a differentiated manner. Substantial evidence has been reported in the literature by several authors that this may take place in the case of proteins (Baird *et al.*, 1976; Lowe *et al.*, 1981; Scawen *et al.*, 1983). However, is it possible that other macromolecules, such as nucleic acids and viruses, could behave in a similar manner (Michael Comer, personal communication)? The present thesis describes preliminary investigations as a basis to verify or invalidate the postulation that individually dyed surfaces are capable of binding RNA, DNA and viral particles in a differentiated, reversible and biospecific way.

1.2 Dyes and pigments: past and present

The history of dyes mingles with the development of societies and has been associated with the artistic and cognitive evolution of humanity. Their use dates back to prehistoric times, when various pigments were used for cave paintings, as a means of visual communication and artistic manifestation. It has always been and still is generally accepted that colour is able to influence people's perceptions, mood and social behaviour. Throughout history, many communities around the world believed that colours possessed magical properties, and used natural pigments for both dyeing purposes and for their healing power (Ardila-Leal *et al.*, 2021; Wells, 2013).

The first evidence of the use of colours is thought to have originated in the Stone Age, when pigments were prepared from a mixture of various soils, saliva and animal fats. Many consider they have been used to draw patterns on the skin surface or cover the skin in order to confer protection against the sun and insects. In addition, some natural pigments like ochre represented the basis for creating paints and were used for colouring various artefacts. It has also been proposed that pigments ingestion by the prehistoric man could have supplemented dietary iron, such as the ochre pigment (Ardila-Leal *et al.*, 2021; Hodgskiss and Wadley, 2017).

All dyes were naturally sourced before the 19th century and invariably consisted of plant or some animal extracts. At that time, the colour range was not as vast, and they did not have such wide applications as they do at present. Evidence of the use of dyes for colouring textiles dates back to Antiquity. The first written evidence of the use of dyes was recorded in China around 2600 BC,

whereas in Ancient Egypt, the cloths used to wrap mummies were dyed with a pigment obtained from madder plant. Other examples include the soldiers of Alexander the Great, who are believed to have covered themselves in a red dye to appear injured to the Persians, thus misleading them. Phoenicians in particular were well known for the manufacturing of dyes, among which a popular one was the “Purple of Tyre”, extracted from murex snails, which was only worn by aristocracy, being totally forbidden to the lower classes. Some natural pigments produced by plants were used as both colouring agents for fabrics, and were also thought to possess healing properties, a belief that has created numerous myths around dyes across the centuries (Bafana *et al.*, 2011; Siva, 2007; Jensen, 1963; Wells, 2013).

Dyes represent coloured compounds which can interact with a suitable substrate in a process that alters their three-dimensional structure, either by being physically adsorbed onto the substrate, mechanically retained, or by forming covalent linkages with salts or metals. A dye’s colour is based on its potential to absorb light in the visible spectrum of electromagnetic radiation, ranging between 400 and 700 nm. Nowadays, dyes are extensively used in the textile, food and cosmetic industries, as well as for printing paper and colouring photographs and play a major role in today’s world economy (Bafana *et al.*, 2011; Kanetkar, 2010).

The field of life sciences recognises the significance and vast use of dyes in many related subdomains. For example, bromophenol blue fulfils important needs in molecular biology, including being used as an acid-base indicator, bearing the ability to change colour from yellow to blue, when shifting from pH 3 to pH 4.6. It is also used as a colour marker of proteins in SDS-PAGE gel electrophoresis, allowing the proteins’ position to be monitored. In addition, bromophenol blue has even been used as an industrial dye. In microbiology, the Gram staining technique uses a dye called crystal violet, a triarylmethane dye, to stain the peptidoglycan cell wall of bacteria, thus enabling the differentiation between so called Gram-positive and Gram-negative microorganisms (PubChem, n.d.; Walker, 1994; Azmi *et al.*, 1998; Budin *et al.*, 2012).

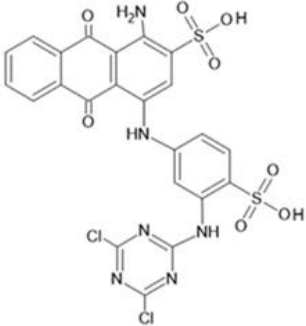
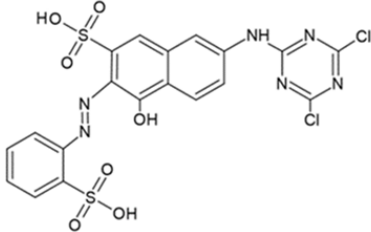
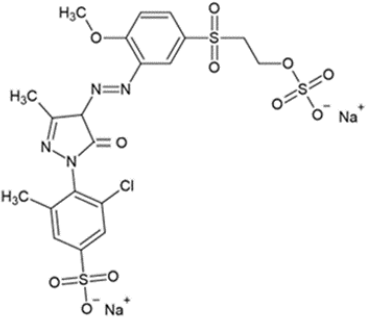
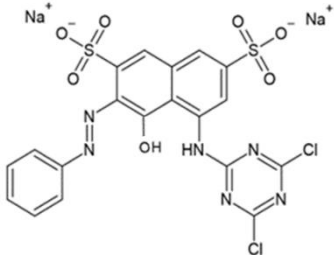
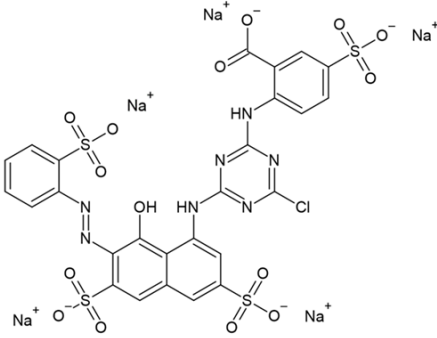
1.3 Procion dyes – chemical structure and uses

Procion dyes are reactive dyes used widely in industrial dyeing processes of textiles, foods, cosmetics, paper and inks production, owing to their increased reactivity and colour durability. An essential characteristic of these dyes is their ability to form covalent bonds with the substrate they interact with, thus undergoing addition or substitution with the functional groups present within the polymer, such as hydroxyl (-OH), amino (-NH₂) and thiol (-SH). These include the azo class of synthetic dyes, characterised by the presence of an azo bond (-N=N-) and aromatic groups, sulfonic groups and sodium ions in their structure. The dyeing process requires that the dye be well fixated

to the substrate, by the addition of a base, such as sodium carbonate or sodium hydroxide, and an electrolyte, like sodium chloride or sodium sulphate. Fixation is achieved by increasing the ionic strength, reducing the double layer thickness of the electrons, thus facilitating the uptake of dye aggregates from the solution onto the polymer. In addition, salt plays a role in overcoming the repulsion between the negatively charged dye and substrate, by concealing their surface potentials. Bases are used in dyeing to elevate the pH, promoting dye fixation via covalent bonding (Rahman *et al.*, 2013; Tappe *et al.*, 2000; Almeida and Corso, 2014; Hariani *et al.*, 2013; Epolito *et al.*, 2005; Hamlin *et al.*, 1999; Ahmed, 2005).

The Procion dyes which have been used in this study are presented in Table 1.1. Among these, all of them, except the Reactive Yellow 14 dye, are part of the class of triazine dyes, molecules containing a six-membered, unsaturated ring, composed of three nitrogen and three carbon atoms (Deng *et al.*, 2020).

Table 1.1 Names of the selection of five Procion dyes used in the present study and their molecular structures (diagrams created using ChemSketch, version 5.0).

<p>Reactive Blue 4 (Procion Blue MX-R)</p> 	<p>Reactive Orange 1 (Procion Orange MX-G)</p> 
<p>Reactive Yellow 14 (Procion Yellow MX-4R)</p> 	<p>Reactive Red 2 (Procion Red MX-5B)</p> 
<p>Reactive Red 29 (Procion Red H-3BN)</p> 	

1.4 Principles of affinity chromatography

Over the past 50 years, an essential requirement for the development of biotechnological innovations has been relying on efficient techniques for purifying proteins. Advancements made in the field of protein research, such as the use of computerised tools to study the structure and interactions with other molecules, the expansion of databases containing key information about the function and conformation of sequences, the improvements in laboratory techniques and manufacturing of specialised kits for handling protein products, have all contributed to more straight-forward and controlled methods for the accurate separation of proteins. The isolation of target proteins is particularly important within the pharmaceutical industry, where the generation of highly pure proteins is indispensable for the production of new vaccines, hormone-based therapies, and antibodies (Ersson *et al.*, 2011; Boyer and Hsu, 1993; Gallant *et al.*, 2008).

Chromatography represents one of the main methods for the purification of proteins, as well as other biological molecules (Boyer and Hsu, 1993). Chromatography refers to a set of laboratory techniques which enable the biophysical separation, identification and purification of the constituents present in a mixture, on the basis of certain characteristics, such as size, shape, hydrophobicity and polarity. The method is carried out by passing the mixture dissolved in a fluid, termed the mobile phase, through a stable, solid structure, called the stationary phase. As a result of the properties mentioned above, the various components will pass through the chromatographic system at different speeds, therefore becoming separated from one another (Charlton and Zachariou, 2008; Coskun, 2016).

The first chromatographic procedures have been known since the 1800, when the method used to be performed by artists to prepare coloured gradients. Later, at the beginning of the 20th century, the Russian botanist Mikhail Tswett introduced the first liquid chromatography column, which he used for separating plant pigments, such as chlorophyll, carotenes and xanthophylls. As the separated elements were coloured, his experiments determined the standardisation of the technique's name to "chromatography" (Greek "chroma", meaning "colour", and "graphien", meaning "to write") (Kumeria and Santos, 2015). The use of immobilised biological agents to segregate particular targets originated a few years later, in 1910, when Emil Starkenstein used this approach for the first time to isolate α -amylase, using insoluble starch as the stationary phase (Priyadarshini *et al.*, 2016; Rodriguez *et al.*, 2020). In 1951, Campbell used the principle of affinity chromatography to purify anti-bovine serum albumin antibodies from rabbit, using a column containing bovine serum albumin and diazotised *p*-aminobenzyl-cellulose, called immunoabsorbent column, which established the basis for immunoaffinity chromatography (Roque and Lowe, 2008).

The three main types of chromatography include gas, liquid, and supercritical fluid chromatography. Liquid chromatography may be further sub-classified into planar chromatography, including paper, thin-layer (TLC) and high-performance TLC, and column chromatography, referring to high performance liquid chromatography (HPLC), ultra-high performance (UHPC), ion-exchange (IEX), size-exclusion and affinity chromatography (AC). Liquid chromatography uses an inert support presenting various chemical groups, which interact with the molecules of interest, thus causing their separation, and is mainly applied for the separation of non-volatile, thermally unstable samples. Such interactions rely on the molecule's charge in ion-exchange chromatography, on specific binding in affinity chromatography, on size in gel filtration or size exclusion chromatography, on hydrophobicity in hydrophobic interaction chromatography and reverse phase chromatography, and on multiple properties in multimodal chromatography (Priyadarshini *et al.*, 2016; Coskun, 2016).

Column chromatography is generally employed for the purification of biomolecules. It is considered a more sensitive method for purifying proteins, due to their various characteristics, such as different sizes, conformations, net charge and binding capacity (Coskun, 2016). Affinity chromatography is a type of liquid chromatography, which uses molecular bonds resembling the biological enzyme-ligand interactions, to separate and identify the components of a sample. A molecule bearing a recognition ability or specificity, called ligand, is immobilised on a suitable insoluble matrix, called a polymer. The passage of the solution containing the binder through the chromatographic column, consisting of the polymeric material, selectively captures the target molecule, under favourable conditions. An eluting solution is then used to desorb the target by adjusting the ionic strength, pH or temperature of the solvent or by using free ligands; these are able to compete for the binding site, thus breaking the interaction between the resin and the macromolecules (Hage, 1999; Denizli and Pişkin, 2001).

When choosing the chromatography resin, the user should consider a number of attributes that the matrix should present, in order to efficiently isolate the target proteins. The support should be inert, thus exhibiting negligible interactions with proteins; it should create a porous network, allowing easy permeation by macromolecules. Its chemical structure must allow the attachment of ligand under normal conditions, and the chemical interactions with the ligand should be stable for the conditions of binding and elution (Roque and Lowe, 2008).

1.5 Applications of the Procion dyes in protein chromatography

Throughout the years, since the introduction of the term “chromatography”, traditional purification protocols have gradually shifted towards affinity chromatography, which is a more selective and elegant method to isolate biomolecules. It is able to simulate naturally occurring biological processes, such as molecular recognition, where the choice of suitable ligands to bind the target is essential. To pinpoint only one process in which ligands play a key role, membrane-associated receptors are worth mentioning, such as cytokine receptors, glycoprotein structures which bind various cytokines and are involved in signal transduction. The recognition site is present on the surface of virtually all biological molecules, which can selectively pair up with the molecule of interest. Thus, exploring the potential of natural ligands and using it in the production of synthetic ones for the separation of molecules is highly advantageous (Lowe, 2001; Novick and Rubinstein, 2012).

Ion-exchange resins containing common ligands have been long used as affinity polymers in protein chromatography. In fact, the most effective method for enzyme purification relies on the interaction with its specific ligands. Most common affinity ligands include peptides, oligonucleotides, antibodies and receptor proteins, all of which bear high biorecognition abilities with the complementary target protein. Affinity chromatography of proteins implies that the ligand binds to an insoluble polymer; thus, depending on the interaction specificity of the enzyme to its ligand, the bond between the enzyme and the polysaccharide resin can be disrupted i.e. the linkage forming between the enzyme and the resin polymer is overcome by the addition of enzyme substrate (Baird *et al.*, 1976; Lowe, 2001).

Dye affinity chromatography represents a convenient purification technique due to a combination of features, which allows the chromatography of some proteins difficult to purify by other methods: the high purification ability of ion-exchange chromatography and the unique selectivity. Today many manufacturers of chromatography matrices supply dye ligand resins. In order to meet the optimal conditions for product binding and elution, the user may need to control the mobile's phase conductivity, thus varying the salt concentration, or to alter the pH of the chromatographic support. In case of increased hydrophobicity, elution may become challenging, therefore the elution buffer could be mixed with a solvent or detergent to aid elution. Generally, low ionic strength buffers, with molar concentrations below 100 mM, promote protein binding, while higher concentrations (up to 1 M) should be used for elution. If the binding is too strong, the modification of pH is recommended (Gallant *et al.*, 2008).

Cibacron Blue F3G-A (CB3GA) was one of the first monochlorotriazinyl dyes to be immobilised on dextran and agarose, proving useful in purifying proteins in affinity chromatography,

particularly efficient in binding kinases, dehydrogenases, glycolysis catalases and proteins present in blood. Cibacron Blue is a reactive monochlorotriazine textile dye, consisting of multiple aromatic rings, of which primary and secondary aromatic amine groups, to which three acidic sulfonate groups are attached (Figure 1.1). The chromophore of blue dextran is believed to function as a nucleotide or coenzyme, by simulating the shape, aromatic structure and charge arrangement of nucleotides. A theory called the “dinucleotide fold hypothesis”, attempting to explain this dye’s ability to bind such a large array of proteins and enzymes, states that the similarity in structure with NAD⁺ moiety enables CB3GA interaction with proteins displaying a dinucleotide fold. A dinucleotide fold represents an evolutionarily conserved structural domain, located at a parallel β -sheet’s C-terminus. However, the absence of a “dinucleotide domain” in some proteins, which still bind CB3GA, seems to invalidate this theory (Lowe *et al.*, 1980; Lowe *et al.*, 1981; Kumar *et al.*, 2009; Andac *et al.*, 2007; Wilson, 1976). Examples of such proteins include serine proteases, cytochrome C and anti-DNA antibodies (Koch *et al.*, 1998; Thompson *et al.*, 1975; Emlen and Burdick, 1983). Thus, some other modes of molecular interactions have been considered, such as hydrophobic, ionic or donor-acceptor bonds (Lowe *et al.*, 1981).

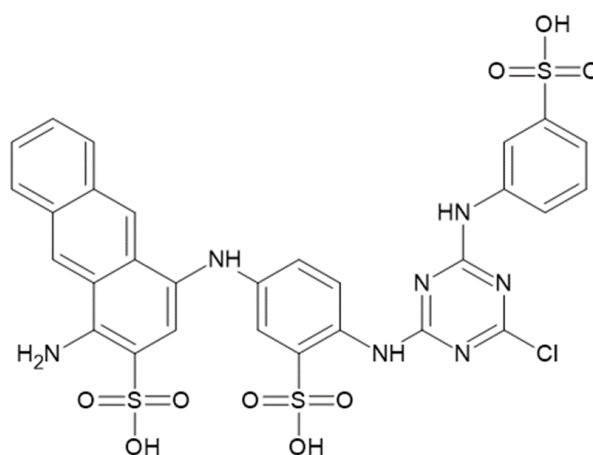


Figure 1.1. Molecular structure of Cibacron Blue F3G-A

(Created using ChemSketch).

The use of Procion dyes for the purification of enzymes has been well studied before. The complex forming between polysaccharide matrices and Procion dyes may be used in affinity chromatography for the purification of enzymes, as strong, covalent bonds establish between the enzyme and the coloured compounds. Procion dyes represent a group of reactive synthetic dyes, with a chemical structure consisting of a chromophore group, giving colour to the compound, and including the anthraquinone, azo and phthalocyanine chromophores, and a reactive part, comprising the triazine ring. There are over 70 triazine dyes, classified into dichlorotriazinyl dyes, including

Procion MX, and the monochlorotriazinyl Procion H dyes. The triazine group reacts with hydroxyl, amino and amide groups, forming stable dye-substrate covalent bonds (Baird *et al.*, 1976; Dudman and Bishop, 1968; Atkinson *et al.*, 1981).

A large variety of proteins have been purified using Procion dyes, immobilised on inert chromatography supports. For example, it was found that inosine 5'-monophosphate dehydrogenase sourced from *E. coli* bound to various Procion dye – Sepharose 4B conjugates, with high specificity. Also, it has been suggested that superior recovery of enzyme and enzymatic activity was obtained upon elution from Procion dyes, in comparison to “true”, highly specific biological adsorbents, like adenosine monophosphate and guanosine monophosphate synthetase (Lowe *et al.*, 1980). Other enzymes purified using Procion dyes were polynucleotide phosphorylase α_3 , isolated using CB3GA – Sepharose (Procion blue H-B), in buffer of low ionic strength, glycerol kinase from *B. stearothermophilus*, linked to Procion Blue MX-3G, Yellow MX-R and Yellow MX-6G. Moreover, carboxypeptidase G from *Pseudomonas* was isolated using various such dyes, with superior binding in terms of recovered activity being observed in the case of Blue MX-R – Sepharose 4B. Another experiment within the same study showed that the enzyme could also be eluted using a buffer consisting of 0.1% Procion HE3B (Drocourt *et al.*, 1978; Scawen *et al.*, 1983; Baird *et al.*, 1976).

Affinity of the proteins to the matrix-immobilised dyes depends on a range of factors, including the type of resin that the dye is bound to, the physical distance between conjugated molecules (spacer arm), temperature, the equilibration buffer's pH, ionic strength, flow rate, and column volume. The inert support should fulfil a number of characteristics in order to form strong interactions with the dye, including hydrophilicity, chemical stability and sufficient number of reactive groups to enable the substitution with the dye. Some matrices may have a higher capacity to bind dyes than others; however, this does not guarantee an increased ability to absorb proteins (Lowe *et al.*, 1980; Lowe *et al.*, 1981).

1.6 Emerging infectious diseases

Throughout history, the spread of infectious diseases has caused considerable suffering due to associated morbidity and mortality. However, over the past decades, humanity has witnessed a major increase in the emergence, incidence and transmission of such diseases, all around the globe. Infectious diseases, also termed “communicable”, represent illnesses caused by pathogens, able to be disseminated from one host to another by various modes of transmission, including airborne, waterborne, bodily fluids, or via contaminated fomites or vectors, such as infected animals and insect bites. In humans, the vast range of pathogenic agents producing diseases includes bacteria,

viruses, fungi, protozoa and worms (Straif-Bourgeois and Ratard, 2005; Platto *et al.*, 2020; Saker *et al.*, 2004; Balloux and van Dorp, 2017). Antimicrobial resistance is imposing a considerable threat to public health, as pathogenic microorganisms no longer respond to treatment, thus increasing the risk of disease spread, prolonging hospitalisations and, consequently, generating negative socio-economic effects (McMichael and Woodruff, 2008; WHO, 2014). Therefore, methods to reduce the pathogenic load, as well as novel treatments, need to be strongly considered in modern day communities, not only to decrease disease incidence, but also to treat specifically potential sources of infection.

Large pandemics have been a leading cause of death for many centuries, among which plagues, such as cholera, smallpox, tuberculosis, influenza and, more recently, coronavirus infections, are noteworthy. In 1995, 17 million out of 52 million deaths had been attributed to communicable diseases, including pneumonia, pathological diarrhoea, tuberculosis, malaria, AIDS and hepatitis B. In recent times, the worldwide disease and death trends have shifted towards non-communicable diseases, such as cardio-respiratory, diabetes, kidney and neurodegenerative conditions. However, according to the World Health Organisation, communicable diseases still represented three out of the top ten global leading causes of death in 2019, among which lower respiratory infections and diarrhoeal diseases are transmissible. In addition, mortality rates due to communicable diseases vary between highly industrialised and non-industrialised countries, with poorer areas being more often stricken by health crises. The poorest fifth of the world population is particularly affected by such illnesses, the rate of multiple infections being higher in low-income regions, in comparison to wealthier countries (Platto *et al.*, 2020; Straif-Bourgeois and Ratard, 2005; WHO, 2000; WHO, 2020; Saker *et al.*, 2004).

Urbanisation and globalisation have resulted in ecological disturbances, which have been linked to the occurrence of new zoonoses. Anthropogenic undertakings have brought humans and wildlife closer together, allowing pathogens to transit between species. Also, the likelihood of infection spread has been associated with densely populated areas, particularly in urban environments, where communities live compactly, use public transportation and are predisposed to interaction with a multitude of international tourists. Thus, the beginning of the year 2020, marked by the emergence of the new SARS-CoV-2 pandemic, was a reminder of how far we still are from eliminating the global burden of infectious diseases, despite the progress medicine has achieved lately. The first cases of the new respiratory disease have been traced back to the Huanan's wild animals' market in Wuhan, China. The 96% nucleotide sequence identity between the new virus and a bat coronavirus, BetaCoV/RaTG13/2013, indicated that the origin of the former may reside in the crossover from an animal to a human host (Platto *et al.*, 2020; Anser *et al.*, 2020; Straif-Bourgeois and Ratard, 2005; Velavan and Meyer, 2020; Bulut and Kato, 2020).

1.7 *Virus biology and bacteriophage T4*

Few areas of science are as compelling as the study of viruses. Viruses represent acellular and anucleated microbiological entities, able to cause diseases by attacking the cells of a host organism, by means of which they survive and replicate. Due to the absence of a nucleus, it is hard to argue whether viruses are living or non-living. In order for a structure to be considered alive, it must incorporate an intrinsic metabolic system, thus meeting specific characteristics, like being able to perform movement, respiration, nutrition, excretion, reproduction and growth by itself. Viruses are unable to carry out these functions independently of a host, which made them be recognised as “obligate parasites”. Viruses possess an infection machinery which they use to reproduce, by inserting their genetic material inside a host, and using the metabolism of the latter to serve their own needs (Villarreal, 2004; Yewdall *et al.*, 2018; Gergerich and Dolja, 2006).

Bacteriophages, or phages, represent a family of viruses which invade bacterial host cells, disrupting their metabolic processes and determining cell lysis. T4 bacteriophage is a large, tailed, double-stranded DNA virus, which infects *Escherichia coli*, being one of the most complex viruses, and known to be able to produce more than 40 proteins. Structurally, T4 phages consist of prolate icosahedral heads called capsids, made of proteins termed capsomeres, which encapsulate the viral nucleic acid. Their tails are made of a contractile sheath, ending in a baseplate, from which multiple projections called tail pins arise (Sulakvelidze *et al.*, 2001; Fokine *et al.*, 2004; Leiman *et al.*, 2003).

1.8 *Molecules bearing the ability to bind pathogens*

Transmission of viruses via fomites occurs when droplets produced by virus-infected individuals fall on various surfaces, from where they can be easily picked up by another host. Despite only being able to replicate inside a host organism, some viruses can remain viable on fomites for several days, just as SARS-CoV-19. Thus, fomites are highly responsible for the spread of viral diseases, in many environments. Consequently, prevention should be the main objective of research aiming to control the dissemination of pathogens, which could be achieved by microbial detection using specialised tools (Castaño *et al.*, 2021; Boone and Gerba, 2007; van Doremalen *et al.*, 2020; Draz and Shafiee, 2018).

Nanoparticles are small, solid particles ranging between 10 to 1000 nanometres (nm), which have become increasingly studied during the past decades. Recent advances in nanoscience have led to the development of nanomaterials designed to identify infectious agents. Thus, among numerous other functions, nanoparticles are currently being used for the development of bioassays

and sensors, and their basic characteristics make them a good candidate for pathogen recognition and capturing (Mohanraj and Chen, 2006; Ray *et al.*, 2012; Mustafa *et al.*, 2017). For example, gold and silver nanoparticles have been used for pathogen detection by observing the alteration in optical signal after the addition of the microorganism of interest to functionalised nanomaterials. Moreover, silver is known to exhibit antimicrobial activity against bacteria, fungi, protozoa and even certain viruses, upon release of toxic ions. Other metal nanostructures like copper and gold/silver-tellurium may be used for modelling nanowires, nanotubes and nanoarrays, which have been shown to express antimicrobial properties (de Azeredo, 2013; Ray *et al.*, 2012).

Pathogen recognition may be achieved by using nanomaterials conjugated with functional groups presenting targeting potential, such as antibodies, organic ligands, antimicrobial peptides and aptamers, which can recognise antigens present on the pathogen's surface with high selectivity. Nanomaterials have large surface areas, allowing a great number of detecting elements to attach to them, thus enabling the identification of multiple pathogens simultaneously (Ray *et al.*, 2012).

Aptamers represent small, single-stranded DNA or RNA sequences, measuring about 3-5 nm, with role in binding specifically and with high affinity to non-nucleic acid targets, such as the epitopes displayed on the surface of bacterial cells. These are synthesised by the SELEX method (systematic evolution of ligands by exponential enrichment) performed in multiple cycles; this consists of three main steps: small nucleic acid sequences are first synthesised *in vitro* and incubated with the target, the unbound sequences are removed, and the bound sequences are used as templates and amplified by PCR. Nanoparticles modified with antimicrobial peptides can attach non-specifically to the negatively charged lipopolysaccharide outer membrane of gram-negative bacteria, or to the peptidoglycan precursors, necessary for the cellular wall synthesis. After detection, pathogenic bacteria undergo photothermal killing, using near-infrared light (Teng *et al.*, 2016; Ray *et al.*, 2012).

Gold nanoparticle-based colorimetric assay can be an easy method for identifying bacteria by monitoring colour changes with the naked eye; the assay relies on the principle of surface plasmon resonance, which refers to the oscillations of free electrons upon excitation with an optical beam, a basic property of metal nanoparticles. The inter-particle distance between gold nanoparticles determines their colour; when the distance between spherical nanoparticles shortens, the phenomenon of interparticle plasmon coupling induces a colour change from red to blue, which can be used for pathogen biosensing by their aggregation on the surface of the micro-organism (Ray *et al.*, 2012; Srivastava *et al.*, 2012; Verma *et al.*, 2015).

Viral detection assays rely on the use of biospecific antibodies. Synthetically engineered antibody fragments with high affinity for the receptor binding site of COVID-19's spike protein proved useful both in identifying viral particles and impeding their entry into the host cell. The

method relies on split-enzyme complementation using two fragments of β -lactamase to generate a fluorogenic signal: when the N- and C-terminal segments of the enzyme attached to antibody fragments recognise two distinct viral epitopes, they can bind to the receptor binding site. The same complex showed promising results in detecting Zika and Ebola antigens (Slezak and Kosiakoff, 2021).

Molecular imprinting may be used for detection of viruses. The technique implies that cavities of high affinity and selectivity are created in polymer matrices using templates, where viruses, which range in size from 10 to a few hundred nanometres, can fit, due to a geometrical match; this way, viruses can be detected, and the mould created in the polymeric surface can be considered an artificial antibody (Hayden *et al.*, 2006).

1.9 Existing mechanisms to prevent transmission of infections

Although infections represent an unavoidable aspect of life, there are numerous available strategies which may help reduce the transmission of communicable diseases. Since 1950, the global life expectancy has increased by 24 years, due to a significant reduction in human mortality caused by infectious diseases. The development of public health services across the globe gave rise to improved medical practices, antibiotics, and vaccination programmes. In addition to these, higher incomes, access to better nutrition, clean water and proper hygiene and sanitation, have led to superior management of epidemics (Drexler, 2010; Anser *et al.*, 2020).

A number of important preventive mechanisms have been in place from the beginning of the COVID-19 pandemic in 2020. Consequently, social distancing, frequent handwashing, the mandatory wearing of face masks, travelling restrictions and testing rules proved essential in reducing the incidence of coronavirus infections worldwide. It has been shown that air samples from patients infected with SARS-CoV-2 which contained viable virions could be collected from 2-4.8 m away from the patients, emphasizing the role of appropriate personal protection to avoid catching the disease (Anser *et al.*, 2020; Lednicky *et al.*, 2020). Face coverings confer protection by lowering the number of virus-containing droplet emissions, which increases with voice amplitude or loudness during speech. Thus, some people may emit high numbers of droplets while speaking and could therefore be super-spreaders. The number of particles ejected during speech range from 1 to 50 per second, increasing to approximately 3000 when coughing once, and equalling as many as 40,000 droplet nuclei during sneezing (Curtius *et al.*, 2021; Zacharias *et al.*, 2021; Cole and Cook, 1998). Interestingly, the systematic use of protective face masks can be traced back to the Spanish Flu pandemic, occurring between 1918-1920. A journal article published in 1919 stated that overcrowded military establishments had been stricken by an increase in influenza

cases, due to exposure to saliva droplets of infected individuals, encouraging the population to wear multi-layered gauze face coverings (Simonetti *et al.*, 2021; Weaver, 1919).

The COVID-19 pandemic has confirmed that our knowledge about the transmission of airborne viruses was rather deficient. The airborne dissemination of respiratory infections has been highly overlooked, suggesting that the traditional understanding of how aerosols are passed on between hosts should be updated. Gatherings in enclosed spaces, such as meeting rooms, offices, schools, and social events taking place indoors, have proved challenging in mitigating the spread of such infections. Close face-to-face human interaction, combined with inadequate ventilation, may facilitate the rapid build-up of viral particles in the air, thus increasing the risk of contracting the respiratory disease. In view of the current situation and considering that further pandemics are likely to occur within the next decades, there is a need for precautionary methods to be planned in advance (Wang *et al.*, 2021; Curtius *et al.*, 2021).

In addition to wearing protective face masks, filtration of air in confined spaces may provide an option for eliminating airborne virions. In this case, the spread of infection is linked to the concentration of breathable pathogens present in the indoor air. Using appropriate room ventilation to dilute and remove contaminated air by redirecting the airflow may reduce the risk of pathogenic transmission. For example, commercial HEPA filters, standing for “high-efficiency particulate air”, appear to be highly efficient in purifying the air, being able to retain around 99.96% of actinophage particles and remove particles with a diameter equal to or larger than 0.3 μm . During WWII, the US military force required filtering instruments, for both individual and shared use, which could confer protection against chemical and biological warfare agents to the soldiers. At the beginning of the war, the British Army captured a gas mask canister from the Germans and discovered a piece of paper contained within, which could trap chemical smoke very efficiently; this was retained as a model for manufacturing protective masks for the troops. Operational headquarters particularly were in need of such units, but the use of unitary gas masks was impractical. Thus, the US Army Chemical Corps developed a safety device known as a “collective protector”, which could act as both a mechanical air blower and a purifier. This consisted of a pleated cellulose-asbestos piece of paper, also used for the fabrication of gas masks, which was the precursor of today’s HEPA filter (Roelants *et al.*, 1968; Medical Advisory Secretariat Ontario, 2005; First, 1998).

Among the measures known to decrease exposure to air contaminants, indoors air filtration may be the most practical compromise between an efficient air purifying system and the comfort of not being required to wear a face mask. Indoor air filtration is an important control measure limiting the inhalation of non-biological air pollutants, such as dust, smoke and volatile compounds; this is also able to reduce the spread of some biological contaminants, including fungi, mould and viruses. Purification of air in enclosed spaces can be achieved by home heating and ventilation systems,

including air conditioning, room air cleaners and purifiers. Such devices that are currently accessible on the market consist of multiple layers, generally incorporating a prefilter, a carbon, an antipathogenic and a HEPA filter. The latter have been initially used in hospitals air filtration systems and have been later included in home air purifiers. Additionally, these are incorporated inside the filtering system of biosafety cabinets of science laboratories (Vijayan *et al.*, 2015; Frey *et al.*, 2020).

Given the known ability of the Procion dyes to bind an extensive selection of proteins, it could be speculated that they may also bind the protein capsid of viruses. If such affinity occurs, it could be possible to immobilise viruses on various dyed surfaces. Procion dyes are primarily used as textile dyes and are inexpensive compounds (Sari *et al.*, 2017). Therefore, the use of Procion dyes in colouring face masks may potentially enhance their efficiency, while providing a cheaper and handier alternative of protection against transmissible respiratory illnesses, in comparison to standard preventive measures. While it is important to note that Procion-dyed face masks, just like standard face coverings, would not provide a replacement for vaccinations, proper hand hygiene and isolation or quarantine, they may be more universally accessible and socially accepted. In addition, they may confer immediate protection and prevention against disease. A disadvantage of using Procion dyes is that they are harmful to aquatic life, caused by the pollution of wastewaters, resulting from the textile colouring industry, and indirectly to human health (Rahman *et al.*, 2013). When in powder form, reactive dyes are known to produce respiratory and skin sensitisation, but only before being applied to fabrics (Docker *et al.*, 1987; Maiphethlo, 2007). However, during intense perspiration, reactive dyes may transfer to human skin and penetrate it. In such cases, the employment of methods to increase colour fastness is recommended, to avoid the occurrence of any allergic reactions (Leme *et al.*, 2014).

1.10 *Aims and objectives of the present study*

The present study aims to investigate the binding of biological macromolecules (including bacterial proteins and nucleic acids) to the Procion dyes, as well as their potential use in binding viral particles (bacteriophage T4). The study will start by testing and confirming the principle that Procion dyes have the ability to bind a large array of proteins, which has been extensively proved in the past, by using a selection of five dyes. Then, the interaction between these and bacterial DNA and RNA will be explored and quantified. Afterwards, in order to examine the ability of Procion dyes to immobilise viruses, potential binding of T4 bacteriophage particles to the dye compounds will be assessed. This will be

approached in two different ways. Firstly, phage will be passed through a chromatography column and eluted. Secondly, pieces of fabric dyed with the choice of five Procion dyes will be incubated with a phage solution, and the change in titre will be monitored.

Exploring the possible application of the Procion dyes in capturing viral particles could be employed to challenge the spread of transmissible viral diseases in the future. As these dyes have been used in the past in the affinity chromatography of a large number of proteins and enzymes, it is reasonable to hypothesize their prospective use in forming chemical linkages with the protein coating of viruses. Consequently, their application in dyeing face masks or other items of personal protective equipment could inactivate and capture viruses due to attachment to the dyed fabrics, thus considerably reducing exposure to the potentially high viral loads present in the air. Additionally, dyeing the filters of air purifiers with Procion dyes might provide a cheap and clever way to boost their filtering capacity and ensure clean, virus-free indoors air, for example in homes, hospitals, schools and other public units, especially during epidemics. Such approaches would be convenient self-protective measures and easy to implement by many people.

2. General materials and methods

2.1 Materials

The initial stocks of *Escherichia coli* β -10 (K12 strain) were provided by Blades Biological Ltd. (Cowden, Kent, UK); the T4 bacteriophage and the specific T4 host *E. coli* K-12 were a kind gift from the University of Liverpool (Liverpool, UK). The DEAE Sephadex A-50 was obtained from Cytiva (US). The Procion dyes, consisting of Blue MX-R, Orange MX-G, Brilliant Red H-3BN, Red MX-5B and Yellow MX-4R, were purchased from Thermo Fisher Scientific (Hempstead, UK) and Sigma-Aldrich (Dorset, UK). General chemicals and growth medium components were purchased from Fisher Scientific, Sigma-Aldrich and Formedium Ltd (Hunstanton, UK).

2.2 Growth of *Escherichia coli* β -10 stocks

The aseptic technique was employed when performing bacterial culturing, by working in a laminar flow safety cabinet and using sterile materials and equipment. An initial stock of *Escherichia coli* was used for growing subsequent colonies, by inoculating Luria-Bertani (LB) agar or yeast agar plates, prepared according to the protocol of Elbing and Brent (2018), by using the streak plate method; the plates were incubated overnight in a convection incubator (Jeio Tech IB-05G, Montreal Biotech Int.), at 37°C. Mini-cultures were prepared by isolating single colonies from the agar plates, using sterile plastic pipette tips and releasing them in individual centrifuge tubes containing 5 ml of LB medium, H, TYGPN, 2× TY or Superbroth medium, prepared according to the protocols of Elbing and Brent (2018). These were incubated overnight (approx. 18h) in an orbital rotating shaking incubator (MaxQ 5000, Thermo Scientific), at 37°C and 180 RPM. Flasks containing 250 ml of the abovementioned media were inoculated with 2.5-3 ml of the mini-cultures and were incubated for at least 20 hours, at 37°C, shaking at 180 RPM. The liquid colonies were poured into 50 ml Falcon tubes, centrifuged at 4500 RPM for minimum 10 minutes (Heraeus Megafuge 8, Thermo Scientific), discarding the supernatant, and the bacterial pellets were stored at -80°C.

2.3 Bacterial protein extraction

Tubes containing frozen bacterial pellets were thawed at room temperature, suspended in an equal volume of sterile 0.1 M PBS, and sonicated using an MSE Soniprep 150 ultrasonic disintegrator, by passing the sample through the probe for 2-3 seconds, minimum 50 times. The lysate was transferred to microcentrifuge tubes, centrifuged for 30 minutes at 11,000 RPM (Heraeus Fresco 17 Centrifuge, Thermo Scientific) at 4°C and the protein-containing supernatant was collected, discarding the pellets. Protein concentration was measured using a DS-11 Spectrophotometer/ Fluorometer (DeNovix), at 280 nm, and the solution was stored at -20°C.

2.4 Bacterial genomic DNA extraction

Bacterial genomic DNA was extracted using a general genomic DNA extraction protocol. The centrifuge tubes containing bacterial pellets were thawed at room temperature, suspended in an equal volume of PBS, and mixed by pipetting. An equal volume of cell lysis buffer was added to the sample and mixed by vortexing. The lysis buffer contained 10 mM Tris solution at pH 8, 100 mM NaCl solution, 10 mM EDTA solution at pH 8, 10% (w/v) SDS solution to a final concentration of 5% and 20 µL of a 20 mg/mL Proteinase K solution per 1 mL of buffer. The sample was incubated in a thermal mixer (Eppendorf Thermo Mixer F2.0, Sigma-Aldrich) for 1 hour, at 56°C and 1400 RPM; alternatively, a water bath set to 56°C and occasional vortexing was used when working with larger sample volumes. The sample was extracted with an equal volume of phenol/chloroform/isoamyl alcohol (25:24:1) (Acros Organics), mixed by inverting, to completely combine the phases, and centrifuged at maximum speed for 5 minutes (14,000 RPM for small sample volume placed in small microcentrifuge tubes) or 25 minutes (4500 RPM for 50 mL Falcon tubes). The upper aqueous layer, containing DNA, was transferred to fresh microcentrifuge tubes, followed by the addition of 1 mL of 100% (v/v) ethanol (RT), and the tube was inverted repeatedly to form DNA precipitates. The sample was left to incubate at room temperature for 15-30 minutes and then centrifuged at maximum speed for 10-25 minutes (for small and large sample volumes, respectively). The supernatant was discarded, and the DNA pellet was washed with 2-5 mL of cold 70% (v/v) ethanol (-20°C), followed by centrifugation at maximum speed for 2-5 minutes. The supernatant was discarded, and DNA was left to dry at room temperature or in an incubator at 37°C. Dry DNA was resuspended in a desired volume of Ultrapure, DNase/RNase-free water (Invitrogen) and stored at -20°C. Alternatively, the pellet may be resuspended in TE buffer at pH 8.

2.5 Bacterial RNA extraction

Bacterial paste was thawed at room temperature and resuspended in 10 volumes of sterile distilled water by continuous pipetting. A volume of 800 μL of suspension was transferred to a fresh microcentrifuge tube, to which 160 μL (a fifth of the culture volume) of TRIzol reagent (Fisher Scientific) was added, followed by the addition of 32 μL of chloroform (a fifth of the TRIzol volume) and the mix was left to incubate at RT for 2-5 minutes. The solution was centrifuged for 15 minutes, at 12,000 RPM and 4°C, and the aqueous phase was transferred to a fresh tube and mixed with an equal volume of 100% (v/v) isopropanol. The mix was centrifuged for 10 minutes, at 10,000 RPM and 4°C, discarding the supernatant. The pellet was resuspended in 70% (v/v) ethanol and centrifuged for another 10 minutes, at 10,000 RPM and 4°C, discarding the supernatant. The RNA pellet was air-dried at 37°C for 10-15 minutes on a heating block, and was resuspended in a desired volume of TE buffer at pH 8.

2.6 Bacteriophage stock preparation and storage

The protocol was first defined by Ceelen (2019). A high titre phage lysate was used for this experiment ($>10^8$ PFU/mL). The lysate was kindly gifted by the University of Liverpool. Its titre was determined by the plaque assay, described in the following section (section 2.7). An LB *E. coli* K-12 mini-culture was prepared and incubated overnight; 100 μL of liquid bacterial culture were used to inoculate 5 aliquots of LB medium, each containing 10 mL, already supplemented with 50 μL of 1 M calcium chloride solution and 50 μL of 1 M magnesium chloride solution. The aliquots were incubated at 37°C, with 180 RPM agitation, for one hour. This was followed by the addition of 100 μL of high titre phage lysate to each aliquot. Another five-hours incubation at 37°C and 180 RPM followed. The aliquots were pooled and centrifuged at 4,000 RPM for 25 minutes, filter-sterilised using a 0.22 μm filter, to remove bacterial cell lysates, and the titre was determined using the plaque assay (section 2.7).

Deep-frozen stocks of both *E. coli* (T4 host) and T4 were prepared, to be easily accessible in further experiments. Multiple aliquots of 400 μL of fresh liquid *E. coli* mini-culture and 400 μL of fresh cell-free T4 lysate were each suspended in 100 μL of 80% (v/v) glycerol, vortexed vigorously and deep-frozen at -80°C, for long-term storage. When needed, these were thawed either at RT or in an incubator, at 37°C.

2.7 The phage plaque assay

This experiment was conducted using the aseptic technique, in a specially designed working space, to avoid contaminating the bacterial cultures. The double-layer agar procedure was adapted from the protocol proposed by Stachurska *et al.* (2021). An *E. coli* K-12 (T4 bacteriophage host strain) LB mini-culture was prepared the night before and diluted, so that $OD_{600} = 0.2 - 0.4$ AU. Soft agar was made by mixing bacto-yeast extract (0.5%), tryptone soy broth granules (1%), sodium chloride (0.5%) and bacteriological agar (0.4%), supplemented with 300 μ L of 1 M calcium chloride solution per 100 mL of soft agar. It was maintained liquid in a water bath, at 42°C. A serial dilution of the initial phage stock was made, from 10^{-1} to 10^{-7} , and 100 μ L of bacterial cells were mixed with 100 μ L of each dilution and incubated for 15 minutes, at RT. The mixtures were used to inoculate 3 mL of soft agar, combining the contents by gentle swirling, and were poured over previously prepared warm LB agar plates (25°C), by evenly spreading the soft agar on the bottom agar surface. Plates were incubated overnight, at 37°C. Next day, phage titre was calculated by multiplying the number of plaque-forming units on each plate by the dilution factor of the serially diluted phage and then by 10, to determine the number of PFU present in a mL of stock (100 μ L of used phage stock = 1/10 mL). Only plates containing between 30 and 300 plaques were considered.

2.8 Preparation of clear and dye-polysaccharide matrices

The methods used for the preparation of dyed matrices were an adaptation of the protocols proposed by Baird *et al.* (1976), Dudman and Bishop (1968) and Scawen *et al.* (1983) and the choice of dyes was made consistent with the ones used by Baird *et al.* (1976). Some of the products listed by Baird and colleagues were not available and were replaced by other dyes, similar in their chemical structure. Thus, in this study, Red H-3BN replaced Red H3B5, Red HE7B, Red HE3B and Red H3B. Additionally, Red MX-5B was purchased. Yellow MX-4R substituted Yellow MX-6G and Yellow MX-R. Cibacron Blue F3G-A, Blue H7GS and Blue MX-3G were substituted by Blue MX-R, which was also used by Baird and colleagues. Therefore, Blue MX-R and Orange MX-G were the only dyes matching the ones used in the research of Baird *et al.* (1976).

A solution containing 1 g of DEAE Sephadex A-50 (Cytiva) dissolved in 20-25 mL of sterile 0.1 M PBS (Gibco PBS tablets, Life Technologies Ltd.) solution was prepared directly in a 50 mL Falcon tube and left to mix on a roller shaker for 5-10 minutes. Another solution containing dry Procion dye powder was prepared by dissolving 50 mg of dye into 5 mL of sterile distilled water.

The slurry and the dye solution were combined and incubated for 5-10 minutes on a roller shaker. Sodium chloride was added to the solution, up to a final concentration of 2% (w/v), followed by another 30 minutes of incubation on the roller. Sodium carbonate was mixed into the solution to a final concentration of 0.1% (w/v) and the tube was incubated for minimum 24-48 hours on the roller shaker, to allow unreacted dye to hydrolyse. Tubes were stored at 4°C.

The use of clear Sephadex A-50 slurry was also necessary as a control in all the experiments. For this purpose, the previous procedure was followed, skipping the step involving the mixture of slurry with the dye solution.

2.9 Traditional method for preparing chromatography columns

For this protocol, 10 mL plastic syringes were used as chromatography columns. The plunger was removed, the syringe tip was packed with a small piece of glass wool, and the column was attached to a vertical stand, with the tip side facing down. A thorough preliminary washing step with distilled water was necessary in order to remove any yellow colouring present in the wool. The

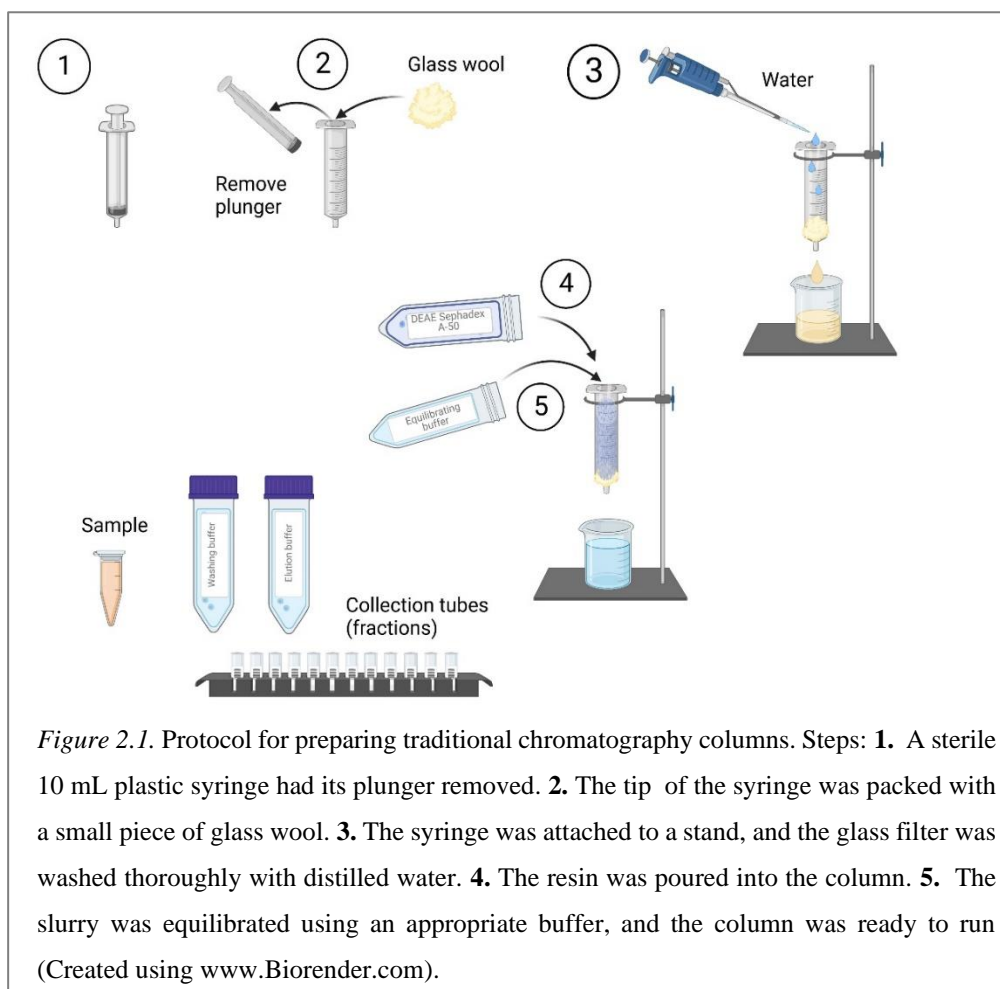


Figure 2.1. Protocol for preparing traditional chromatography columns. Steps: **1.** A sterile 10 mL plastic syringe had its plunger removed. **2.** The tip of the syringe was packed with a small piece of glass wool. **3.** The syringe was attached to a stand, and the glass filter was washed thoroughly with distilled water. **4.** The resin was poured into the column. **5.** The slurry was equilibrated using an appropriate buffer, and the column was ready to run (Created using www.Biorender.com).

clear or dye-tagged DEAE Sephadex A-50 slurry was poured into the syringe and the extra liquid was allowed to drip down the column into a waste beaker. The column was washed with 3 column volumes of equilibrating buffer, depending on the experiment (Figure 2.1).

2.10 *Dyeing of natural fabrics with Procion dyes*

Undyed cotton and silk were a kind gift from Calico Laine Ltd. (Wallasey, United Kingdom). The methods used for fabric dyeing were adapted from two online protocols (Holland, 2015; FastColours.com, n.d.), which are believed to be adaptations of techniques described by Clark (2011). Although these protocols are designed for the use of Procion MX dyes, they were also followed for dyeing the fabrics with Procion Red H-3BN (Reactive Red 29). The cloths were first washed thoroughly, to remove any unwanted residues and ensure better dye adsorption. Small, rectangular pieces of completely dried fabric were cut and weighed out on a fine scale, measuring approximately 5 cm long and 3 cm wide and weighing approx. 303 mg (cotton) and 53 mg (silk).

Sterile distilled water at 40°C or slightly below was used for dyeing cotton. When using colder water, as the online protocol requires, dyeing results were not satisfactory. The cotton was first soaked in distilled water and squeezed well; water was added to a small glass beaker, using 30 ml for each gram of cotton (9.096 mL of water in this case). Then, 1 g of dye was added for every 100 ml of water (90.96 mg of dye) and stirred well on a magnetic stirrer; the fabric was added to the beaker and stirred. The protocol advises the use of 40 g of NaCl per each 100 ml of water, which in this case represented a slightly high salt concentration (363.84 mg of NaCl in total), leading to insufficient adsorption of dye in previous attempts; therefore, 200 mg of NaCl were added to the beaker, 10 minutes after the addition of fabric. Similarly, a lower amount of Na₂CO₃ was added (121 mg), instead of 2 g for every 100 ml of water, after 30 minutes. The contents of the beaker were transferred to a Falcon tube, and incubated on a shaking roller overnight, at 35 RPM.

For dyeing silk, 3 L of sterile distilled water at 40°C were used for every gram of fabric (160.5 mL of water in this case) and were added to a flask. Due to very low fibre weight, using 1 g of dye per 100 g of silk, as specified in the protocol, resulted in 0.535 mg of dye, which was impractical to measure and very low for the quantity of water calculated; therefore, 100 mg of dye were stirred into the water instead. Wetted silk was added to the dye solution and the flask was incubated on a roller shaker for 10 minutes, at 35 RPM. 80 g of NaCl were necessary for each 100 g of silk; however, the quantity was quite high for the dye content, according to previous dyeing attempts, thus only 30 mg of NaCl were used, instead of 42.8 mg. After 30 minutes, 6 g of Na₂CO₃ were added for every 100 g of silk (3.21 mg) and the flask was incubated on the roller overnight.

The next day, the fabrics were washed sequentially, by transferring them to separate flasks containing sterile, distilled water, placed on a shaker roller; used water was replaced regularly with fresh, sterile water, until no more dye was visibly leaking. For intensely coloured fibres, the fabrics were stirred gently in a 5% (w/v) NaCl solution for a couple of hours and rinsed well, to allow further colour removal; this was necessary in order to prevent any colour leaking during future experiments. The fabrics were dried in an incubator and allowed to cool down until further processing.

An extra piece of silk was dyed using 1000x more RB4 dye (100 g of dye per 100 g of silk). The other steps and the quantities of salt and sodium carbonate were followed as per the previously described recipe.

2.11 *Statistical analyses and figures*

Minitab (version 1.9.0) and Microsoft Excel (version 2206) were used to conduct statistical analyses and produce graphs. SDS-PAGE gel images were modified using Image Lab (version 6.1). Collection of data on protein bands' intensity was performed using ImageJ (<https://imagej.nih.gov/ij/>). P-values equal to or lower than 0.05 were considered statistically significant. Other figures and diagrams were created and edited using BioRender (www.biorender.com), ChemSketch (version 5.0) and PowerPoint (version 2209).

3. Testing the binding affinity of bacterial proteins to the Procion dyes

As mentioned, Procion dyes represent reactive coloured compounds, able to interact with various types of substrates, including fibres and resins. Due to this key property, they have been extensively used as chromatography affinity ligands for the purification of a broad range of proteins, as indicated by the studies of Scawen *et al.* (1983), Baird *et al.* (1976) and many others.

Chapter 3 investigates the interaction between the selection of five Procion dyes and the total *E. coli* β -10 protein extract, divided into two experiments. The first experiment, in which the binding of bacterial proteins to the Reactive Blue 4 dye was examined, lays the foundational groundwork for the subsequent experiment. Here, the interaction was tested in tubes, without recovery of bound protein. The second experiment explored the affinity of bacterial proteins to all of the five Procion dyes, by using a highly creative method, based on SDS-PAGE gel electrophoresis technology, which is not known to have been used in the past. This method evaluated the dye-protein interplay, by assessing the binding of proteins to dyed resin, subsequent washing, elution and the inability to recover some proteins.

The methods described here aimed to validate the findings of Scawen *et al.* (1983) and other similar studies, which indicated an affinity of various proteins to the Procion dyes. These analyses serve as a preliminary step for subsequent experiments, described in the following chapters.

3.1 Methods

3.1.1 Testing the affinity of bacterial proteins for the Reactive Blue 4 dye

Bacterial protein was extracted using the protocol defined previously (section 2.3) and was diluted to the desired concentration (gDNA concentration ranged between approximately 30 – 80 ng/ μ L throughout the experiments). Tubes containing clear DEAE-Sephadex A-50 and resin tagged with the RB4 dye (see section 2.8 for preparation of clear and dye-conjugated matrices) were incubated at RT for 30 minutes. 200 μ L of each slurry were added to microcentrifuge tubes, preparing triplicates for each resin type. Initial protein concentration was measured using the DeNovix DS-11 Spectrophotometer/ Fluorometer (DeNovix). A volume of 150 μ L of protein solution (27.499 mg/mL) was added to each tube, and these were incubated for 1, 5, 10, 30 and 60 minutes on a roller shaker, at 35 RPM. Tubes were centrifuged at maximum speed (Eppendorf Centrifuge 5424, Sigma-Aldrich) for 30 seconds after each incubation, and protein concentration in the supernatant was measured spectrophotometrically.

3.1.2 *Testing the affinity of bacterial proteins for the Procion dyes by SDS-PAGE gel electrophoresis*

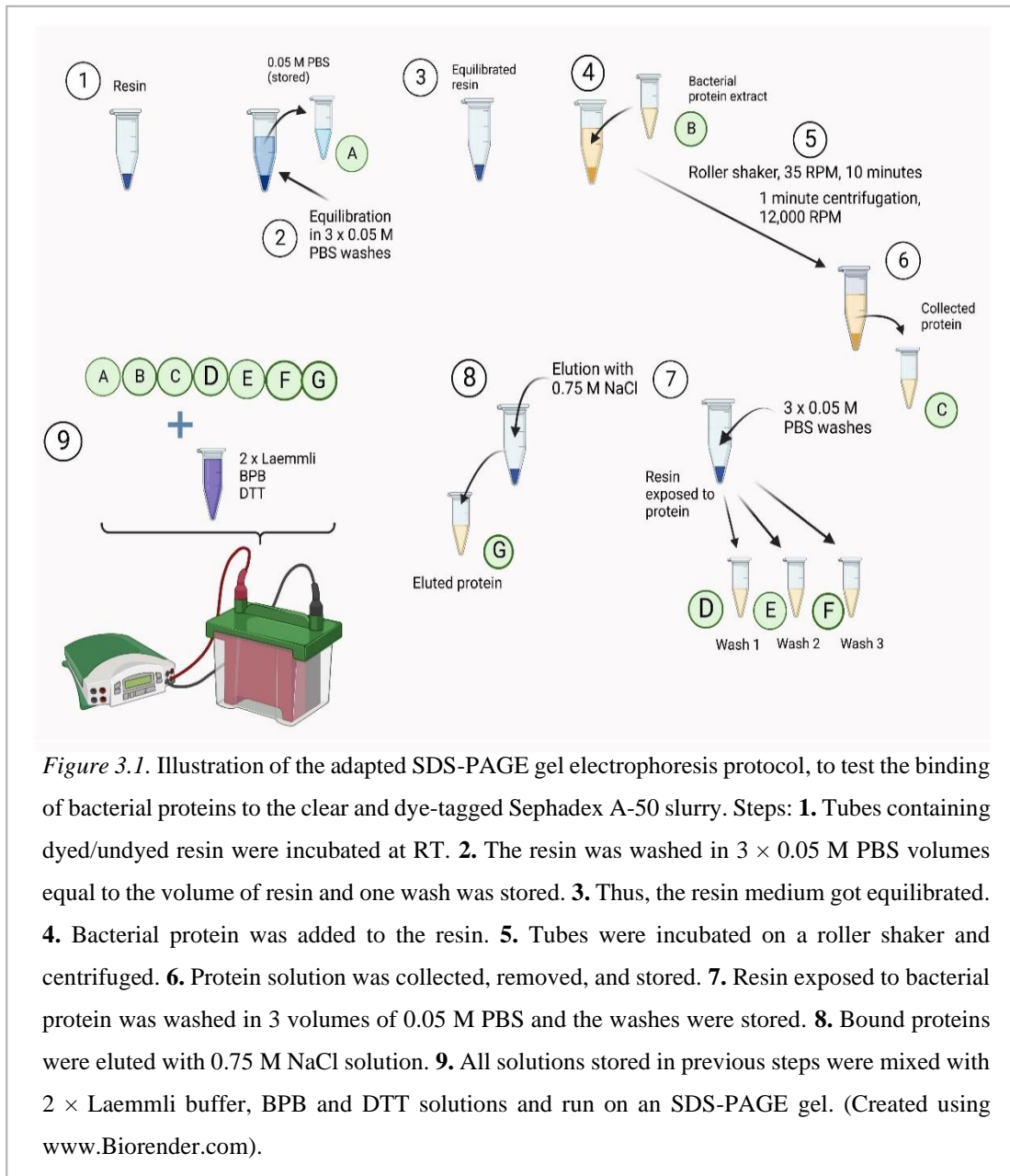
The bacterial protein extract was first diluted to approx. 10 mg/ml in 0.05 M PBS (see section 2.3 for extraction of bacterial protein), and left to incubate at RT for 30 minutes, along with clear and Procion dye-tagged DEAE Sephadex A-50 (see section 2.8 for preparation of clear and dye-tagged matrices). The following steps were repeated for each resin. A volume of 0.5 mL of slurry was added to a microcentrifuge tube and equilibrated in 3 volumes of 0.05 M PBS at RT. Beads were centrifuged at 12,000 RPM for 1 minute, removing and storing the supernatant (for controls). A volume of 0.5 mL of dilute protein mixture was added to the tube. Tubes were incubated on a roller shaker at 35 RPM and RT, for 10 minutes. Tubes were centrifuged, and the supernatant was collected. Unbound proteins were removed by 3 consecutive washes in 0.5 ml of 0.05 M PBS, vortexing tubes for 2 seconds after each wash, and storing the supernatant. Bound proteins were eluted with 0.5 mL of 0.75 M NaCl, ensuring collection of supernatant after each step. 75 μ L of a stock solution containing 940 μ L of 2 \times Laemmli buffer (10% (w/v) SDS –40% of the final volume (v/v), glycerol –20% of the final volume (v/v), 0.5 M Tris – HCl pH 6.8 – 24% of the final volume (v/v), distilled water – 16% of the final volume (v/v)) and 35 μ L of 1 M DTT were added to each tube collected in previous steps (including the controls). Samples were denatured at 95°C by incubation on a thermal block and were immediately placed on ice afterwards. 1 μ L of 100 \times BPB was added to 24 μ L of each sample and tubes were centrifuged briefly. SDS – PAGE gels measuring 1.5 mm in thickness were prepared, consisting of 12% acrylamide resolving gels and 4% acrylamide stacking gels. The SDS-PAGE gels were prepared according to the recipe in Table 3.1. A volume of 25 μ L of each sample was loaded on the gel, including 10 mg/mL bacterial protein control, the 0.05 M PBS control, along with 3 μ L of protein ladder (PageRuler™ Prestained Protein Ladder, Fisher Scientific, UK). The gel was allowed to run for approximately 2 hours at 100 mV, followed by a 1-2 h incubation on a shaker at 55 RPM in Coomassie Blue stain solution. The gel was then gradually destained in a solution containing 10% (v/v) glacial acetic acid and 20% (v/v) methanol, and imaged using the ChemiDoc™ Touch Imaging System (BioRad) (protocol illustrated in Figure 3.1).

The following protocol represents a modified version of the method defined by Yan (2019), initially described for quantifying bands' intensity on Western blots. In order to quantify SDS-PAGE gel protein bands' intensity, all gels' images were gathered in one JPG file, using the Image Lab (version 6.1) application. Individual gel images were edited, by modifying the brightness, sharpness and contrast; the file was then opened in the ImageJ software. The image's colours were first inverted using the appropriate software function; a box was drawn around the protein band of

interest using the cursor, and data was saved in a separate window by pressing the keys “Ctrl” + “M”. This combination of keys converts the colour intensity of the box of interest into a numerical value. The box was dragged along the gel until reaching the other band of interest, using the arrow keys, thus maintaining the box size; background data was also copied by dragging the box onto an area of the gel containing no bands, and numerical values were produced by repeating the previous step. The corresponding bands in the protein control (positive control) were copied for comparison. Data was copy-pasted into an excel sheet. Intensity of bands was calculated by subtracting the background value from the bands’ value. Relative bands’ intensity was calculated by dividing each of the numbers resulting from the previous step by the positive control’s value. Five protein bands were selected for analysis, based on intensity and differential binding pattern to the dyed and undyed resin. These bands are shown in Figure 3.2.

Table 3.1. SDS-PAGE gel recipe (for 1 gel)

Stacking gel – 4%		Resolving gel – 12%	
ProtoGel 30% (National Diagnostics, UK)	0.6 mL	ProtoGel 30% (National Diagnostics, UK)	4 mL
0.5 M Tris- HCl (pH 6.8)	1.25 mL	1.5 M Tris-HCl (pH 8.8)	2.5 mL
10% SDS	50 µL	10% SDS	100 µL
10% APS	25 µL	10% APS	100 µL
Distilled water	3.05 mL	Distilled water	3.3 mL
TEMED	5 µL	TEMED	10 µL



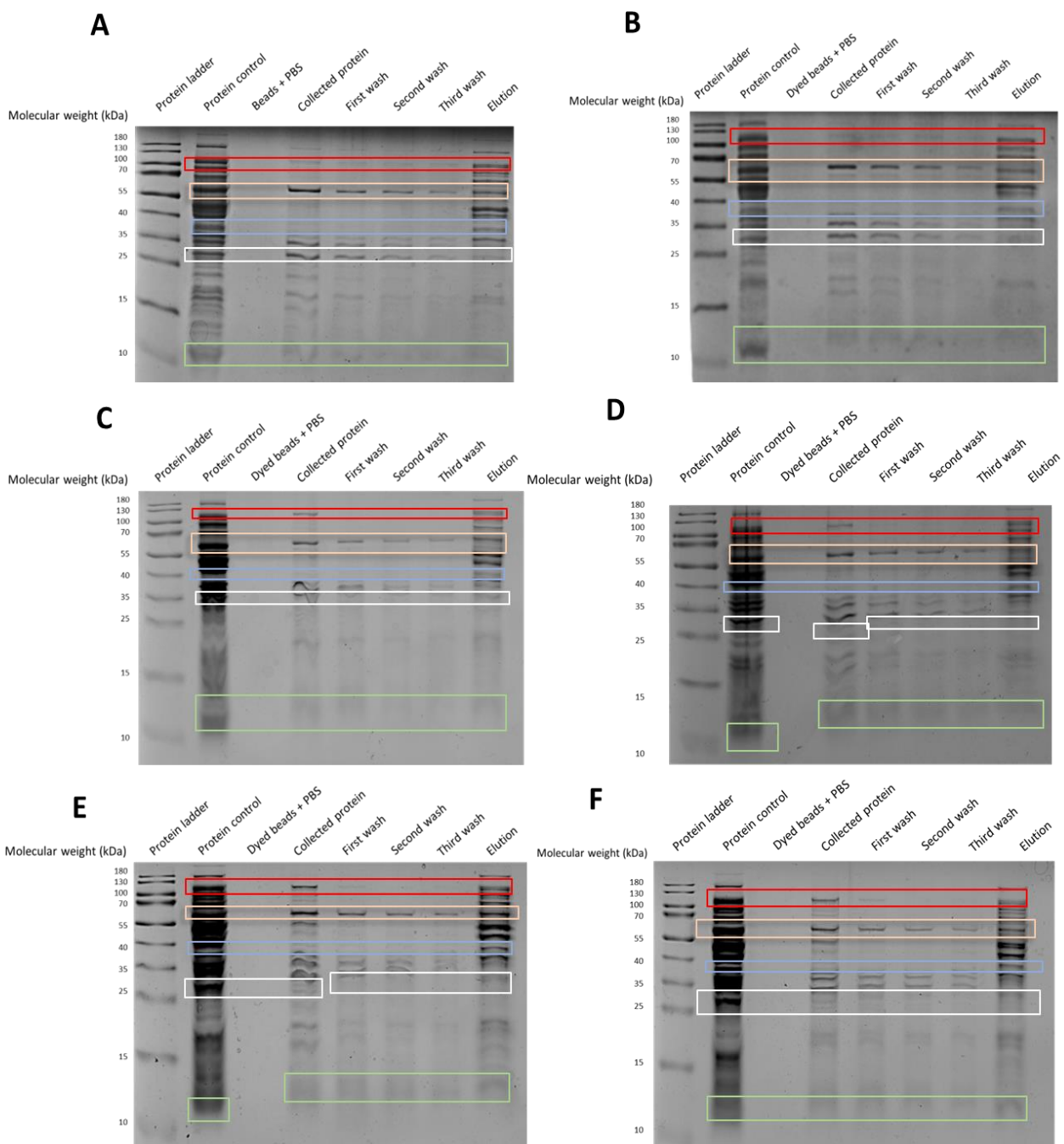
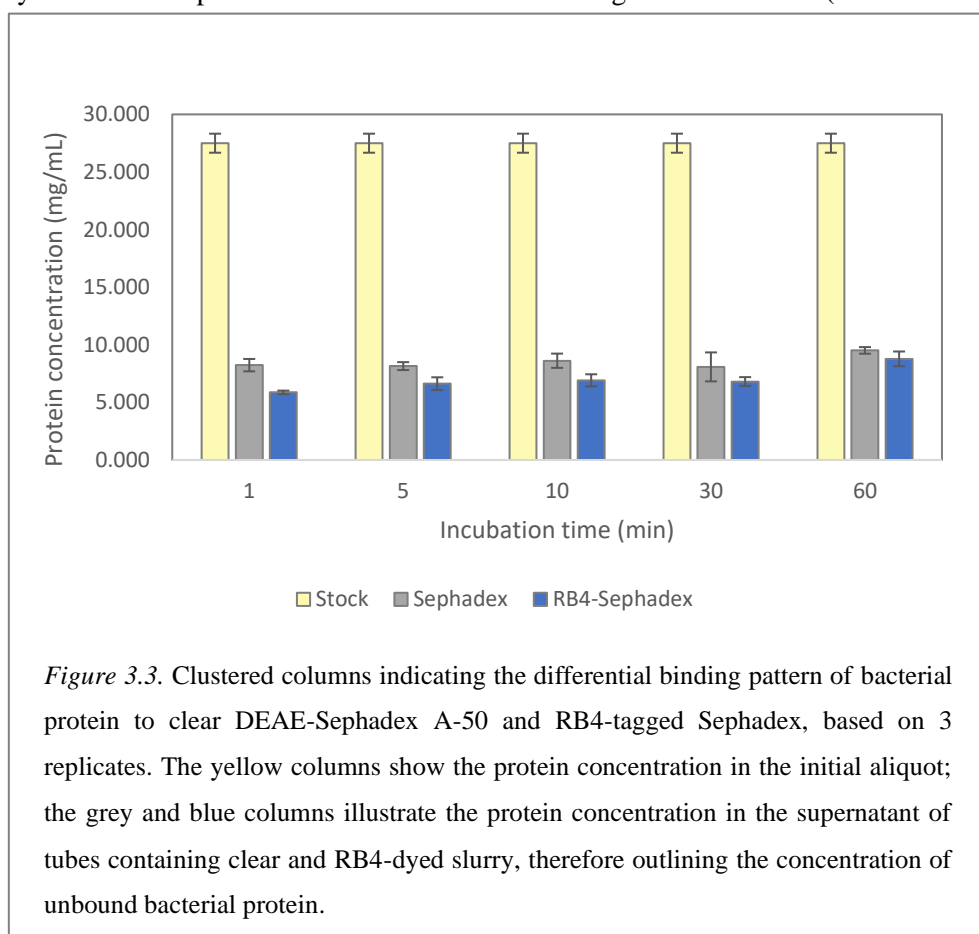


Figure 3.2. SDS-PAGE gels showing the binding pattern of bacterial proteins to the clear and dyed Sephadex slurry. Coloured boxes indicate the protein bands of interest, analysed using ImageJ. **A.** Clear Sephadex A-50; **B.** RB4-tagged resin; **C.** Red H-3BN-tagged resin; **D.** Yellow MX-4R-tagged resin; **E.** Orange MX-G-tagged resin; **F.** Red MX-5B-tagged resin. **Beige box:** Protein 1 (60 kDa); **Red:** Protein 2 (120 kDa); **Blue:** Protein 3 (40 kDa); **White:** Protein 4 (30 kDa); **Green:** Protein 5 (13 kDa). NOTE: Boxes only indicate the position of the bands of interest. These differ from the box areas drawn around the bands of interest for the analysis in ImageJ. Approximate protein sizes are specified.

3.2 Results

3.2.1 Testing the binding affinity of bacterial proteins to the Reactive Blue 4 dye

Data representing bacterial protein concentration in tubes where the protein mixture was incubated with clear and dye-tagged Sephadex A-50 was mainly normally distributed. It did not follow a normal distribution after 10 minutes of incubation with the clear resin, as indicated in Table 10.1 (appendix). Statistical analyses testing the differential binding of bacterial protein mixture to the undyed DEAE Sephadex A-50 and RB4-conjugated slurry are shown in Table 10.2 (appendix). These suggest that mean protein concentration was significantly different between the stock and the tubes containing clear and dyed resin after 1, 5, 30 and 60 minutes (P -values < 0.001). After 10 minutes of incubation, the difference between means was not significant (P -value = 0.081, Mann-Whitney test). It should be noted that for this incubation time (10 minutes), performance of a Kruskal-Wallis test resulted in a significant difference between protein concentration in the initial stock, in the supernatant of protein solution incubated with clear resin and that exposed to RB4-tagged Sephadex (P -value = 0.027). However, the Mann-Whitney post-hoc test conducted to identify the different pairs of means resulted in a non-significant P -value (P -value = 0.081). The



discrepancy may be due to the lack of sufficient statistical power of the non-parametric Mann-Whitney test. This could be a result of the very small sample size (three groups were tested). However, as a conclusive test result was not reached, the difference was considered insignificant.

Protein concentration was higher upon exposure to clear Sephadex A-50, in contrast to the tube where bacterial protein was exposed to RB4 slurry, at all incubation times (Figure 3.3). Mean protein concentration from all time points in tubes with clear resin was 8.519 mg/mL; thus, the overall decrease from the stock was 29.94%. In the case of RB4-tagged slurry, mean protein concentration was 6.999 mg/mL, meaning that the overall difference from the initial protein stock was equal to 25.45%. Therefore, the reduction in protein concentration was greater in the case of RB4-tagged slurry, in comparison to clear slurry. Comparison between incubation times indicated no significant difference between protein concentration upon exposure to clear resin (P-value = 0.159); however, the variation was significant upon exposure to RB4-tagged Sephadex A-50, where protein concentration was different after 60 minutes of incubation, compared to 1, 5, 10 and 30 minutes (P-value < 0.001, Table 10.3, appendix).

3.2.2 *Testing the affinity of bacterial proteins for the Procion dyes by SDS-PAGE gel electrophoresis*

Data describing the protein concentration of samples ready to run on the SDS-PAGE gels was normally distributed, as indicated by the results of Ryan-Joiner tests (Table 10.4, appendix). One-Way ANOVA tests comparing the mean protein concentration in each of these protein samples revealed a significant difference between proteins exposed to the six types of slurry. Differences were found between the following: “Collected protein”, “Wash 1”, “Wash 3” and “Elution” samples (P-values < 0.001), with no difference being observed between the “Wash 2” samples (P-value = 0.432). Details of the significantly different pairs of means are shown in Table 10.5 (appendix). In comparison to protein concentration data (Table 10.5), in the case of band intensity data (which is based on protein concentration) these were not significantly different between gels (Figure 10.7).

Figure 3.4 illustrates the protein concentration in samples containing bacterial protein mixture, prepared for running SDS-PAGE gels. The columns’ pattern shown in Figure 3.4 should be predictive of the pattern described by protein bands’ intensities in Figure 3.5. Thus, it should reflect the model described by the overall protein bands’ intensities shown in Figure 3.6. However, differences can be observed between the three figures. Consequently, bands’ intensities shown in Figure 3.6 are not visibly different from one another. However, data analysis revealed differences between these, for bands generated using samples washed and eluted from: clear resin (P-value =

0.003), Red H-3BN – slurry (P-value < 0.001), Orange MX-G – resin (P-value = 0.001) and Red MX-5B – slurry (P-value < 0.001). These are indicated in Figure 10.6 (appendix). In terms of statistical analyses of protein concentration data from Figure 3.4, the column describing the protein concentration in the control protein mixture is highly different from the rest of the samples i.e. “Collected”, “Wash 1”, “Wash 2”, “Wash 3” and “Elution” (P-values < 0.001, Table 10.6, appendix). Still, Table 10.6 and Figure 10.6 show different patterns. For example, intensity of bands produced based on the Yellow MX-4R – tagged resin and RB4 – tagged slurry are not different (Figure 10.6), whilst analysis of protein concentration data indicated highly different means for all matrices (Table 10.6).

Analysis of normalised relative intensity of bands was performed with two gel replicates per type of slurry (clear and dyed with one of the five dyes). Band intensity data was normally distributed, as resulting from the corresponding P-values of the Ryan-Joiner tests (P-values > 0.100, Table 10.7, appendix). The results of the One-Way ANOVA tests analysing the difference of mean bands intensity of Proteins 1 - 5, with Tukey’s comparison, are shown in Figures 10.1 – 10.5 (appendix). Almost all P-values were higher than 0.05, indicating no significant difference between bands’ intensities between samples. The six SDS-PAGE gels, produced using bacterial proteins washed and eluted from clear and dyed Sephadex A-50, are shown in Figure 3.5.

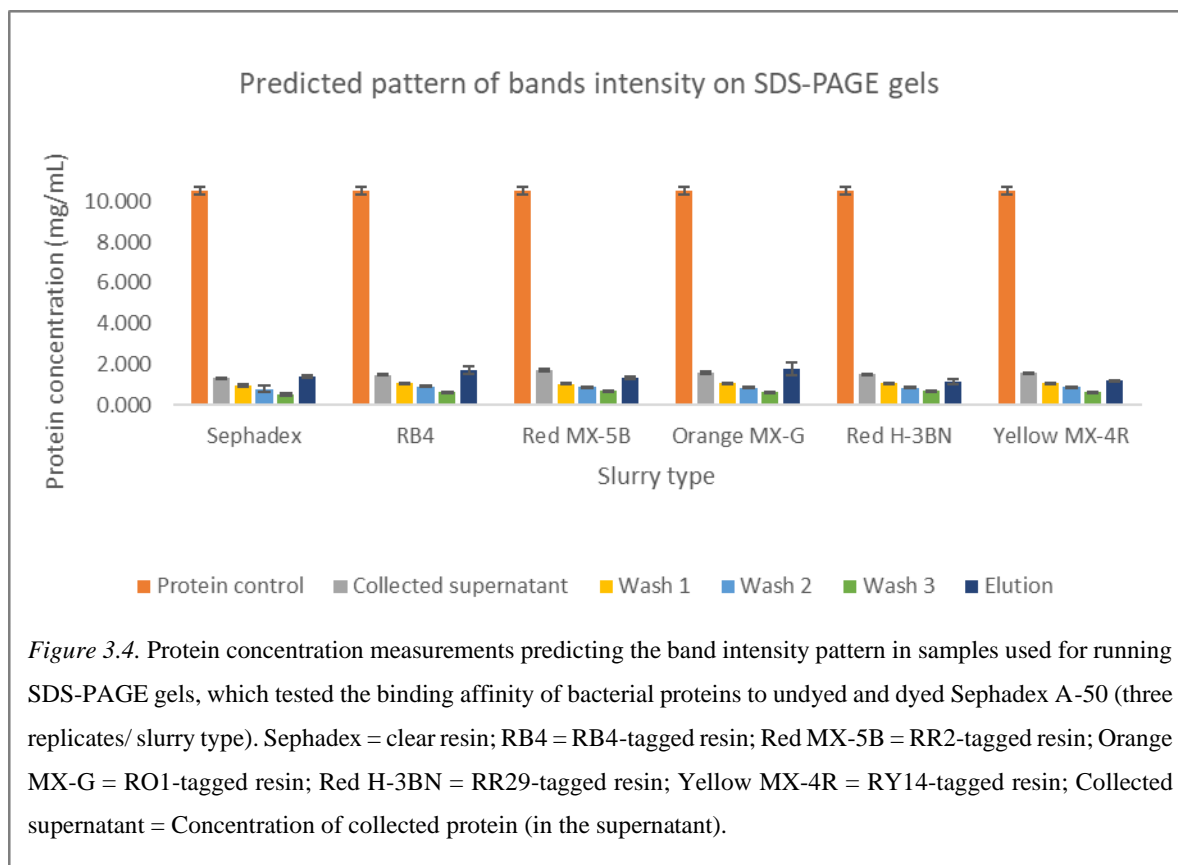
The resulting P-value of the ANOVA test run on “Elution” intensity data for Protein 1 was marginal, due to being close to the 0.05 cut-off (P-value = 0.055, Figure 10.1, appendix), where the difference of means between the RB4 gel (0.635521) and the Yellow MX-4R gel (0.4258) was nearly significantly different. No other differences between gel lanes were reported for Protein 1. In the case of Protein 5, bands’ intensities in the “Elution” lane were significantly different between the clear Sephadex and Red H-3BN gels (P-value = 0.05, Figure 10.5, appendix). No significant differences of bands’ intensities produced by the rest of the proteins (Proteins 2, 3 and 4) were recorded between the slurries (Figures 10. – 10.4).

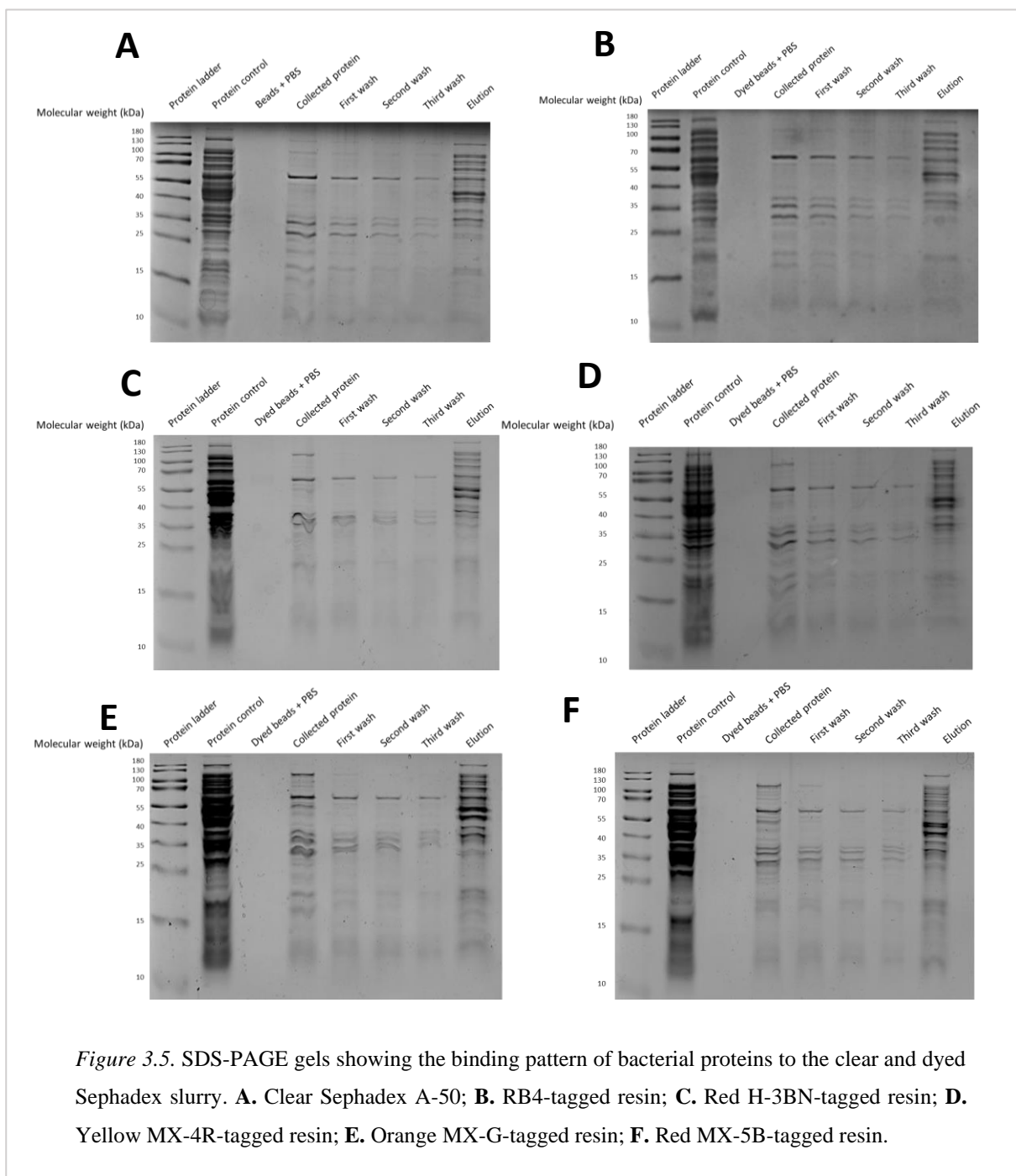
Figures 10.6 and 10.7 (appendix) illustrate the outcomes of One-Way ANOVA tests comparing the difference of mean band intensity data between whole protein lanes, located on the same gel or on various gels, respectively. Differences between whole lanes’ intensities were found between lanes corresponding to clear slurry, to Red H-3BN – slurry, to Orange MX-G – slurry and to Red MX-5B – slurry (Figure 10.6). Significantly different mean lanes’ intensities corresponding to the clear resin gel were found between the protein control and the PBS, negative control. For the gels lanes produced using the Red H-3BN and Orange MX-G dyes, the protein control, elution and PBS control lanes were found to be significantly different. In the case of protein lanes based on the Red MX – slurry, the protein positive control, elution, PBS control and the other lanes (collected protein,

wash 1, wash 2, wash 3) were significantly different. In the case of protein lanes' intensities compared between gels, no significant differences were found (Figure 10.7, appendix).

Figures 3.7 – 3.9 depict the intensity of a selection of five proteins, compared between the six SDS-PAGE gels, and thus the patterns described by individual protein bands in these figures are neater and more precise, in contrast to the pattern described by overall bands' intensity in Figure 3.6. All graphs shown in Figures 3.6 – 3.9 are modelled in a similar fashion, with the “Protein control” lane being the greatest in intensity, decreasing gradually across the washes and increasing again in the “Elution” lane, in most cases.

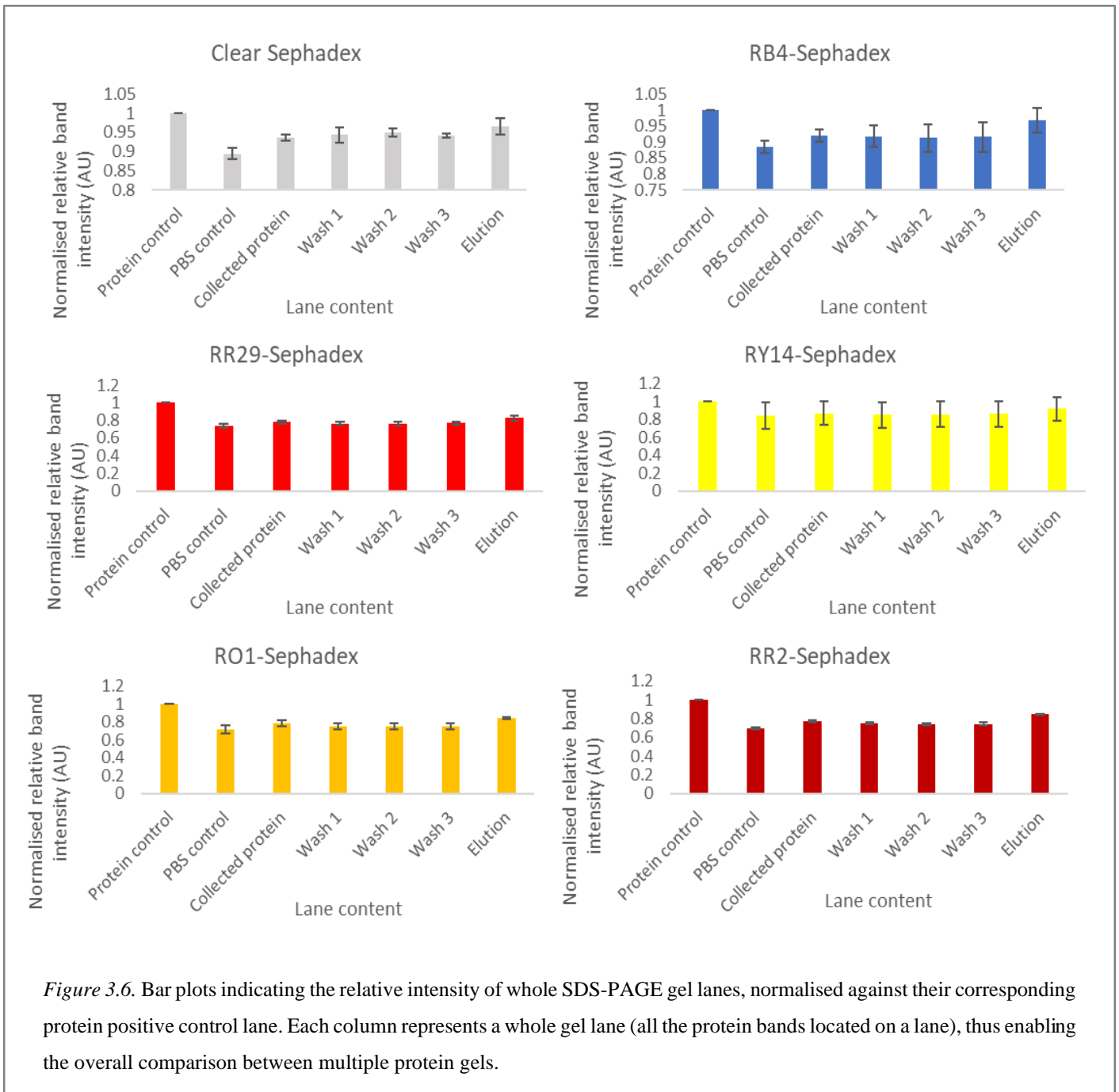
It should be noted that columns describing the bands' intensity of “PBS control” lanes appear to be quite high in some graphs e.g. Figure 3.7: Protein 2 – RY14 Sephadex: and Protein 2 – Clear Sephadex; Figure 3.8: Protein 3 – RY14 Sephadex; Figure 3.9: Protein 5 – RB4 Sephadex etc. Great differences between the bands' intensities corresponding to the “Wash 3” and “Elution” lanes have been observed in the case of Protein 1, 2, 3 and 4, bound to RB4, RY13, RR29, RO1, and RR2. In the case of Protein 5, the same differences were observed, with the exception of RY14 and RB4, where the bands' intensities did not vary greatly between the two lanes. In the case of clear Sephadex, the difference between lanes was not evident for the intensity of Proteins 2, 3, and 4, and almost unnoticeable for Proteins 1 and 5. In fact, the columns describing Protein 5's intensity on Clear Sephadex varied the least amongst all SDS-PAGE gels (Figures 3.7 – 3.9).





In terms of comparison of the bands' intensities produced by Proteins 1 – 5, variability was observed for the following samples: “Elution” from clear Sephadex, “Collected protein” and “Wash 1” from Red H-3BN, the first two washes from Orange MX-G and the three washes from Red MX-5B (Table 10.8, appendix). Table 10.9 (appendix) details the significantly different protein bands and which protein produced the most intense and the faintest bands, from those found to be significantly different in intensity, showed in Table 10.8. Protein 5 band eluted off Sephadex was the most intense, whilst Protein 3 band was the least intense. In the case of collected proteins from

Red H-3BN – slurry, Protein 1 produced the most intense band, whilst Protein 3 generated the faintest band. In fact, Protein 3 bands were found to be mostly faint in comparison to the rest of Proteins. In contrast, Protein 5 was found to produce the most intense protein bands in most cases.



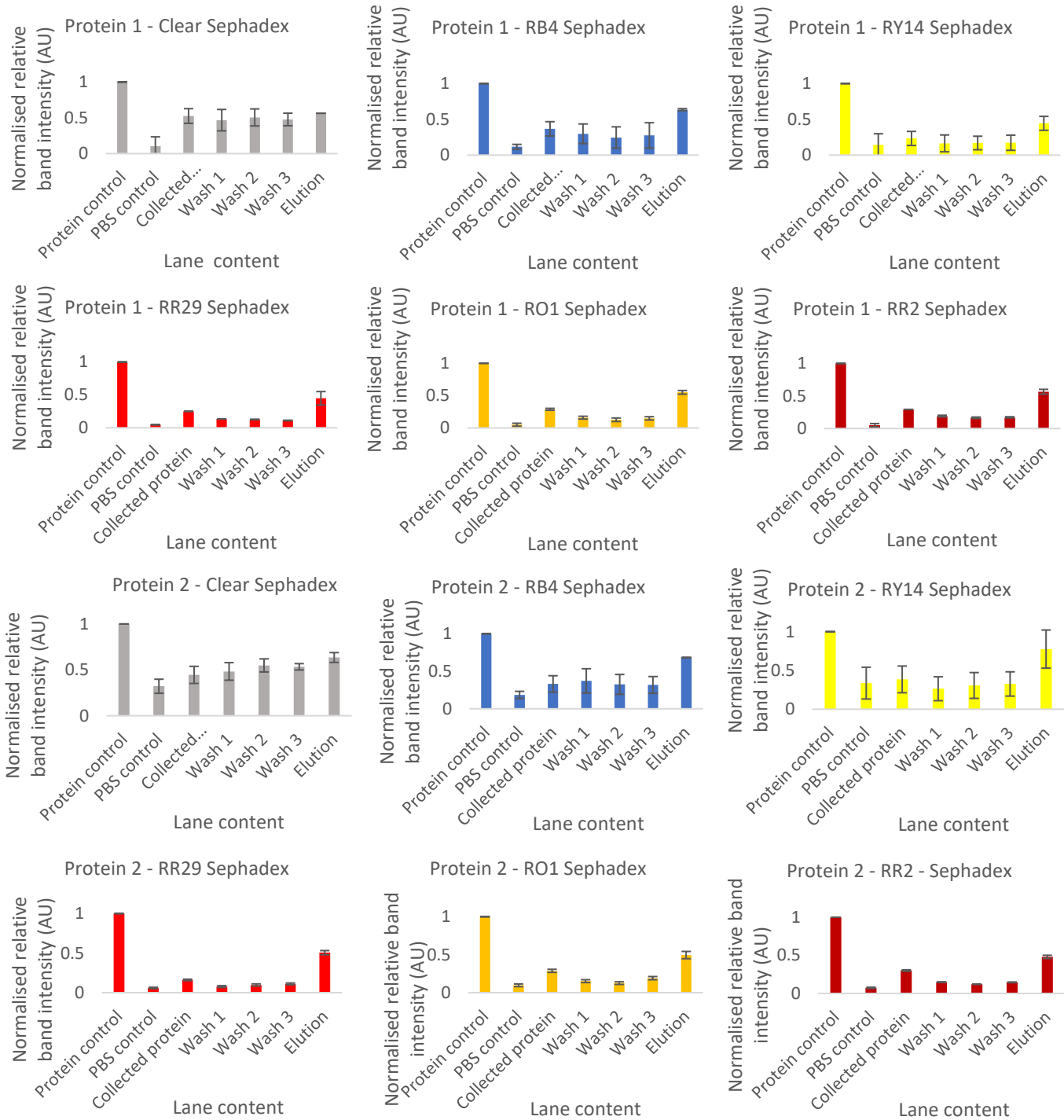


Figure 3.7. Bar plots indicating the relative bands intensity of Protein 1 and 2 in the lanes of all SDS-PAGE gels, normalised against their corresponding bands in the protein positive control lane.

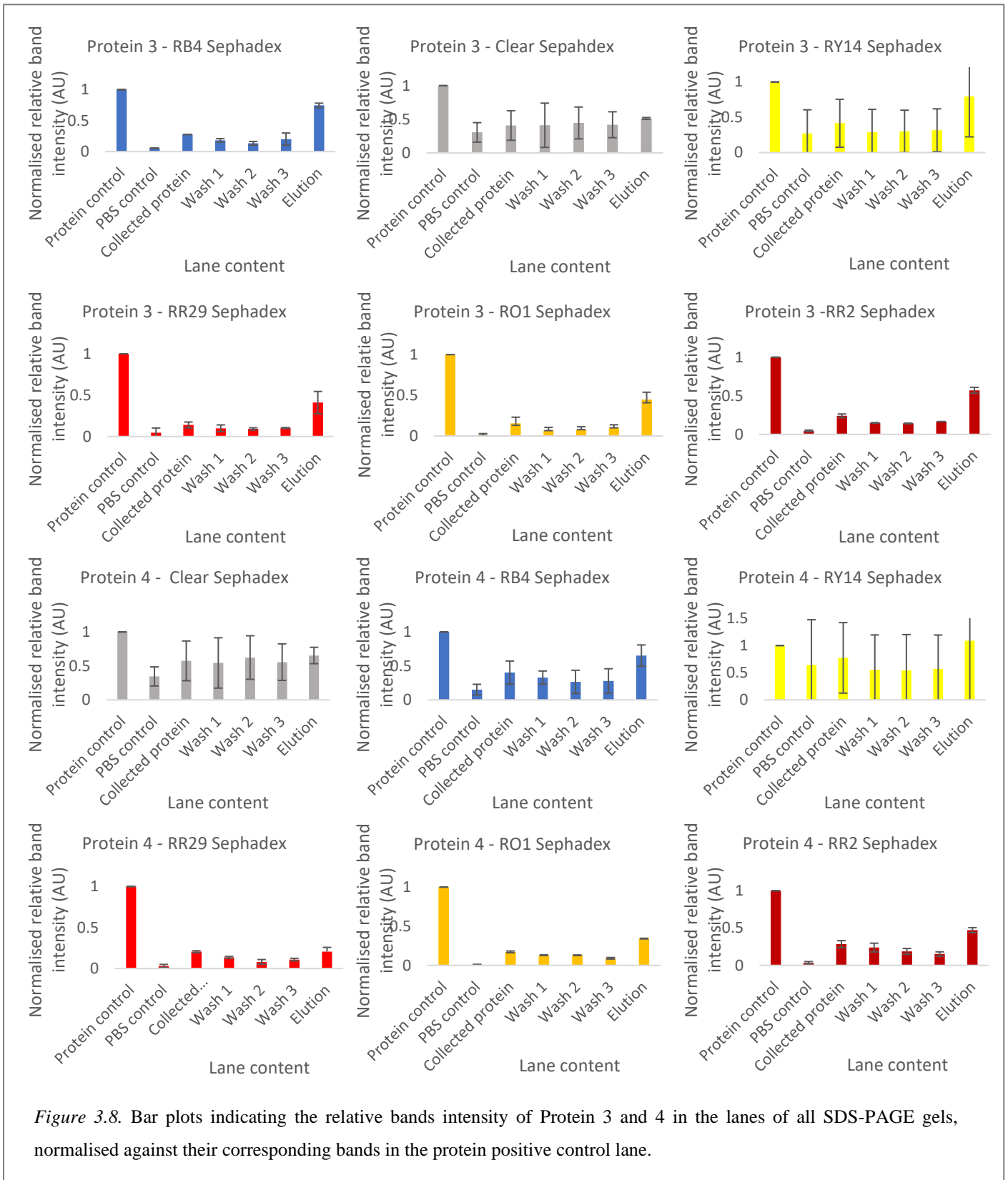
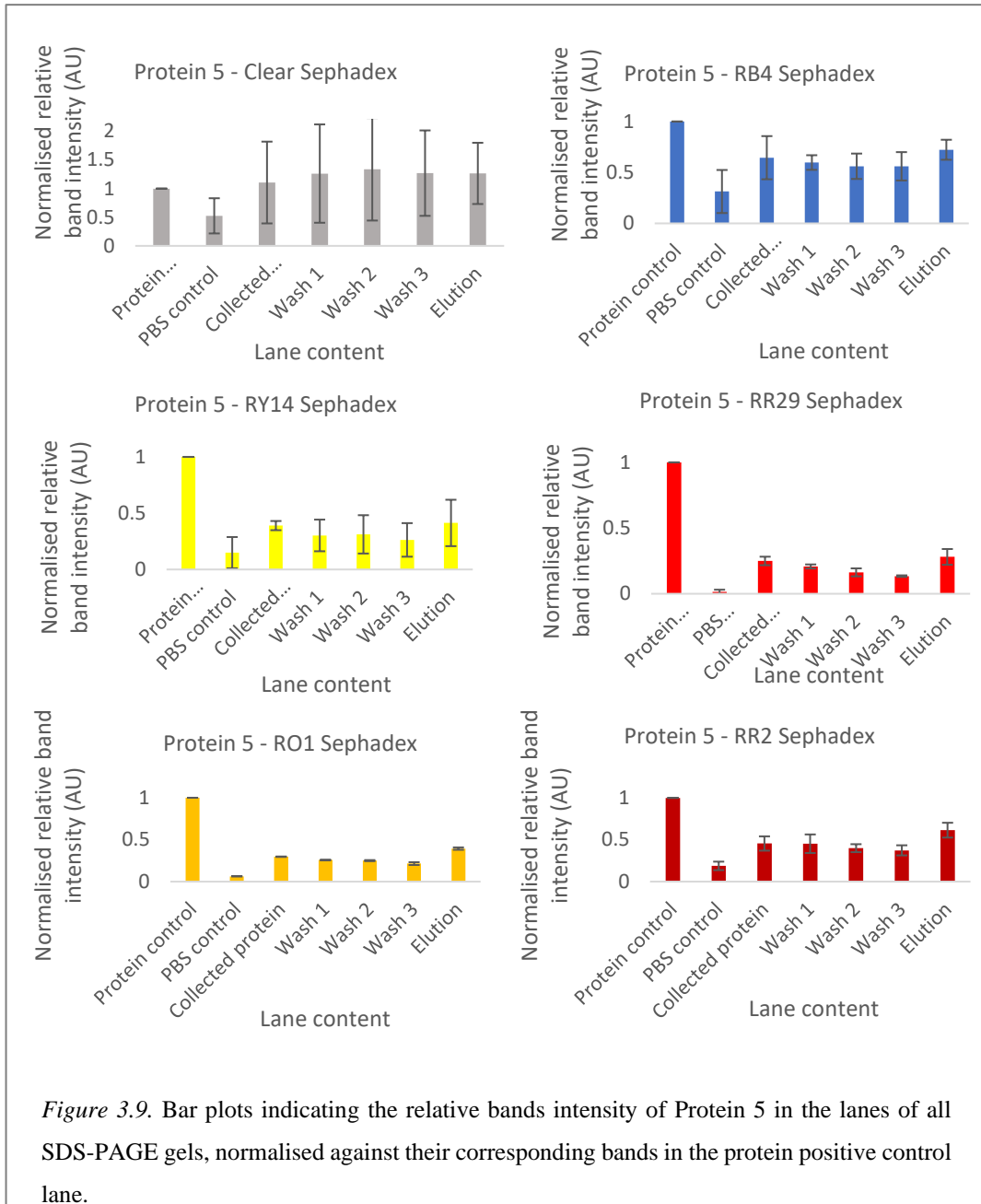


Figure 3.8. Bar plots indicating the relative bands intensity of Protein 3 and 4 in the lanes of all SDS-PAGE gels, normalised against their corresponding bands in the protein positive control lane.



3.3 Discussion

The present experiments tested the binding of a large array of bacterial proteins to five Procion dyes. Incubation of bacterial protein mixture with the undyed and RB4-conjugated Sephadex A-50 resulted in a remarkable decrease in protein concentration between the initial protein stock and the supernatant of tubes where protein had been exposed to the polysaccharide matrices. Table 10.2 (appendix) indicates that after 1 and 5 minutes of incubation the difference in protein concentration was recorded between the initial stock, the mixture incubated with clear resin and dyed resin. In these cases, protein concentration was significantly lower after exposure to the dyed beads, in comparison to the clear slurry, possibly suggesting superior binding due to the presence of RB4. After 10 minutes of incubation, no significant difference between the three was recorded. After 30 and 60 minutes, the difference was significant between the stock and the two types of matrices, but no differential binding was recorded between the two. This could indicate that initially proteins tend to bind to the dyed resin, but in time the interaction is weakened and some of the proteins gradually come off the dye.

In the case of changes in protein concentration upon exposure to clear resin, no differences were observed between the five incubation times, meaning that protein concentration stayed steady throughout. This may suggest that once proteins bind to the clear slurry, they do not come off easily. For the RB4-tagged resin, protein concentration was significantly different from the concentration recorded after 5, 10, 30 and 60 minutes, after 1 minute of exposure (Table 10.3, appendix). After 60 minutes, unbound protein concentration rose significantly in contrast to the one found after 1 minute of incubation. This may suggest that protein adsorption to RB4 is observed immediately after exposure, but this diminishes in time, resulting in some proteins detaching from the dye approximately an hour after exposure. Given the nature of the used resin, one could presume that the binding capacity exhibited by the dye-matrix conjugate is what leads to such a dramatic reduction in protein concentration, and not the RB4 itself. DEAE Sephadex A-50 represents a cross-linked dextran, weak anion exchanger with a high binding ability, where the ion exchanger is represented by the positively charged diethylaminoethyl group. The functional group binds to the negatively charged molecules it comes in contact with. Thus, these groups interact with negatively charged ions of the substance that is passed through the slurry, replacing the counter-ions (Agrawal and Goldstein, 1965; Cytiva, n.d.). In addition, a protein's electrical charge depends on its isoelectric point. Consequently, a protein is negatively charged above its isoelectric point, which enables the binding to anion exchangers, and positively charged below it (Jungbauer and Hahn, 2009). In this study, a protein extract consisting of the whole *E. coli* proteome was used, which implies that the binding ability to both clear and RB4-dyed Sephadex A-50 was specific to every protein, due to their unique characteristics.

Images illustrating the SDS-PAGE gels indicate that a large array of bacterial proteins bind to the five analysed Procion dyes. This statement is proved by the presence of bands of higher intensity in the “Elution” lanes, as opposed to the “Wash 1”, “Wash 2” and “Wash 3” lanes (Figures 3.5 – 3.9). Dyes have been used for the purification of enzymes and other proteins for many decades, the first one being Cibacron blue F3G-A, the chromophore of Blue Dextran, which selectively binds enzymes like pyruvate kinase, glutathione reductase and some factors involved in blood coagulation (Thompson *et al.*, 1975). The principle of dye-ligand chromatography relies on the biomimetic characteristic of the triazine dyes, which interact with proteins similarly to natural receptors binding target proteins. Baird *et al.* (1976) suggested that strongly acidic sulfonic groups within the dyes’ molecules are highly reactive and determine the binding of dyes to the protein substrate. On the other hand, Dudman and Bishop (1968) proposed that the dichlorotriazinyl group reacts with hydroxyl, amino and amide groups of the substrate. The structure of the dyes used here comprise either both sulfonic groups and chlorotriazine rings or $-SO_3H$ attached to the rings, which explains their high reactivity (Table 1.1). Proteins have been shown to have a high affinity for such dyes, thus scientists have preferred them to other affinity ligands, also for being particularly inexpensive at the beginning of the dye-ligand affinity chromatography era. In more recent years, their costs have increased on the science supply market, most likely as a result of the growing demand for their use in protein purification (Magdeldin and Moser, 2012; Baird *et al.*, 1976; Giuliano, 1992; Stellwagen, 1993; Stellwagen, 1995).

Protein concentration was found to vary significantly between wash and elution samples resulting from undyed and dyed matrices (Table 10.6, appendix). Thus, protein concentration in the “Protein control” sample was much higher than that in the “Elution” sample, in the case of all matrices, as shown in Figure 3.4. Unlike protein concentration values, data describing the overall bands intensity shown in Figure 3.6 (where one column is the equivalent of a whole protein lane) shows minimal differences between bands’ intensities in the “Protein control” and “Elution” lanes. Theoretically, it could be argued that the overall intensity of bands in the lane containing the positive protein control represents the “sum” of the bands’ intensities in all the other lanes. In practice, neither the pattern of measured protein concentration, nor that of the bands’ intensity could prove this affirmation in the present study (Figure 3.4, compared to Figures 3.5 and 3.6). There are multiple reasons which could explain this result. Firstly, using ImageJ for quantification of band intensity may not represent a highly accurate strategy to indicate the amount of protein represented by a protein gel band. Secondly, the equipment used for measuring protein concentration may not be sensitive enough. On one hand, using 2 μ l of sample for estimating total protein concentration in a sample is a good way to minimise sample waste while operating the DS-11 Spectrophotometer; on the other hand, such a low volume may be insufficient for a precise approximation, even when repeating measurements. This error was minimised by vortexing the sample-containing tube prior

to measuring protein concentration, although even this step cannot guarantee a perfectly homogenised solution. Yet, using a low volume overcomes the need to transfer the whole sample into a cuvette and measure protein concentration with a traditional spectrophotometer, which is prone to substantial sample loss.

Overall, all the SDS-PAGE gels' lanes followed a quite precise and neat pattern, with slight differences being observed between clear and dye-tagged DEAE Sephadex A-50 and between various dyes. Bands' intensities faded away gradually with each washing step and their strength increased dramatically after elution. This may provide good evidence that binding was strong enough to not be overcome by the salt content present in 0.05 M PBS (Figure 3.5). When using the ImageJ method for generating and analysing bands' intensity data, it is essential to divide the relative intensity of each band by the corresponding band intensity in the protein control lane. This way, a comparison between different gels can be made, as the intensity of each band is related to its positive control. If non-normalised band intensity data is used for analysis, only protein bands found on the same gel can be compared to one another.

The washing procedure represents a crucial step for the removal of any unbound proteins and is followed by the elution of bound molecules. Generally, such experiments are performed in chromatography columns and the washing is carried out with a 0.1 M salt solution, whilst the elution is performed using a 0.1 – 0.4 M salt gradient. DEAE Sephadex A-50 is a polysaccharide resin that should be mixed with and stored in saline solution, as per manufacturer's guidelines. Water should not be used, as it causes the beads to swell. In the present study, the resin was mixed and preserved in 0.1 M PBS. However, salt concentration in PBS is already quite high, measuring 137 mM NaCl, in addition to the presence of other salts, potassium chloride in a concentration of 2.7 mM and potassium dihydrogen phosphate, in a concentration of 1.5 mM (Gallant *et al.*, 2008; Thorat and Suryanarayanan, 2019). All of these components may have the ability to overcome the dye-protein complex bonds, leading to early elution of bound proteins. Here, washing was performed using a 0.05 M PBS solution, in order to satisfy two important needs: maintenance of true beads size, given by the presence of salt, while avoiding the premature elution of bound proteins. Addition of a 1 M NaCl solution to the dyed resin determined the dyes to "bleed off" the beads in a preliminary experiment. Therefore, a 0.75 M NaCl buffer was used to elute bound proteins.

Five protein bands have been compared between gels, in order to examine any differential protein binding patterns between the dyes and between dyed and clear resin. Thus, it was demonstrated that some proteins might have greater affinity for a particular dye, whilst being easily washed off others due to a lack of such structural compatibility. Also, the binding of some proteins is more evident to undyed resin in comparison to the dyed one. For example, statistical analysis of bands' intensities corresponding to Protein 5 indicated that these were not significantly different in

the “Collected protein”, “Wash 1”, “Wash 2” and “Wash 3” lanes, but were highly different in the “Elution” lane, when the comparison was made between all the SDS – PAGE gels (Figure 10.5, appendix). This difference was recorded between clear Sephadex and Red H-3BN-tagged slurry, where a greater amount of Protein 5 detached from the clear resin than from the dyed one, upon addition of 0.75 M NaCl. This finding may suggest that the binding affinity of Protein 5 was higher to the Red H-3BN dye in comparison to undyed slurry. Other slight differences between the six gels can be noted for the other four proteins, by just looking at the gel images shown in Figure 3.5; however, they are not statistically meaningful (Figures 10.1 – 10.4, appendix).

Analysis of differences between the intensity of bands produced by the five proteins within the same gels indicated some binding variability. For example, the band produced by Protein 5 in the “Elution” lane was the strongest from all the five proteins, whilst the faintest band in this lane was generated by Protein 3 (Table 10.8, appendix). This could suggest that Protein 3 bound better to the clear Sephadex in comparison to the other proteins. It also indicates that Protein 5 was eluted from the clear slurry the most easily, after addition of 0.75 M NaCl, suggesting a weak interaction between the clear beads and the protein. In fact, bands generated by Protein 5 were generally found to be the most intense of all; thus, the linkages formed between Protein 5 and the dyed resins were easily overcome by the addition of the washing or the eluting buffer, suggesting that the binding of this protein to the Procion dyes was the weakest of all. In contrast, Protein 3 bands in the “Collected protein”, “Wash 1” and “Wash 2” lanes had a more reduced intensity compared to the other proteins in gels based on samples washed off the Red H-3BN, Orange and Red MX-5B matrices, respectively. This could indicate that Protein 3 demonstrated superior binding to these dyes. However, Protein 3 was generally significantly different from Protein 5, but not different from Proteins 1, 2 and 4. For example, in the “Wash 1” lane on the SDS – PAGE gel based on the Orange MX-G slurry, Proteins 1, 2, 3 and 4 generated bands of similar intensity. This may suggest that the bonds they form with the orange dye are similar in strength. Additionally, on the gel based on the Red MX-5B dye, bands’ intensities in the “Wash 1” lane were similar for Proteins 5 and 4, and bands produced by Protein 1, 2 and 3 were similar to those of Protein 4, whilst being highly different from those of Protein 5. This could indicate that Protein 5 bound the least strongly to RR2, Protein 4 bound better to this dye, and Proteins 1 – 3 showed the strongest binding. The variability in binding could be explained by the fact that each proteins have different sizes, conformations, charge and binding affinity and capacity (Coskun, 2016).

Using a standardised internal protein control, like actin, as an alternative to using the total bacterial protein extract, may offer some advantages, including standardisation, normalisation and accurate quantification of the amount of protein binding to the clear and dye-conjugated Sephadex resin. Incorporating actin as an internal protein standard in each lane could provide a consistent reference point for comparison between lanes and between various gels, to account for various

procedural errors. Therefore, addition of a fixed volume of actin in each protein sample after sample collection (i.e. after performing the washing and elution steps) would help clarify if differences in bands' intensities between lanes are indeed an indication of protein binding and washing off the resin, or represent a result of loss of protein during gel loading. Moreover, intensity of various protein bands could be compared against the intensity of the actin band. However, if actin bands' intensity across lanes or gels differed when analysed by ImageJ, that could denote an operational or technical error, such as: variations in protein loading, lane cross-contamination/spillage, differences in gel composition, variable electrophoresis conditions (voltage, buffer composition, running time etc.).

Although using ImageJ for analysing bands intensity is not a definitive method for measuring protein concentration, it could provide some insights into the ways in which bacterial proteins bind to these dyes, by quantifying bands' intensities and comparing them against the protein-lacking background. Such a method presents many limitations. First of all, the size of the box drawn around the protein band of interest is important because it needs to be maintained throughout the whole process of collecting band intensity data. Accidentally clicking anywhere on the image opened in the application would cause the current box to disappear irreversibly. Therefore, the initial box size becomes lost, and the process must be started all over again, by drawing a new box. Preserving the same box size throughout is important in order to avoid any variability given by procedural errors, which is incredibly time consuming and meticulous.

The ImageJ method can sometimes be inconvenient because the box should be positioned identically among bands. Misplacing the box could generate different values and the comparison between bands would vary substantially. In addition, the box size should be universal for all the protein bands among all the gels. Some bands may have different dimensions, some can be longer, more streaked, and thus the box would not be large enough to enclose them. This size variability occurred quite often in these gels, probably due to residual detergent or scratches on the surface of the glass plates between which the gel is poured. Non-ionic detergents in household dish soap are generally not accepted for washing protein gel glass plates and should have been avoided. Also, vertical streaks occurred on the gel produced with protein samples washed off the Yellow MX-4R – tagged resin (Figure 3.5.D). These probably appeared due to loading a high protein mixture or due to protein-containing debris, such as skin flakes. Moreover, samples in the “Protein control” lanes were sticky, probably due to the presence of nucleic acids which tend to coagulate (Gallagher, 2012). All these could have affected the size of the protein bands. Thirdly, any minor protein cross-contamination that might occur while loading the samples into the wells can generate wrong values in ImageJ. Such spillage may not be visible with the naked eye, but can be easily picked up by the software and spoil bands' intensity in neighbouring lanes. For example, if any unwanted proteins ended up in the negative control lane (PBS) or in the protein ladder lane (usually, the empty spaces

between consecutive bands in the ladder lane have been used for background data), such fault would lead to numerical inaccuracies.

An automated protein purification system could not be used in the present experiment. Early attempts to perform a chromatographic run using such equipment, namely the AKTA Start Protein Purification System from Cytiva, have proved unsuccessful. AKTA protein purification systems represent great automated tools for the isolation of biomolecules and are extensively being used in laboratories all around the world (Yoo *et al.*, 2014; Gotesman *et al.*, 2022; Duranti *et al.*, 2021). However, the resin used in the present study was not compatible with the AKTA system. It has been observed that the overall protein binding pattern was not significantly different between the control (clear Sephadex) and the dye-tagged matrix. DEAE Sephadex A-50 is an anion exchanger and has been commonly used for the purification of enzymes for many decades (Miranda *et al.*, 1970; Nakamura *et al.*, 1974; Scawen *et al.*, 1983; Farag and Hassan, 2004). Usually, Procion dyes have been attached to neutral chromatography supports, such as Sepharose CL-2B, Sepharose CL-2D or cellulose (Roque and Lowe, 2008; Scawen *et al.*, 1983; Baird *et al.*, 1976; Lowe *et al.*, 1980; Dudman and Bishop, 1968), to minimise or even prevent any interaction that may occur between proteins and the matrix. However, many attempts to bind the dyes to such matrices have failed in the present study. Initially, Sepharose CL-2B and Sepharose CL-4B in suspension were washed thoroughly and the methods of Baird *et al.* (1976) and Scawen and colleagues (1983) were used for dyeing the polymers. Unfortunately, even after incubating the slurry with the Procion dyes for one week on the roller shaker, minimal binding was observed. Also, washing the unreacted dye with water led to dye removal from the resin. A later attempt to dye dry Sepharose 4B with RB4 was successful, but the amount of available resin was insufficient, and the time left until project completion was limited. Superior binding of dyes to the DEAE Sephadex A-50 slurry was observed from the beginning, and therefore it was used throughout the experiments.

The AKTA Start System has many features incorporated, including a screen monitoring the change in absorbance over time, a mixer for creating gradients, a peristaltic pump and glass columns, which are generally recommended for purification. The flow path is designed in a way that prevents the formation of air bubbles inside the slurry, thus preventing it from drying. Moreover, pre-installed automated purification methods allow easy handling of the sample, and the system does not need to be supervised during the run, thus saving time and effort (Cytiva Life Sciences, n.d.). Yet, in the current study it is unknown whether the binding of proteins was influenced to some extent by the ionic nature of the chosen resin. Thus, when using an equilibration buffer with an insufficient salt content on Sephadex A-50, the beads swelled considerably, increasing the pressure inside the column and blocking the flow path. Based on this observation, the experiment had to be carried out in tubes and plastic syringes, with improvised glass wool filters, therefore, many experimental aspects being difficult to control. Some of these include relying only

on gravity as driving force for running the sample through the column, because of lacking a peristaltic pump, using an improvised filter which may also interfere with the proteins, having to manually push the tubes rack to collect fractions, as well as having to count drops to ensure equal volumes in each fraction.

As a conclusion, the present chapter demonstrated that an extensive variety of *E. coli* β -10 proteins are able to bind to the five chosen Procion dyes. Analysis of the interaction patterns between five bacterial proteins and the coloured compounds indicated varying degrees of affinity. These five proteins bound differentially to RO1, RB4, RR2 and RR29. Proteins bound superiorly to RB4-tagged Sephadex A-50 than to clear resin. Despite not using an automated protein purification system, the aim of this section was eventually reached.

4. Testing the binding ability of nucleic acids to the Procion dyes

Obtaining highly pure nucleic acids is an essential first step for many subsequent molecular biology applications. Purification of nucleic acids is currently performed using various methods, such as ethanol precipitation, spin-column kits, or gel electrophoresis and band excision (Ali *et al.*, 2017; Zeugin and Hartley, 2985; Dehasque *et al.*, 2022; Cone, 2015). Here, we present a novel alternative for the purification of nucleic acids.

The present chapter researches the binding affinity of bacterial genomic DNA and RNA to clear and Procion RB4-tagged DEAE Sephadex A-50, by means of two experiments. The first experiment was a preliminary step performed to test if any interaction can occur between nucleic acids and the two types of slurry. This was carried out in microcentrifuge tubes, by monitoring the decrease in nucleic acid concentration upon exposure to Sephadex resin in time, without an elution phase.

As a result of obtaining a positive outcome, a second experiment was performed using traditional syringe columns. Clear resin and resin conjugated with the five Procion dyes were used as affinity matrices and the procedure involved binding, washing and elution steps, while collecting fractions.

Several studies have investigated the purification of DNA and RNA using chromatography matrices (Sander *et al.*, 1966; Bautz and Hall, 1962; Chandra *et al.*, 1992; Easton *et al.*, 2010; Holmes *et al.*, 1975). However, to this date, there are no known studies to have explored the affinity of nucleic acids to Procion dye-tagged resin.

4.1 Methods

4.1.1 Testing the binding of bacterial nucleic acids to the Reactive Blue 4 dye

Details on extraction of bacterial nucleic acids and preparation of dye-tagged resin can be found in sections 2.4, 2.5 and 2.8, respectively. Tubes containing clear DEAE Sephadex A-50 and Reactive Blue 4-tagged resin were incubated at RT. A volume of 200 μL from each slurry was added to microcentrifuge tubes, ensuring the preparation of 6 replicates for each resin. Bacterial RNA and DNA samples were thawed at RT for 30 minutes, and mixed by repetitive pipetting; nucleic acids concentrations were measured, using the DeNovix DS-11 Spectrophotometer/Fluorometer (DeNovix). A volume of 150 μL of DNA solution was added to 3 tubes containing clear Sephadex and 3 tubes containing dye-tagged slurry. Tubes were incubated on a roller shaker, at 35 RPM, for 1, 5, 10, 30 and 60 minutes. After each incubation, tubes were centrifuged at

maximum speed for 1 minute (Eppendorf Centrifuge 5424, Sigma-Aldrich), to allow beads to settle, and DNA concentration in the supernatant was measured. The procedure was repeated with RNA.

4.1.2 *DNA binding to clear and dye-tagged DEAE-Sephadex A-50 in columns*

This experiment was performed on traditional syringe columns (section 2.9), because the low salt concentration in the equilibrating buffer determined the Sephadex beads to swell, blocking the AKTA system's flow path. Dyed resin (section 2.8) was poured into a column and equilibrated by constant washing (2-3 CVs), with a 1:1 mix of 1× TE buffer and 0.1 M PBS, at pH 8, ensuring the removal of any unreacted dye. A volume of 2 ml of DNA was poured onto the column. Unbound DNA was removed by washing the slurry with minimum 2 CVs of the same buffer. Bound nucleic acids were eluted using minimum 1 CV of 0.75 M NaCl, collecting 1 ml fractions.

4.2 *Results*

4.2.1 *Testing the binding of bacterial nucleic acids to the Reactive Blue 4 dye*

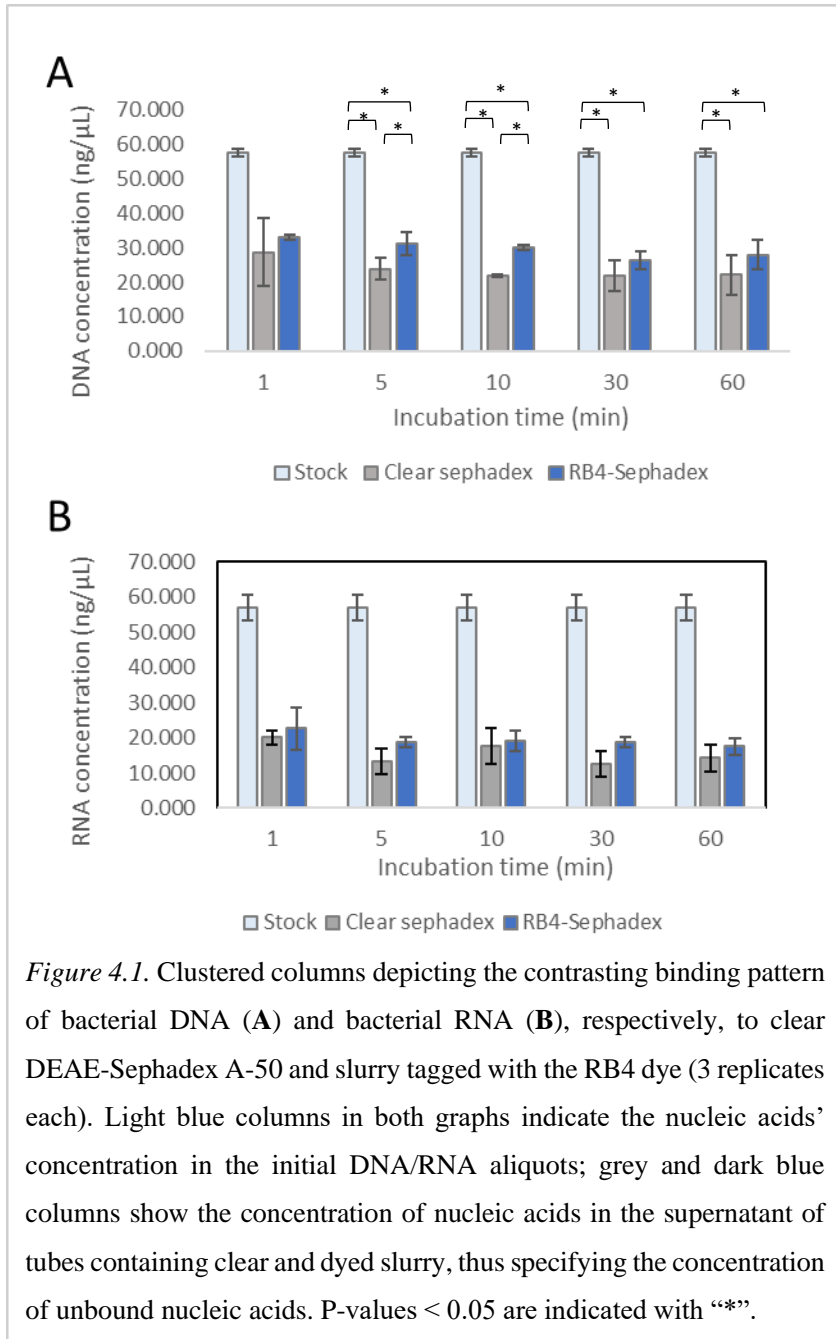
Data describing the initial concentration of DNA and RNA and the nucleic acid concentration which has not bound to clear and RB4-tagged Sephadex followed a normal distribution (Table 10.10, appendix). Concentration of unbound bacterial DNA exposed to clear and RB4-tagged Sephadex was significantly different from the concentration in the initial stock, after being incubated for 5, 10, 30 and 60 minutes (P-values < 0.001, Table 10.11, appendix). After 1 minute of incubation, the concentrations were not significantly different between the three (P-value = 0.061). Therefore, DNA concentration did not decrease substantially upon immediate exposure to clear or RB4 – tagged resin, a 5 – minute incubation being necessary for a relevant reduction to occur. After 5 and 10 minutes, DNA concentration differed significantly in tubes containing nucleic acid stock (control), dyed and clear resin, the lowest concentration being recorded upon interaction with clear resin. After 30 and 60 minutes of incubation, initial DNA concentration was significantly different from tubes containing dyed and clear slurry, but no notable variation was observed between resins.

Concentration of unbound bacterial RNA, after exposure to clear and RB4 slurry, was not significantly different after 1 (P-value = 0.066), 5 and 30 minutes (P-values = 0.027 by Kruskal-Wallis test, infirmed by post-hoc Mann-Whitney test with resulting P-value = 0.081). Also, no

different means were recorded after 10 (P-value = 0.061) and 60 minutes of incubation (P-value = 0.051), indicated in Table 10.11 (appendix).

Comparisons between the five incubation times revealed no significant difference in the concentration of DNA bound to clear resin (P-value = 0.483) and RB4-dyed resin (P-value = 0.087). In the case of RNA, concentration of unbound nucleic acids did not vary significantly between the five incubation times for clear Sephadex (P-value = 0.199) and RB4 slurry (P-value = 0.463), as shown in Table 10.12 (appendix).

In the case of gDNA, the mean overall decrease in concentration between the stock and the supernatant of clear Sephadex among all incubation times was 33.87 ng/ μ L equalling 58.82%, whilst the difference between the stock and the supernatant of RB4-Sephadex was 27.86 ng/ μ L, representing a 48.40% reduction in concentration (Figure 4.1.A). For bacterial RNA, the mean overall decline in concentration between the initial stock and the tube containing clear resin, considering all incubation times, was 42.04 ng/ μ L, meaning that a 72.69% fall in nucleic acids concentration occurred on the whole. In the case of RNA exposed to RB4-tagged slurry, the variation between the stock and the supernatant of tubes containing dye-conjugated slurry was 65.96% or 37.52 ng/ μ L of RNA (Figure 4.1.B).



4.2.2 DNA binding to clear and dye-tagged DEAE-Sephadex A-50 in columns

Data specifying the DNA concentration in fractions washed and eluted from clear and Procion dye-tagged DEAE Sephadex A-50 was distributed normally (Table 10.13, appendix). It is important to mention that these DNA concentrations are expressed as percentage values of the initial DNA concentration in the aliquot used for chromatography, not as absolute values. DNA concentration in processed aliquots was different for each resin. Consequently, the conversion from absolute to

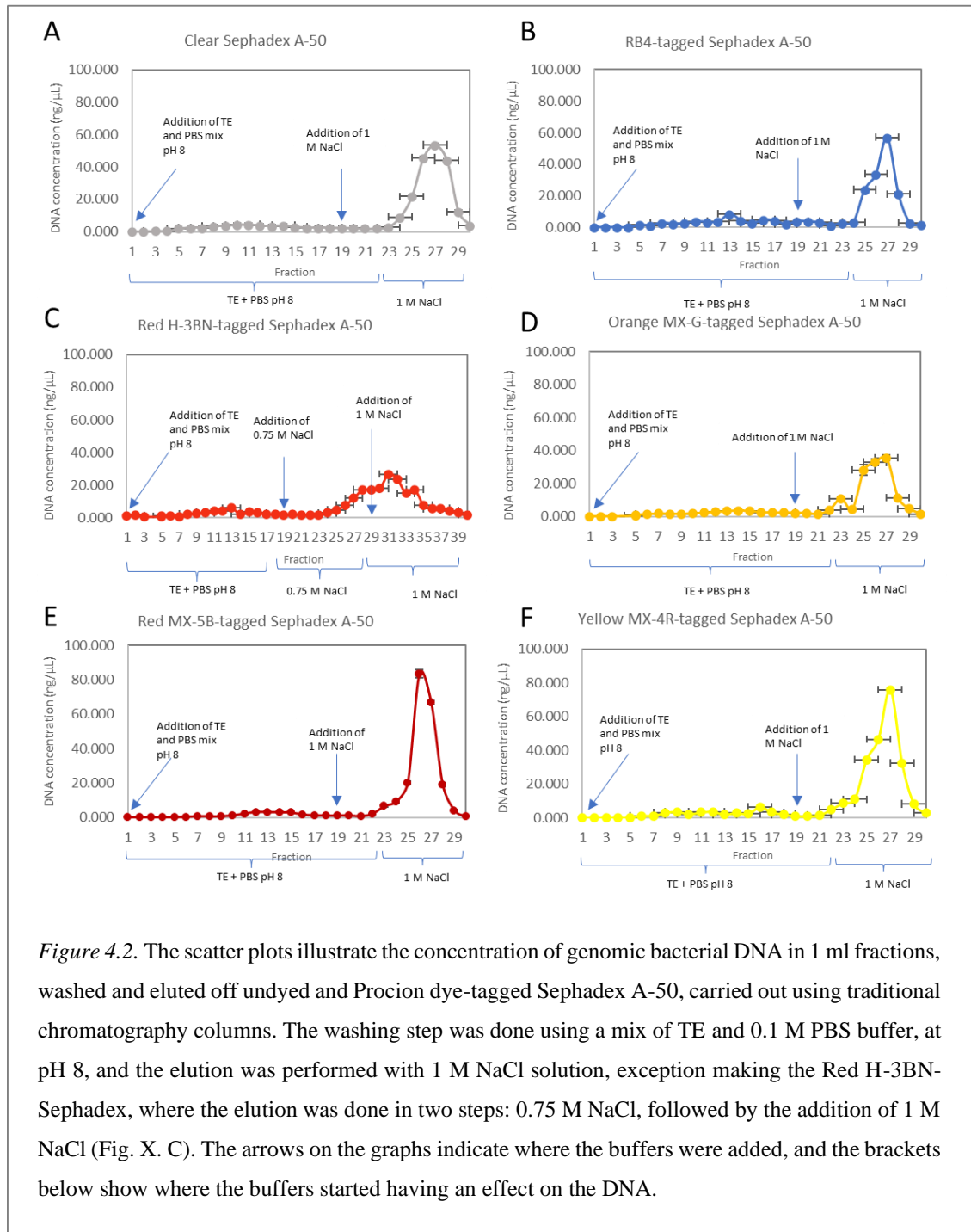


Figure 4.2. The scatter plots illustrate the concentration of genomic bacterial DNA in 1 ml fractions, washed and eluted off undyed and Procion dye-tagged Sephadex A-50, carried out using traditional chromatography columns. The washing step was done using a mix of TE and 0.1 M PBS buffer, at pH 8, and the elution was performed with 1 M NaCl solution, exception making the Red H-3BN-Sephadex, where the elution was done in two steps: 0.75 M NaCl, followed by the addition of 1 M NaCl (Fig. X. C). The arrows on the graphs indicate where the buffers were added, and the brackets below show where the buffers started having an effect on the DNA.

relative values was necessary to compare fractions eluted from various resins. Absolute values can be found in Table 10.14 (appendix).

One-Way ANOVA tests indicated significant differences between the mean bacterial DNA concentration in corresponding chromatography fractions, eluted from clear DEAE Sephadex A-50 and the resin conjugated with the five Procion dyes. Complete statistical analyses with associated P-values and the outcome of Tukey's post-hoc tests are indicated in Table 10.15 (appendix). It should be noted that 40 fractions were collected for the Red H-3BN – tagged slurry, whilst only 30 fractions were obtained from resin dyed with the other four dyes. Therefore, only fractions 1 – 30 were compared against one another.

The highest DNA concentration off all fractions shown in Figure 4.2 was recorded in fraction 26, eluted from Red MX-5B – tagged resin (83.410 ng/μl). However, initial DNA concentration in the aliquot used for this run was 242.627 ng/μl and other aliquots had a higher concentration e.g. the aliquot run on RB4 slurry, where the initial DNA concentration was 349.864 ng/μl (Figure 4.2.F). In the case of Red MX-5B, 97% of the initial DNA was recovered, as the sum of concentrations in all fractions was 235.673 ng/μl. For RB4, only 207.491 ng/μl were recovered (59%). The second highest peak was produced by the nucleic acid concentration in fraction 27, eluted from Yellow MX-4R – dyed slurry (Figure 4.2.E). Initial DNA concentration run on the yellow resin was 249.793 ng/μl, with complete recovery. In the case of bacterial DNA run on Orange MX-G – Sephadex, the initial concentration was quite high, equalling 311.120 ng/μl, but the highest peak located on the specific graph (Figure 4.2.D) was relatively low in comparison to the other dyes, equalling only 35.679 ng/μl. However, this could be the case because another smaller peak had been produced earlier, by fraction 23, where DNA concentration was 10.894 ng/μl. Also, total concentration of recovered DNA was 170.568 ng/μl, which is about half of the initial amount (almost 55%). DNA concentration in fractions 11, 12, 14, 18, 28 and others was found to be the highest when washed from the clear slurry, in comparison to dye – tagged resin.

For Red H-3BN – tagged slurry, the peak corresponded to fraction 31, with a DNA concentration of only 26.737 ng/μl, as a result of the addition of 1 M NaCl solution (Figure 12.C). Nonetheless, this graph contained the highest number of peaks, in fractions 13, 15, 27, 31 and 34. High amounts of DNA were lost throughout the chromatographic run, as the initial DNA concentration was high, equalling 317.800 ng/μl. In addition, elution was performed in two steps, firstly starting at fraction 25, using 0.75 M NaCl, and secondly, starting at fraction 31, with 1 M salt solution. Total recovered DNA was only 243.165 ng/μl (77%).

4.3 Discussion

4.3.1 Testing the binding of bacterial nucleic acids to the Reactive Blue 4 dye

This chapter examined the binding of bacterial nucleic acids to five Procion dyes. Bacterial gDNA behaved differently when exposed to undyed and dyed Sephadex A-50 beads (Figure 4.1). The observed binding pattern to the two types of resin may outline that initially DNA forms stronger interactions with clear Sephadex in comparison to dye-tagged slurry. This could indicate that the presence of dye may restrict the binding of DNA to the beads, between 5 – 10 minutes of incubation. It should still be noted that there is a significant decrease from the concentration of DNA present in the initial stock, but RB4 does not contribute to superior DNA binding, in comparison to the Sephadex beads alone. In time (30 to 60 minutes), differences in binding between the two resins became insignificant. Also, the decrease in DNA concentration in both tubes containing clear and dyed slurry did not vary significantly from one incubation time to another suggesting that the variation may be attributed to random chance.

For bacterial RNA, reduction in concentration from the initial stock was not evident after exposure to either clear or dye-tagged resin throughout the 60 minutes period of incubation. However, due to the small sample size ($N = 3$) and not-normally distributed RNA concentration data in the initial aliquot, a non-parametric test was conducted. These types of tests are known to have lower statistical sensitivity in comparison to parametric tests, with great chance of producing false-negative results (Sedgwick, 2015). Regarding the observed RNA binding pattern to the beads, this could be caused by randomness, as no significant interaction was observed throughout the 60 minutes incubation period.

Overall, reduction in nucleic acids concentration from the initial stock was greater in the case of RNA in comparison to DNA, upon exposure to both clear and RB4 – tagged slurry (see section 4.2.1). This finding could suggest that bacterial RNA may bind better to both undyed and dyed Sephadex beads in contrast to DNA. In other words, Sephadex and RB4 – tagged Sephadex may have a greater binding capacity to RNA than to DNA, meaning that larger amounts of RNA can attach to these beads. Double stranded genomic DNA contains a sugar called deoxyribose, consisting of a hydrogen attached to the second carbon in the pentose ring, whilst single – stranded RNA contains ribose, which consists of an extra -OH functional group, in comparison to its counterpart. The presence of a reactive hydroxyl group in the RNA molecule makes it more reactive than DNA. Moreover, RNA contains the uracil base, lacking a methyl, whilst DNA comprises thymine in its structure, to which a methyl group is attached. Methyl groups are typically unreactive,

therefore their presence on the thymine base determines more stability in the DNA molecule in comparison to the RNA one (Burge *et al.*, 2006; Alberts *et al.*, 2002; Klecker and Nair, 2017).

4.3.2 DNA binding to clear and dye-tagged DEAE-Sephadex A-50 in columns

Figure 4.2 displays the bacterial DNA washing and elution steps from clear and dye-tagged chromatography matrices, where DNA concentration measurements represent absolute values. First DNA elution off the dye-conjugated chromatography resin was performed using Procion Red H-3BN. Elution was performed in two steps, using 0.75 M NaCl and 1 M NaCl (Figure 4.2.C), just as a preliminary test of the effect of various salt molarities on the dye-bound DNA. Thus, more fractions were collected. Upon addition of 1 M NaCl, residual nucleic acid came off the chromatography column, proving that the higher salt molarity was superior in eluting the DNA. Therefore, 1 M NaCl was used in subsequent experiments.

Despite running equal volumes of DNA on each type of resin (2 mL aliquots), the DNA concentration varied among aliquots, due to performing chromatography runs on different days. Thus, the amount of DNA concentration in each fraction had to be converted to a percentage value of the concentration in the initial aliquot, used for the chromatographic run. By using relative values as opposed to absolute values, a comparison between corresponding fractions was possible.

Mean nucleic acid concentrations were significantly different amongst all corresponding fractions of different matrices. The most notable difference between resins was observed in case of fraction number 27. In the case of RR29-tagged Sephadex, these differences are most likely a consequence of using a different salt molarity (0.75 M NaCl solution), in comparison to the other resins (1 M NaCl solution). However, these findings could suggest that DNA may bind better to Red H-3BN and Orange MX-G, in contrast to Yellow MX-4R.

Highly different means were observed between slurries in the case of fractions 26 and 27, probably due to the differential effect of 1 M salt on the strength of DNA – dye linkages (Table 10.14, appendix). Thus, one could hypothesise that the high amount of nucleic acid coming off RR2-resin in fractions 26 (34.378%) and 27 (27.520%) may suggest that the DNA-dye bond was more easily overcome by the addition of 1 M NaCl in the case of Red MX-5B, as opposed to other dyes. This may be a potential indication of a weak chemical bond. Fraction 26 coming off the RB4 – resin contained the lowest DNA concentration of all corresponding tubes, equalling 9.678% (not considering fraction 26 produced by the elution from Red – H-3BN, as this included a two-step elution). Also, the total amount of recovered DNA was only 59.306% in the case of RB4 – resin, which could potentially indicate a strong affinity of bacterial DNA to the RB4 dye. The same pattern

was observed in the case of Orange MX-G, where only 54.824% of the initial DNA was recovered. Similarly, unpublished data of Michael Comer (Comer, personal communication) indicated a superior affinity of the enzyme glycerol kinase to RO1, in comparison to other dyes, such as Procion Yellow MX-R, Red H-3B, Blue H7-GS and Cibacron blue F3G-A. In his case, elution was performed using a solution containing adenosine triphosphate and magnesium chloride. In contrast to Comer's findings, Baird *et al.* (1976) reported low adsorption of carboxypeptidase G on RO1-Sephadex 4B conjugates, with better enzyme binding in case of Procion Blue MX-R (Reactive Blue 4). Such contrasting results could arise from the major structural differences between the molecules of DNA and those of proteins, where the nucleic acids may be exposing various other potential binding sites. In addition, DNA has an overall negative charge, conferring it a superior binding capacity to the cationic Sephadex beads, whilst the electrical charge varies from one protein to another, depending on its amino acid composition (Yamasaki *et al.*, 2001; Schasfoort *et al.*, 1990).

DNA concentration in some fractions eluted from undyed Sephadex was found to be higher in comparison to corresponding fractions in the case of dyed resin. Additionally, DNA concentration was never found to be the lowest amongst corresponding fractions. This finding could suggest that washing DNA off the clear resin led to easy detachment. In other words, it could be hypothesised that generally DNA bound superiorly to the dyes than to the undyed matrix. Insoluble polymeric supports have been used in the past for the chromatography of nucleotides, such as thymidylate-cellulose matrix, complementary strands of nucleic acids bound to cellulose or Sephadex, but no studies investigating the binding of double stranded DNA to dyed chromatographic resins were found (Sander *et al.*, 1966; Bautz and Hall, 1962; Chandra *et al.*, 1992). Thus, the present findings suggest that Procion dyes immobilised on inert chromatography matrices may provide a novel strategy for the purification of DNA.

The structure of double stranded DNA comprises the major and minor grooves. DNA binding sites represent short sequences that proteins or enzymes attach to, with varying degrees of affinity. Proteins interact with DNA more easily via the major groove, which exposes the nucleotides' edges, thus enabling proteins to recognise specific DNA sequences. The phosphate-ribose groups form the backbone of the DNA molecule, conferring it its overall negative charge. Procion dyes are known to be negatively charged as well, resulting from the presence of sulfonic groups, which should theoretically inhibit their interaction with DNA. However, the present experiment demonstrated that bacterial DNA bound to the dyes, as elution required the addition of a high-concentration salt buffer. Therefore, it could be hypothesised that the binding of DNA to the Procion dyes occurs in a similar fashion as the protein-DNA binding interactions. Thus, such binding may rather be a result of geometrical complementarity due to the chemical conformation of DNA, rather than to

electrochemical interactions (Ades and Sauer, 1995; Meng and Ducho, 2018; Maffeo *et al.*, 2014; Rahman *et al.*, 2013).

It is arguable that DNA was present in the first few fractions collected from the RR29-slurry. These spectrophotometer readings could have resulted from the presence of other molecules, which can also absorb light at this wavelength. These molecules could have originated from the initial DNA aliquot, as well as from the glass wool filter. In fact, this observation could apply to many other fractions. For example, the total amount of recovered DNA from RY14-tagged slurry was 106.13% of the initial concentration, which is clearly an error. The use of qualitative chromatography filters and sensitive automated purification equipment is essential for the isolation of various macromolecules in many industries (Labrou, 2014). However, the aim of the present experiment was to prove a concept, rather than produce highly pure nucleic acids, and this specific target was eventually reached by using an improvised chromatography system. Nevertheless, these experiments should be repeated multiple times, using a larger number of replicates to confirm the results.

Therefore, these experiments provided a basis of evidence that bacterial nucleic acids bind to the choice of Procion dyes. Double stranded DNA and RNA were found to bind in different manners to both clear and dye-tagged matrices, possibly indicating various degrees of affinity. However, the small sample size cannot guarantee the validity of the present findings.

5. Testing the binding of phage to the Procion dyes

The emergence of the COVID-19 pandemic has emphasised the need for scientific research into ways to limit the spread of transmissible diseases. Discovering means to immobilise viruses on various surfaces could provide an invaluable tool to potentially reduce the transmission of respiratory infections.

Chapter 5 aimed to test the binding of T4 bacteriophage to the Procion dyes, including all the preliminary experiments undertaken in preparation for this. Firstly, production of a high-titre phage stock was performed based on the growth curve of an *E. coli* liquid culture. Secondly, the effect of salt solutions of varying molar concentrations on T4 survival was investigated. The third experiment consisted of mixing phage solution with clear and RB4-tagged Sephadex slurry, pouring the mixtures into traditional syringe columns, and washing and eluting any potentially bound phage, by using salt solutions. Binding of T4 to pieces of fabrics dyed with the five Procion dyes was then tested, by adding coloured cloths to the phage solution and monitoring the change in T4 concentration over time.

In order to rule out the possibility that binding of phage to fabrics was due to adherence to the cloth's dry surface, LB pre-wetted pieces of undyed silk and cotton were mixed with phage stock, and the change in phage density was tracked. Then, in order to test if exposure to a greater amount of Procion dye could lead to superior T4 binding, RB4 deeply dyed silk was mixed with phage, monitoring viral concentration. Finally, validity of the obtained results was assessed by examining electron microscopy images of fabrics exposed to T4 bacteriophage. So far, no studies are known to have tested the interaction between Procion dyes and viruses.

5.1 Methods

5.1.1 *E. coli* growth curves

The appropriate time for phage addition to an *E. coli* liquid culture was determined by monitoring the rise in absorbance at 600 nm of a liquid bacterial culture over time, until the optical density started to increase exponentially i.e. reaching the exponential growth phase. The growth curves of two bacterial liquid cultures, one as a control and the other infected with T4 bacteriophage, were tracked in parallel. An overnight *E. coli* "mini-culture" was used to inoculate two flasks containing 150 mL of LB medium. These were incubated in an orbital shaking incubator at 37°C and 180 RPM, taking the OD₆₀₀ every hour, until reaching 0.5 - 0.65 AU. A volume of 3 mL of high

titre phage lysate (over 10^7 PFU/mL) was added to one of the flasks and absorbance readings were recorded every 15 minutes, between repeated incubations at 37°C and 180 RPM, up to 3 hours. 0.5 mL of phage-infected culture were collected in microcentrifuge tubes at each reading. These were centrifuged at maximum speed for 5-10 minutes. A serial dilution of the centrifuged phage sample was prepared and 100 μ L of each dilution were mixed with 100 μ L of an overnight *E. coli* starter culture with an OD₆₀₀ between 0.2-0.4 AU. The mixture was incubated at RT, for 15 minutes. This was added to 3 mL of warm soft agar and was poured on pre-warmed (25°C) LB agar plates, and incubated at 37°C overnight.

5.1.2 *Testing the effect of sodium chloride on phage survival*

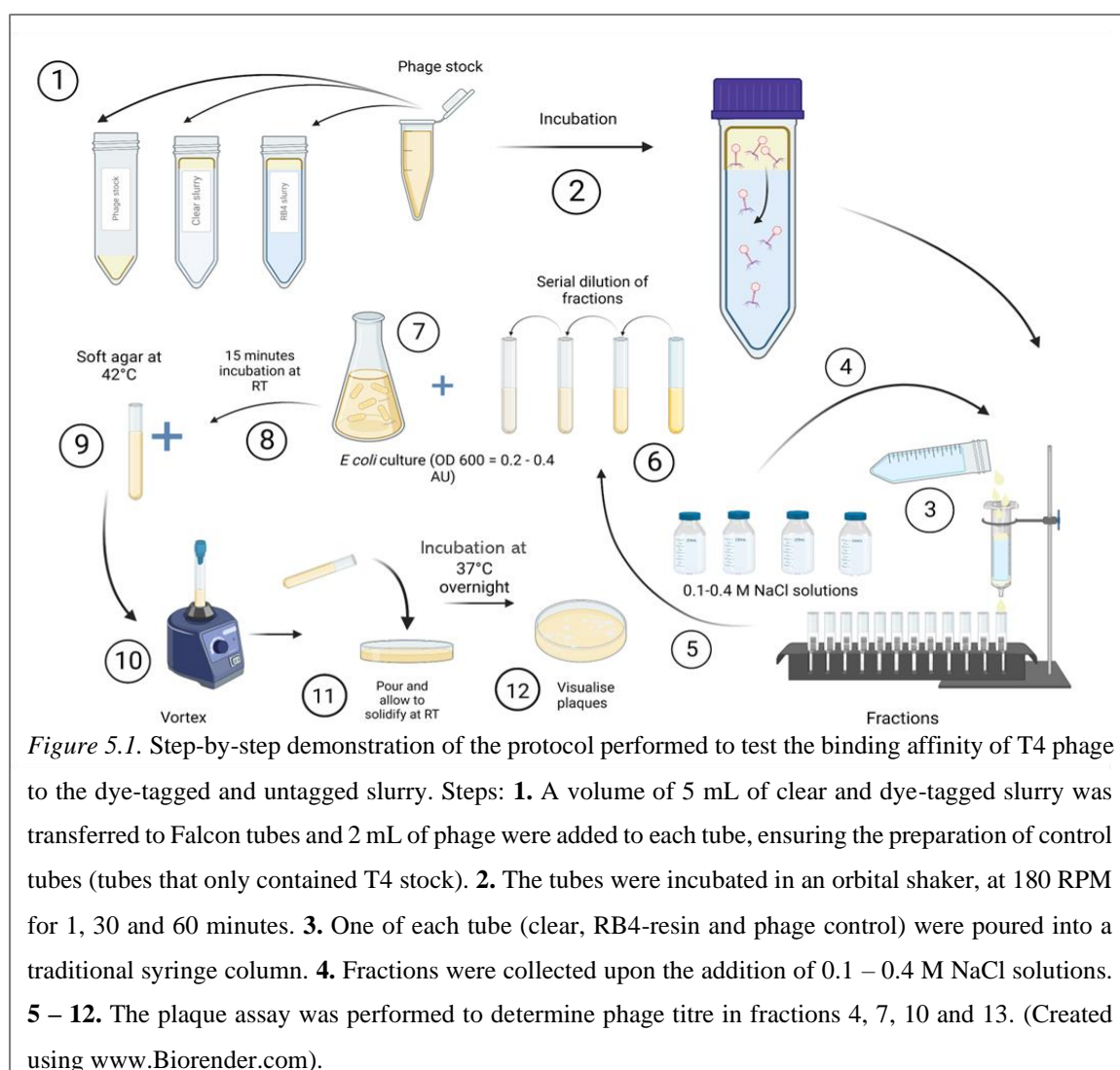
The effect of salt on bacteriophage survival was determined in a preliminary experiment, before eluting phage potentially bound to dyed and undyed Sephadex slurry. The phage stock was incubated at RT for approx. 30 minutes. 2 M, 0.8 M, 0.6 M, 0.4 M and 0.2 M NaCl solutions were prepared, autoclaved and allowed to cool down, to RT. Equal volumes of each solution and phage stock were mixed and incubated at RT for 30 minutes; this step caused both the NaCl and phage solutions to dilute by 50%. The phage-salt mixtures were used to determine the phage titre by the plaque assay (section 2.7).

5.1.3 *Testing the binding of phage to polysaccharide matrices*

A T4 bacteriophage stock solution, clear DEAE-Sephadex A-50 slurry and RB4-tagged slurry were incubated at RT for 30 minutes. A volume of 5 mL of slurry was added to sterile 15 ml Falcon centrifuge tubes, ensuring the preparation of 2 replicates per slurry; tubes were centrifuged briefly (1500 RPM, 30 seconds) to allow the beads to settle, and the supernatant (PBS) was removed. A volume of 2 mL of phage stock was added to each tube; controls were prepared by adding 2 mL of phage solution to 2 empty tubes. Tubes were incubated in an orbital shaker, at 180 RPM and RT, for 1, 30 and 60 minutes, and beads were centrifuged for 1 minute. A volume of 200 μ L of phage supernatant was collected from each tube after every incubation, which was then used to determine the phage titre by the plaque assay (Figure 5.1, steps 1 – 2; see section 2.7 for the assay).

5.1.4 Phage elution from the polysaccharide matrices

Traditional syringe columns were prepared by the method described previously (section 2.9). The contents of each tube from the previous section (section 5.1.3) were poured into separate syringe columns. The first 2 ml of liquid dripping down the columns were collected. This volume represented the amount of residual phage solution which did not get adsorbed into the Sephadex slurry. Volumes equal to 8 mL of 0.1, 0.2, 0.3 and 0.4 M NaCl solutions were sequentially added to the column, to wash and elute any potentially unbound or bound viral particles. A number of 15 other fractions of 2 mL were collected in microcentrifuge tubes. Phage titre was determined in fractions 1, 4, 7, 10, and 13 by the plaque assay (section 2.7), where each fraction, with the exception of the first, corresponded to one NaCl molar concentration (Figure 5.1, steps 3 – 12).



5.1.5 *Testing the binding of phage to natural fabrics*

Small rectangular pieces of dyed and undyed fabrics were cut from previously dyed cloths (section 2.10). It was ensured that all pieces of fabric of the same kind weighed identically (cotton – 15.3 mg; silk – 6.4 mg). Triplicate fabric pieces were prepared for each cloth type and colour. Undyed fabrics were used as controls. A volume of 1.5 mL of a 10^3 PFU/mL stock was added to 2 mL microcentrifuge tubes. Sterile pincers were used to transfer one piece of fabric to one tube and allowed to incubate for 1, 30 and 60 minutes on the roller shaker, at 35 RPM. Tubes were vortexed briefly (1-2 seconds, 3000 RPM) after each incubation and 100 μ L from each tube were collected; these were used for the plaque assay (section 2.7; protocol illustration in Figure 5.2).

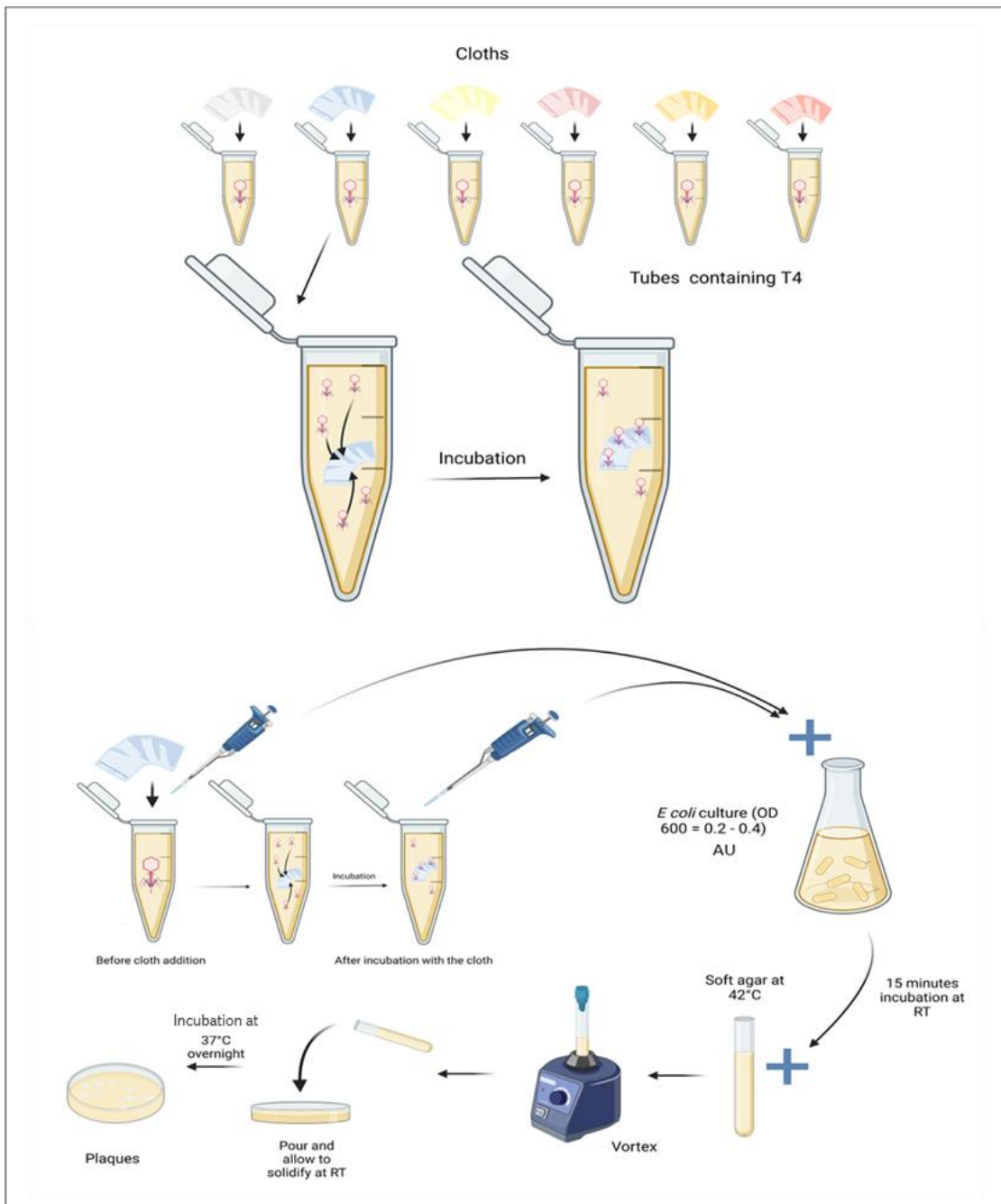


Figure 5.2. Illustration of the plaque assay protocol, adapted to test the binding affinity of T4 phage to the dyed and undyed (control) fabrics. Procion dye-tagged and undyed fabrics were added to tubes containing T4 solution and were incubated for 1, 30 and 60 minutes. A small volume of phage solution was removed from the tubes before the addition of cloths and after each incubation, which were then used for the plaque assay. (Created using www.Biorender.com).

5.1.6 *Testing the binding of phage to pre-wetted silk and cotton and dry dark-RB4 silk*

Pieces of undyed silk and cotton of the same weight as measured in the previous section (section 5.1.5) were wetted in LB solution, placed in a Pierce protein concentrator with a 10K molecular weight cut-off (Thermo Scientific, Hempstead, UK), and centrifuged for 2 minutes at 4000 RPM to remove excess liquid, whilst keeping the cloths moist. These were used to test the binding of phage, as described in the previous section (section 5.1.5). Dry pieces of silk deeply dyed with the RB4 dye were processed as in the previous section (section 5.1.5).

5.1.7 *Analysis of fabrics using Scanning Electron Microscopy*

The table-top SEM system (Hitachi TM4000plus) and the TM4000plus software (version 1.5) were used to analyse some of the fabric samples exposed to phage and control fabrics. Samples were mounted onto the specimen holder and then placed into the sample chamber. A vacuum pressure (10^0 to 10^1 Pa) was applied to the samples; the software was opened with the correct specimen holder selected. SEM images were obtained using an accelerating voltage of 5 kV surface with Backscattered electron + Secondary electron detector (MIX), with an appropriate vacuum of 30 Pa. The images were taken at 100 \times , 250 \times and 800 \times magnification.

5.2 Results

5.2.1 *E. coli* growth curves

Figure 5.3 describes the steps followed to produce an optimal concentration of T4 bacteriophage stock. Figure 5.3.A illustrates the rise in absorbance at 600 nm of an *E. coli* liquid culture over time, whilst Figure 5.3.B indicates the bacterial concentration at each time point shown

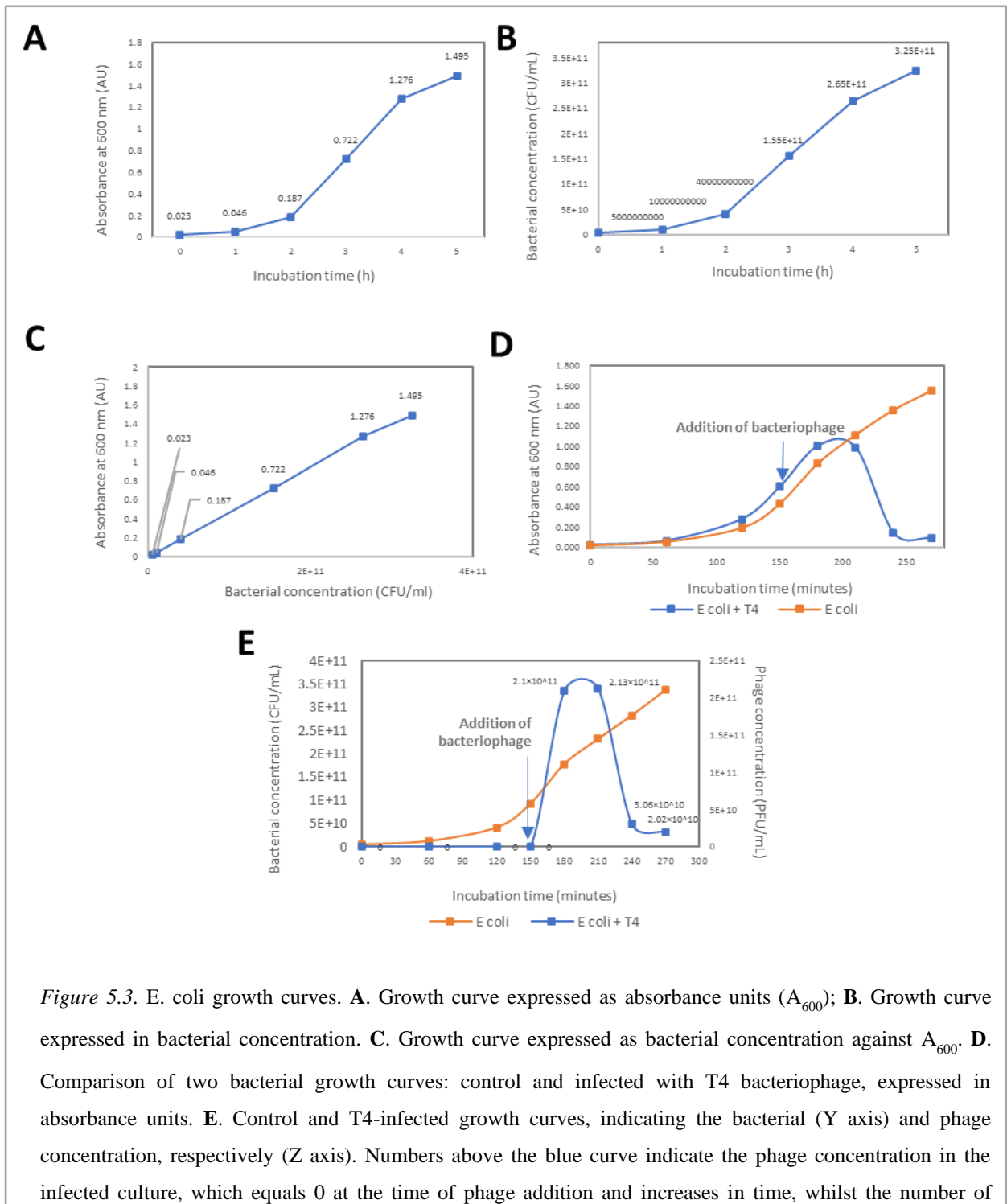


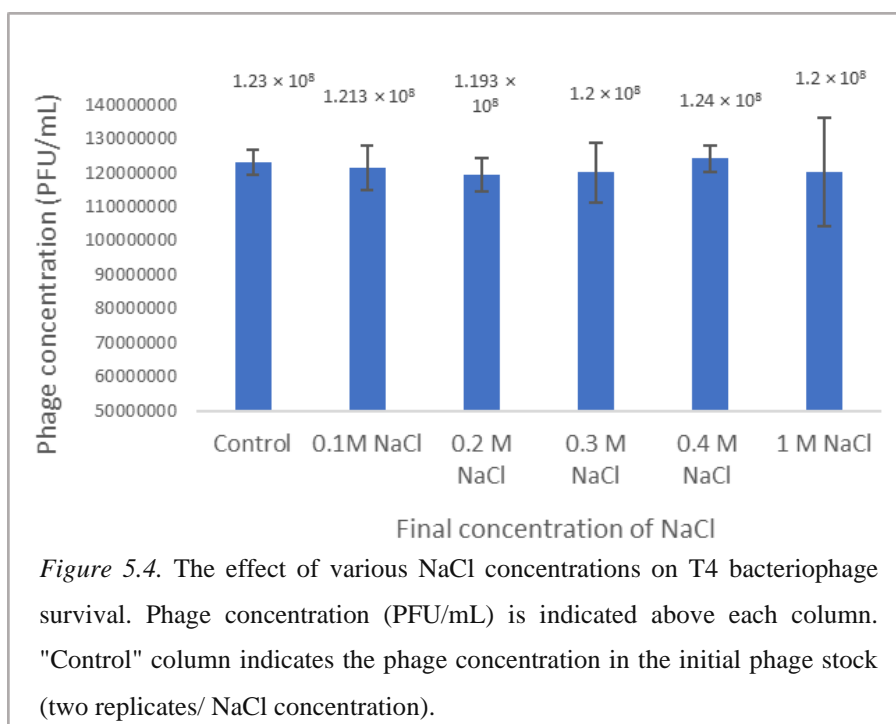
Figure 5.3. *E. coli* growth curves. **A**. Growth curve expressed as absorbance units (A_{600}); **B**. Growth curve expressed in bacterial concentration. **C**. Growth curve expressed as bacterial concentration against A_{600} . **D**. Comparison of two bacterial growth curves: control and infected with T4 bacteriophage, expressed in absorbance units. **E**. Control and T4-infected growth curves, indicating the bacterial (Y axis) and phage concentration, respectively (Z axis). Numbers above the blue curve indicate the phage concentration in the infected culture, which equals 0 at the time of phage addition and increases in time, whilst the number of

in the previous section, plotted against time. The optimal time for infecting an *E. coli* culture was found to be after approximately 2 – 2.5 hours (120 to 150 minutes) of incubation, or when the absorbance reached between 0.200 – 0.500 AU. Figure 5.3.C plots the absorbance at 600 nm of the bacterial culture, against the concentration of bacteria, creating a straight graph line, which validates the number of CFU/mL determined in the previous section (Figure 5.3.B).

The growth curves of two *E. coli* liquid cultures were monitored in parallel, one infected with T4 and one not infected (control), as shown in Figure 5.3.D. Here, the exponential increase in absorbance of the control culture (orange curve) starts after 2 hours of incubation at 37°C, and the curve begins to flatten between 200 and 250 minutes. In contrast, the addition of T4 in the other culture (blue curve) causes a decrease in absorbance around minute 150, 30 minutes after its addition to the *E. coli* culture. Figure 5.3.E indicates both the bacterial concentration (Y axis, where values relate to the orange curve) and the phage concentration (Z axis, where values relate to the blue curve) of the two cultures. Thus, the blue curve describes a downward motion to indicate the drop in bacterial concentration over time, whilst the numbers shown above the curve denote the number of PFU/mL, which increases with time.

5.2.2 *Testing the effect of sodium chloride on phage survival*

This experiment was conducted using 2 replicates per sample. Phage concentration data was normally distributed, as shown by the results of Ryan-Joiner normality test, where P-values > 0.100 (Table 10.16, appendix). Salt solutions of various molar concentrations, including 0.1, 0.2, 0.3, 0.4 and 1 M did not have any significant effect on phage concentration, as indicated by the insignificant P-value, resulting from the One-Way ANOVA (Table 10.17, appendix), where P-value = 0.262. The experimental outcome is depicted in Figure 5.4.



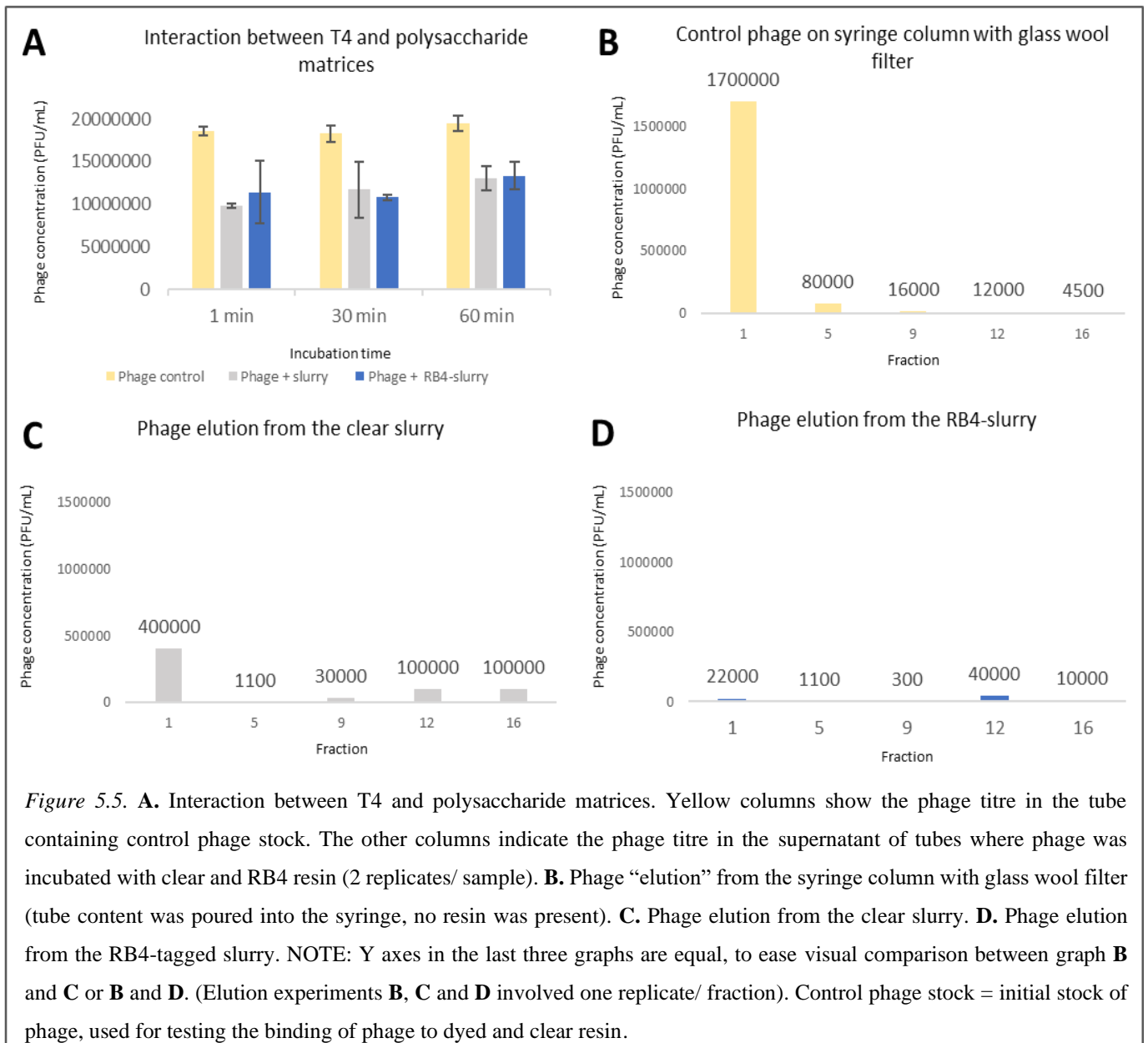
5.2.3 Testing the binding of phage to polysaccharide matrices

The experiments in this section were carried out using two replicates per sample. Data representing phage titre in stock (control) and in the solution exposed to clear and RB4 – tagged Sephadex slurry followed a normal distribution (P – values > 0.100, Table 10.18, appendix). One-Way ANOVA tests showed no significant difference between phage concentration in the stock control, in the supernatant of clear slurry and that of RB4 resin, after 1 minute of incubation (Table 10.19). However, the associated P-value was 0.051 for this comparison, close to the 0.05 cut-off value. Thus, the post-hoc LSD Fisher pairwise comparison showed a significant difference between phage titre in the tube containing phage control and the other two tubes, although Tukey’s test did not indicate any differences between means; therefore, the variation was not considered significantly different. After 30 minutes of incubation, no significant difference between the three was noted by ANOVA (P-value = 0.057); still, the LSD Fisher test indicated a significant difference between the control and the other two tubes. A significant P-value of 0.028 resulted from the analysis of the three, by One-Way ANOVA, the difference being observed between the control and each treatment group, after 60 minutes of incubation (Figure 5.5.A).

Analysis of the difference between incubation times by One-Way ANOVA revealed no significant difference between tubes containing control phage stock (P-value = 0.424), tubes

containing clear resin (P-value = 0.408) and those with RB4-tagged resin (P-value = 0.580). This is indicated in Table 10.20 (appendix) and depicted in Figure 5.5.A.

The highest phage concentration was recorded in fraction 1, corresponding to the control tube (Figure 17.B). All plated fractions eluted from dyed slurry contained fewer phage than those eluted from clear one, except for fraction 5, where titres were identical between resins (Figures 17.C and D).



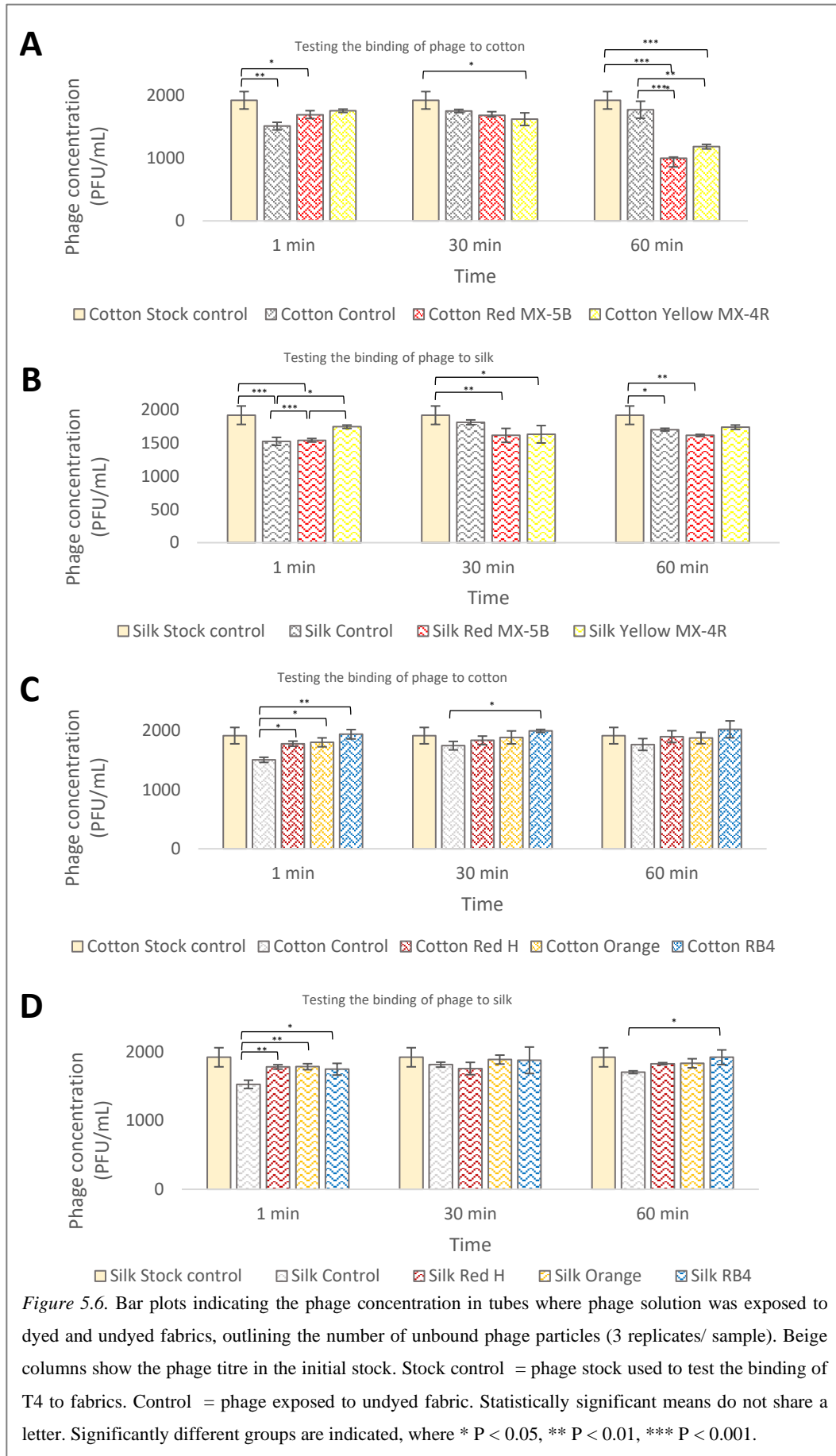
5.2.4 *Phage elution from the polysaccharide matrices*

These experiments were carried out using one replicate per fraction i.e. phage titre was determined using one replicate. Thus, data analysis could not be conducted. Fractions number 1 in Figures 5.5.**B** - **D** consisted of a volume of phage solution that did not get adsorbed onto the beads or glass wool and was allowed to drip off the column, before the addition of NaCl solutions. In fraction 1, Figure 5.5.**B**, the bacteriophage concentration was remarkably higher, in comparison to Figure 5.5.**C** and **D**. Similarly, the number of phage particles in fraction 5 was greater in the case of control phage, in contrast to the corresponding fractions coming off clear and RB4-tagged resin. The mean PFU/mL value showed in fraction 9, Figure 5.5.**B** was lower in comparison to the corresponding fractions in Figure 5.5.**C**, with the lowest concentration being recorded in Figure 5.5.**D**. For fractions 12, the highest phage concentration was reported in figure **C**, followed by figure **D** and then **B**. Similarly, in fractions 16, the top phage concentration was recorded in the case of clear resin, and was followed by the corresponding fractions coming off RB4 slurry and glass wool in the phage control column.

5.2.5 *Testing the binding of phage to natural fabrics*

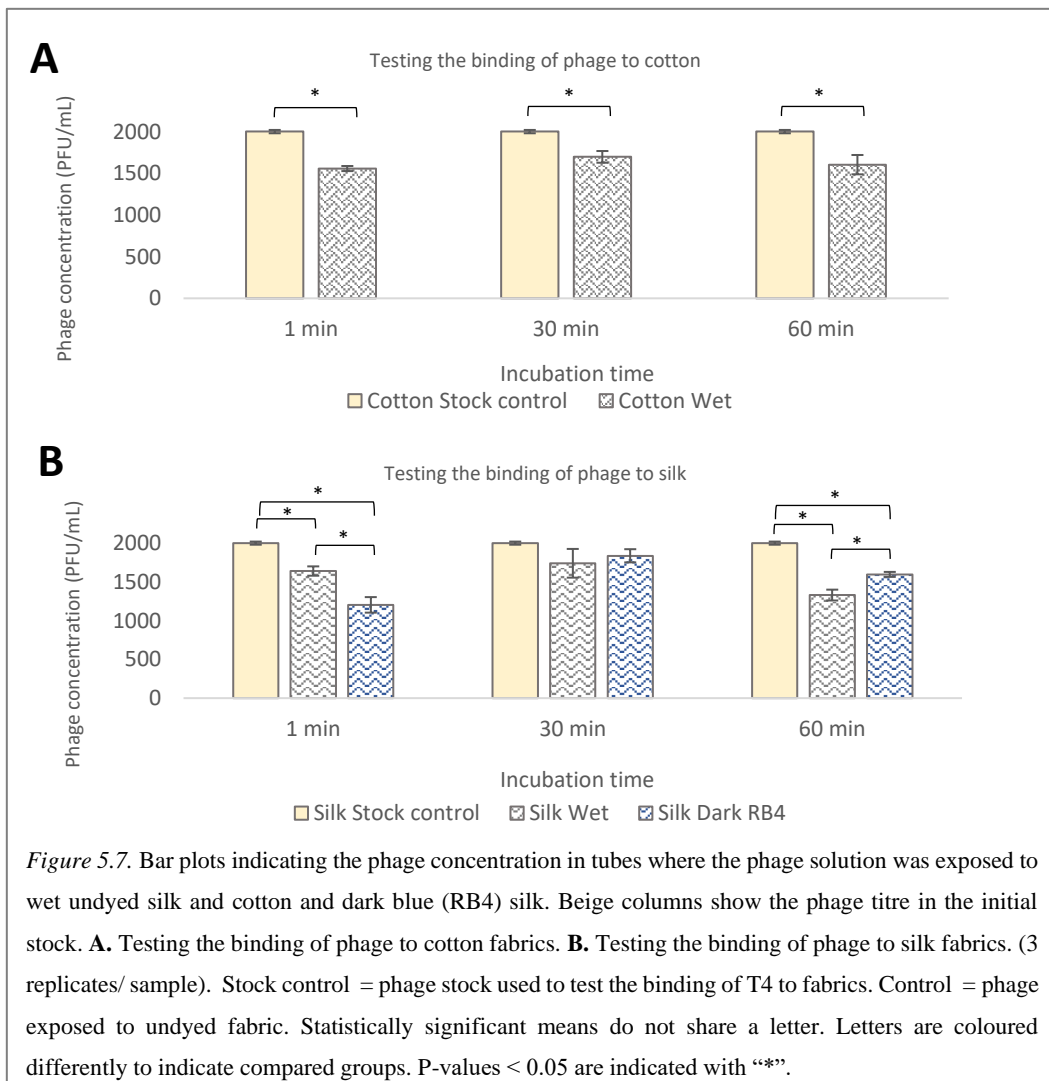
Data representing the number of bacteriophage particles in the stock solution before and after exposure to undyed and dyed fabrics was distributed normally, as indicated in Table 10.21 (appendix, P-values > 0.100). One-Way ANOVA analyses comparing titre variability after exposing phage to Procion dyed and undyed cotton and silk, indicated highly significant differences after 1, 30 and 60 minutes of incubation (P-values detailed in Table 10.22, appendix). Details of the significantly different pairs of means are shown in Table 10.23 (appendix), for both cotton and silk fabrics.

Comparisons between incubation times were conducted using One-Way ANOVA tests, for pieces of cotton and silk (Table 10.24). Differences were observed between 1 and 30 minutes of incubation in the case of control, undyed cotton (P-value = 0.034), between 1 and 60 minutes for undyed cotton (P-value = 0.024), Red MX-5B (P-value < 0.001), and yellow (P-value < 0.001). After 1 minute, the different titres were found between stock and undyed cotton, and between stock and Red MX-5B – cotton. Between 30 and 60 minutes, variations were reported for Red MX-5B (P-value < 0.001) and yellow (P-value < 0.001). In the case of silk, differences were observed for undyed fibre, between 1 and 30 (P-value < 0.001), 1 and 60 (P-value = 0.005) and 30 and 60 minutes (P-value = 0.043), as indicated in Table 10.25. These results are illustrated in Figure 5.6, where figures **A** and **C** show the binding of phage to cotton, and **B** and **D** indicate the binding to silk.



5.2.6 Testing the binding of phage to pre-wetted silk and cotton and dry dark-RB4 silk

Data indicating the number of PFU/mL in the phage stock, in the T4 solution exposed to wetted undyed cotton, and silk and dark RB4 silk was normally distributed (P-values > 0.100, Table 10.26, appendix). One-Way ANOVA tests comparing the phage titre after exposure to pre-wetted cotton, silk and dry dark RB4 silk indicated a significant difference from the stock after 1 minute (P-value < 0.001), 30 minutes (P-value = 0.037) and 60 minutes of incubation (P-value < 0.001). Differences were observed between stock and wet cotton, wet silk and dark RB4 silk after 1 minute. Half an hour incubation resulted in significant differences between stock and wet cotton. After 60 minutes, stock titre differed greatly from the titre of the sample exposed to wet cotton, silk and dark RB4 silk (Table 10.27, appendix). Differences between incubation times were reported for pre-wetted silk (P-value = 0.013) and deeply dyed RB4 silk (P-value < 0.001, Table 10.28, appendix). For undyed fibre, significant variations were reported between 1 and 30, and 1 and 60 minutes. For dark



RB4-dyed silk, differences were observed between all incubation times. Figure 5 depicts the experimental outcome.

5.2.7 Analysis of fabrics using Scanning Electron Microscopy

SEM images of silk and cotton fabrics exposed or unexposed to phage, either undyed or dyed with some of the five Procion dyes, are shown in Figures 5.8 – 5.10. Areas marked with an orange box indicate examples of ovoidal structures, presumably bacteriophage particles bound to fabrics exposed to T4 (Figure 5.10), or other units of similar shape, present on the surface of cloths unexposed to the T4 solution (Figures 5.8 and 5.9). The fabrics imaged here are identical to the ones used in the preceding sections (sections 5.2.5 and 5.2.6). However, not all fabrics tested previously have been imaged. Images were produced 1 – 3 days after fabrics had been exposed to T4.

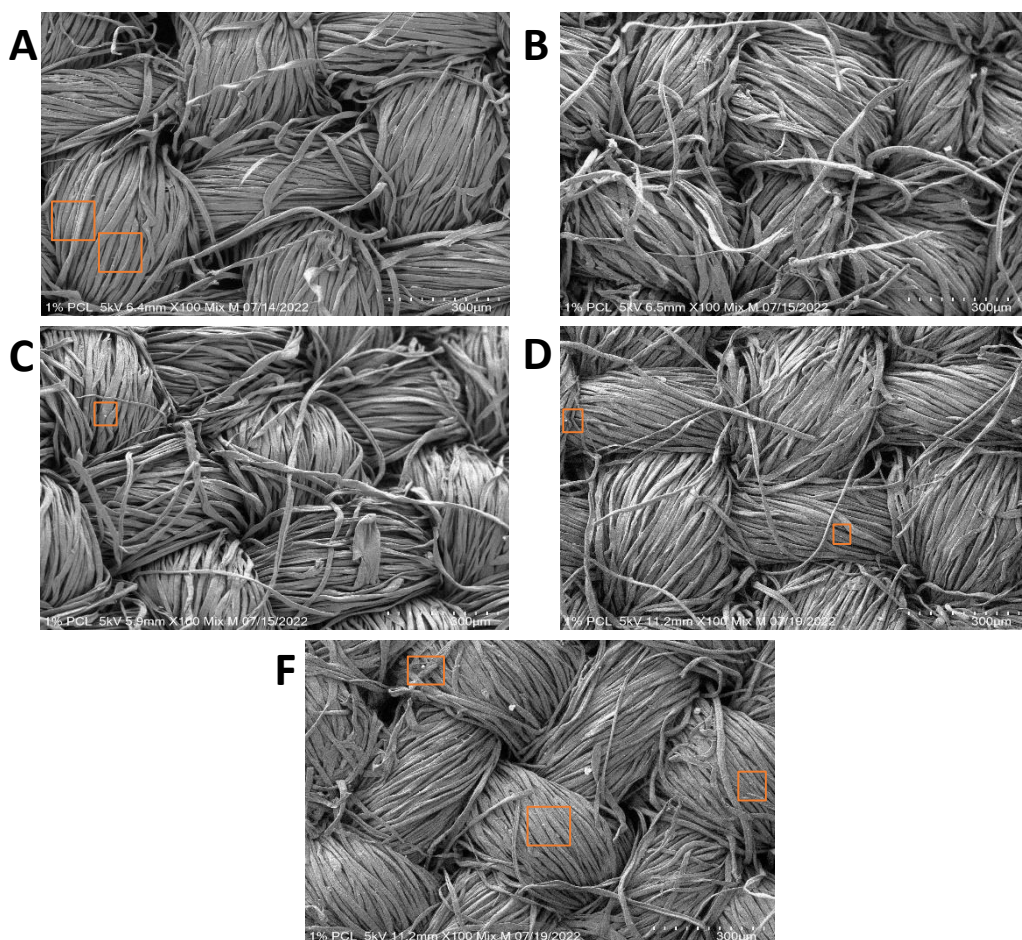


Figure 5.8. SEM images showing various cotton fibres (100× magnification), unexposed to T4 bacteriophage. **A.** Undyed cotton **B.** Cotton dyed with Procion Orange MX-G. **C.** Cotton dyed with Procion Red MX-5B. **D.** Cotton dyed with RB4 **F.** Cotton dyed with Red H-3BN.

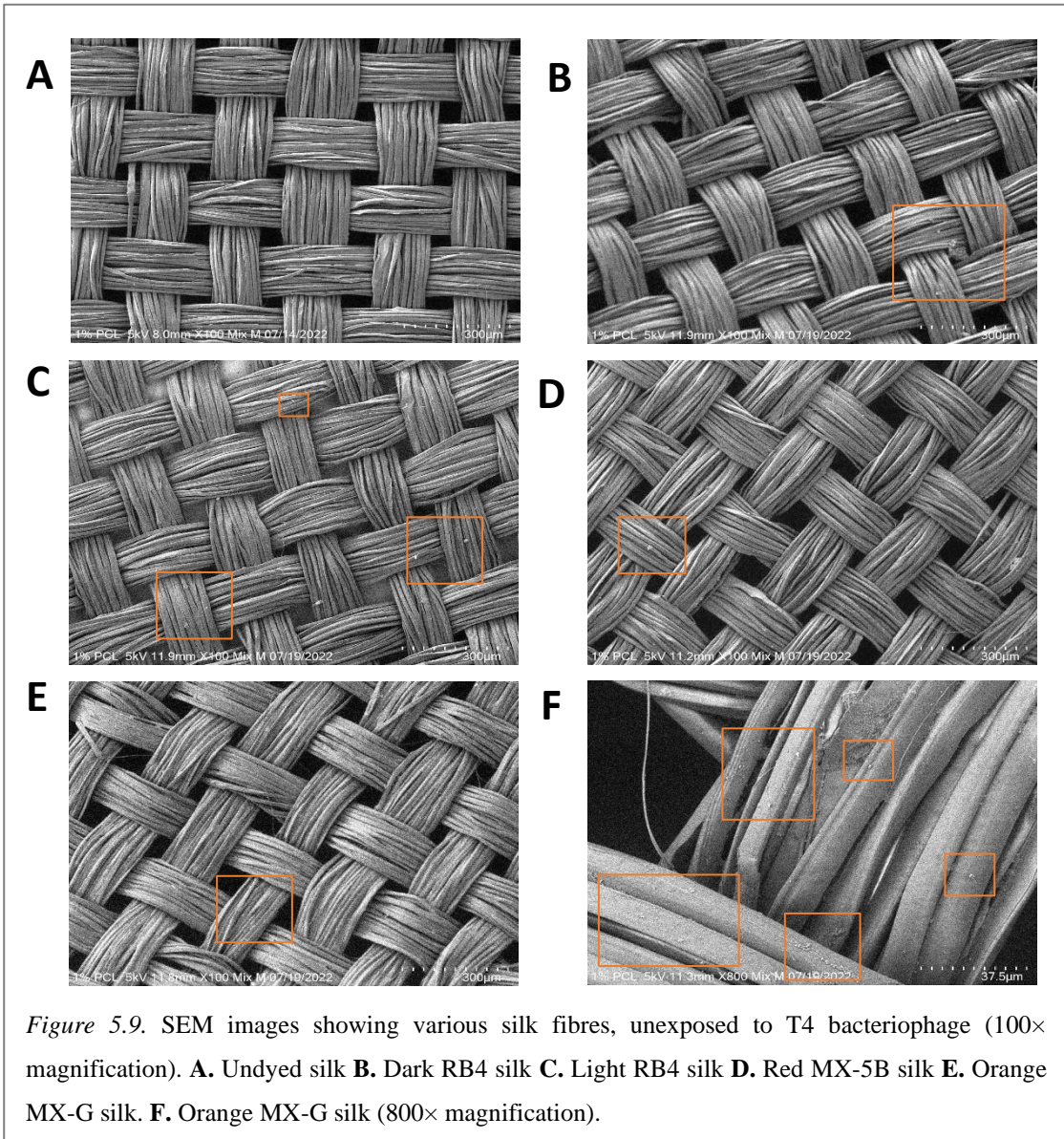


Figure 5.9. SEM images showing various silk fibres, unexposed to T4 bacteriophage (100× magnification). **A.** Undyed silk **B.** Dark RB4 silk **C.** Light RB4 silk **D.** Red MX-5B silk **E.** Orange MX-G silk. **F.** Orange MX-G silk (800× magnification).

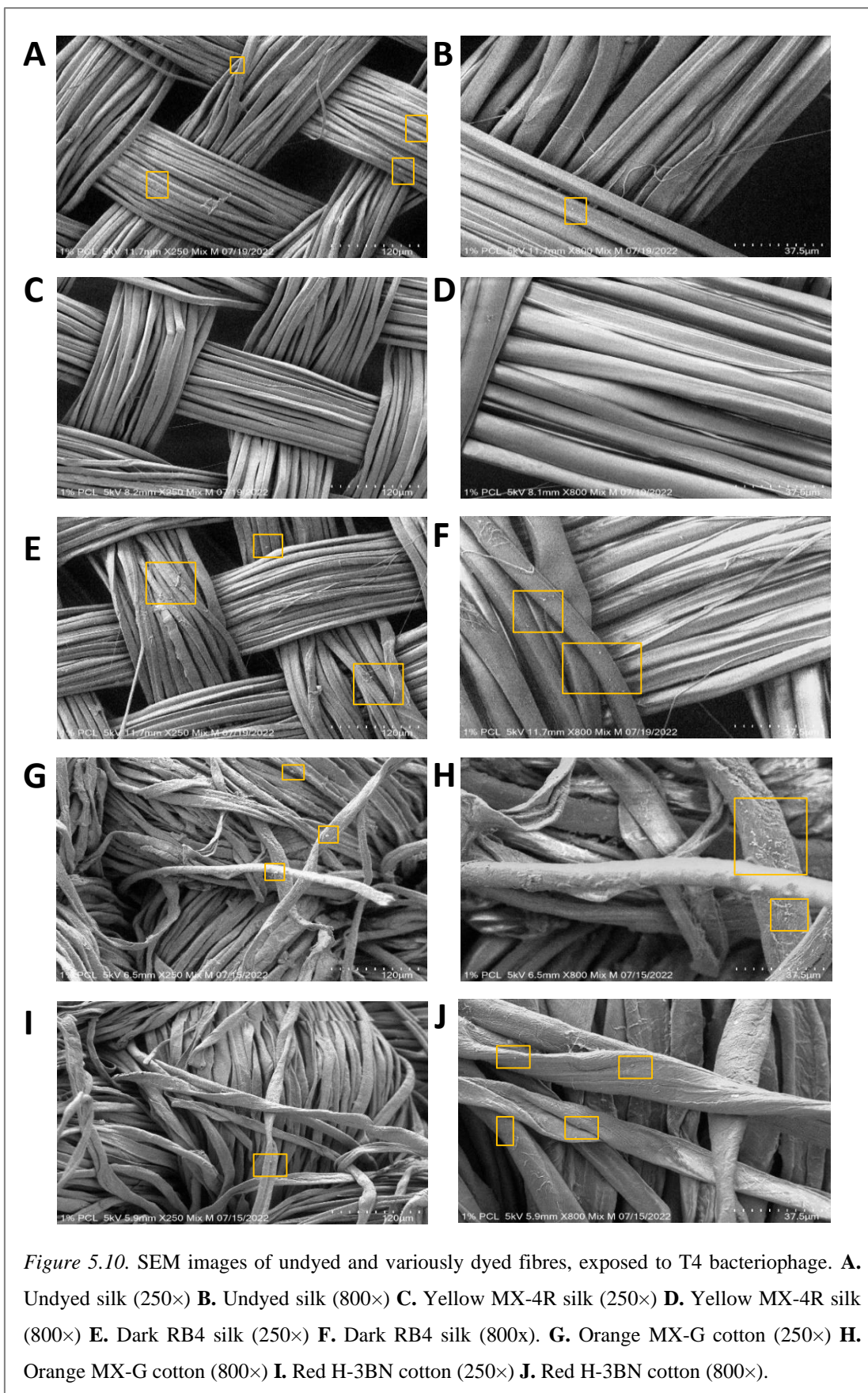


Figure 5.10. SEM images of undyed and variously dyed fibres, exposed to T4 bacteriophage. **A.** Undyed silk (250×) **B.** Undyed silk (800×) **C.** Yellow MX-4R silk (250×) **D.** Yellow MX-4R silk (800×) **E.** Dark RB4 silk (250×) **F.** Dark RB4 silk (800×). **G.** Orange MX-G cotton (250×) **H.** Orange MX-G cotton (800×) **I.** Red H-3BN cotton (250×) **J.** Red H-3BN cotton (800×).

5.3 Discussion

5.3.1. Testing the binding of phage to polysaccharide matrices

The current investigation aimed to analyse the binding of T4 bacteriophage to the choice of five Procion dyes. Initial attempts to concentrate the viral stock by either incubating the T4 with an *E. coli* liquid culture of high cellular density or for longer periods of time (section 5.2.1/ figure 5.3 **A** and **B**) proved unnecessary for the final stage of the present study. The first *E. coli* growth curve monitored the rise in absorbance of a liquid culture in time, in order to identify an appropriate time to infect the culture, for optimal phage production. Microbial growth includes three phases: lag, exponential and stationary. During the lag phase, bacteria adapt to the new environment, until starting to take advantage of it by beginning to metabolise the “new” nutrients around them, and no significant division is observed; the exponential, or log phase, represents the stage at which cells divide fast, bacterial numbers growing exponentially, doubling in numbers every 20 or 30 minutes; when reaching the stationary phase, bacteria start dying, as nutrients become limited (Buchanan *et al.*, 1997; Elbing and Brent, 2018). Therefore, the appropriate time for phage addition is the beginning of the lag phase, which is indicated by the quick rise in absorbance. Such approach would lead to the generation of maximal numbers of viral particles.

For the second part of the experiment (Figure 5.3.C, **D** and **E**), bacterial concentration was estimated. Then, the number of organisms was plotted against absorbance, information which was further used to estimate the increasing number of PFU, concomitant with the fall in CFU numbers. Accordingly, an optimal phage generation was achieved in stocks, which were used in future experiments.

Establishing if binding of T4 to the RB4-tagged and clear Sephadex resin could occur required an experiment aiming to elute potentially bound phage off the matrices. Thus, traditional syringe columns were used for this purpose. Affinity chromatography includes three steps: incubating the sample with the affinity support to enable the target to bind to the ligand, washing off unbound molecules and eluting bound target molecules from the ligand immobilised on an inert support. Concentration of salt in the washing and elution buffers should be increased gradually, thus allowing a stepwise elution of the target. In dye ligand chromatography, it is advisable to increase buffer's ionic strength from a concentration of 100 to 1000 mM, thus favouring protein elution. Sodium chloride solution is one of the most used buffers in protein purification. During the passage of the salt-containing eluent buffer through the chromatographic column, NaCl dissociates in Na⁺ and Cl⁻ ions, which start competing with the analyte ions, to bind to the functional groups present

on the surface of the stationary phase (Magdeldin and Moser, 2012; Gallant *et al.*, 2008; Acikara, 2013).

Considering that the chromatographic target consisted of bacteriophage particles, the effect of table salt on T4 survival had to be tested prior to conducting the above-mentioned experiment. Incubation of phage with salt solutions of increasing molarities did not have an effect on bacteriophage survival and infectability, findings which enabled the subsequent use of NaCl buffers for phage elution from dyed and undyed matrices. Leibo and Mazur (1966) described an experiment in which suspending bacteriophages T4B and T4D in concentrated salt solutions determined a sudden osmotic shock inside the phage heads, followed by immediate dilution in water, to reduce osmotic pressure. Here, phage particles were mixed with salt solutions and incubated for 30 minutes before being serially diluted and undergoing the plaque assay; therefore, the immediate effect of NaCl on phage survival was not monitored. Scribner and Krueger (1937) reported that addition of 0.25 M NaCl to the mixture of a *Staphylococcus aureus*-specific bacteriophage and its susceptible host determined an increase in the amount of phage produced; however, no significant difference in the number of produced phage was observed when phage alone was incubated with NaCl for 4 hours, at 37°C, prior to titration. In the present study, various NaCl concentrations did not have a significant effect on phage titre, in comparison to the control, and so, slight variability in phage concentration among tubes was most likely due to random chance.

The procedure mentioned above, generally followed in protein chromatography, was applied for phage elution from resin. Although the effect of 1 M NaCl buffer on T4 had been tested previously, this buffer was not used for phage elution. Phage titre varied significantly between stock and tubes containing phage-resin mixture, with no differences between dyed and undyed resin. Therefore, it is unlikely that the presence of RB4 led to better phage adsorption onto Sephadex. Phage titre did not vary with time in either of the tubes, suggesting that longer incubation times do not lead to superior binding to the matrices.

It was found that a great amount of phage got adsorbed onto the clear and dyed resin. Differential binding of phage to the two types of slurry was observed from fraction 1. All plated fractions eluted from dyed slurry contained fewer phage in comparison to those eluted from clear Sephadex. This could possibly indicate a stronger interaction between phage and dyed slurry, in contrast to clear one. However, conclusions cannot be drawn, as the experiment was only conducted once, and the titre was determined using only one replicate per fraction. Repeating this experiment or plating all 16 fractions for all three tubes (control, clear and dyed slurry) was both time-consuming and wasteful, so the fabrics approach was taken afterwards.

Unfortunately, it was difficult to assess the binding capacity of the dyed beads to the viral particles. Bacteriophage particles were found in the first collected fractions and thus it was

hypothesised that their concentration was too high to bind such a small volume of dyed resin (5 mL). Another possible explanation was that the binding could not have occurred because of the incubation at 180 RPM, where the agitation was too vigorous for optimal dye-phage interaction. Additionally, in order to ensure the binding was not taking place due to the resin's biochemical nature (anion exchanger), the dyed fabric approach was taken.

5.3.2. *Testing the binding of phage to natural fabrics*

Due to working in small-scale, it was sensible to assume that such small pieces of fabric could not capture a very high number of viral particles. Consequently, the T4 stock was diluted to the minimum concentration detectable by the plaque assay, without the need to perform a serial dilution, which was 10^3 . To clarify this argument, in our case the number of PFU detected on a plate was approximately 10^2 , which represents the PFU concentration in 100 μ L of stock; multiplying this number by 10 would give the PFU concentration in a millilitre. Due to time constraints, the protocol was established and followed for all the dyes, without diluting the stock any further (by 50%, for example, to give a concentration around 10^1). Furthermore, tubes containing fabrics were incubated on a gentle roller shaker at 35 RPM, to allow potential binding to take place.

Some variation in the concentration of T4 was observed upon exposure to dyed and undyed fibres. Results indicated a significant decrease in titre upon exposure to both white and red cotton, suggesting that the presence of Red MX-5B did not influence phage binding. Other differences were reported between white and Red H-3BN – fibre, white and orange and white and blue cotton. Nonetheless, stock phage titre was not highly different from tubes with T4 exposed to cotton dyed with these three dyes. This indicates that the presence of the Red H-3BN, orange and blue dyes did not produce a dramatic decrease in phage titre, after 1 minute of incubation. Incubation for 30 minutes led to a significant decrease in phage after exposing the T4 sample to yellow-dyed cotton. Other differences between the stock and dyed cotton were not observed. The observed binding pattern of phage to the dyed cloths may suggest that phage binds to the yellow dye, as opposed to the other dyes. Also, it may suggest that Red MX-5B and Yellow MX-4R have the potential to bind or inactivate T4, due to a decrease in titre upon exposure to them.

Phage titre was compared between incubation times, after exposure to dyed and white fibres. The observed pattern could indicate a potential binding behaviour of phage to undyed fabrics. For white cotton, it seems that there is an immediate adsorption of phage, followed by desorption after half an hour, from which point the titre stabilises. For undyed silk, the pattern seems to involve initial adsorption, followed by desorption and final reabsorption. This may indicate an unstable interaction between phage and white silk. Other major differences were observed between stock

and T4 exposed to Red MX-5B and Yellow MX-4R cotton. For coloured silk, changes were not evident. This inconsistency could be explained by the fact that fine, silk fibres absorbed less dye in comparison to densely packed cotton, leading to less dramatic phage binding.

The observed potential binding pattern of phage to undyed cloths occurred throughout the 60 minutes incubation: initial adsorption – desorption – final reabsorption. This was initially hypothesised to be due to “assimilation” of phage onto dry fabric, to a better extent than to wet one. However, our findings inquired the initial hypothesis. as the same pattern was observed for both pre-wetted and dry white fibres (Figures 5.6 and 5.7). Thus, adsorption of phage onto undyed fabrics was most likely not influenced by the level of moisture in them. With this in mind, it could be postulated that generally binding of phage to white fabrics was superior to the binding to RB4, Orange MX-G and Red H-3BN. The explanation could be that the presence of these dye on the fabrics’ surface may conceal the area that phage particles interact with. On the other hand, exposure of T4 to deeply dyed silk fabric led to an immediate and significant reduction in titre, in contrast to exposure to light RB4-silk. This may suggest that the fibre which absorbed more RB4 dye bound more phage than the lightly coloured silk.

Despite observing some significantly different phage concentrations between samples exposed to various fibres, only three replicates per sample were used in each case. This determined very low sample sizes, which significantly limits conclusions’ accuracy, due to lower statistical power of tests. Therefore, it is unclear whether the observed effects are real or if false positive results simply arose from the small number of replicates.

Scanning electron microscope images produced in this study were meant to assess qualitatively any potential binding of phage to the dyed and undyed fabrics, rather than quantitatively. It could be hypothesised that the areas marked with orange boxes could likely indicate bacteriophage particles bound to the silk and cotton fabrics, as the round structures present on the fibres’ surfaces resemble in shape with T4. No such structures were observed in Figures 22 C and D. This could be explained by the fact that some areas of interest may be overlooked when visualising fabrics under the microscope. Thus, multiple sections of the same fabric should be inspected and imaged. In addition, some such structures could “hide” between the thin fibres of both cotton and silk and would be impossible to image.

Figures 5.8 and 5.9 illustrate images of undyed cotton and silk fibres, respectively, that have not been exposed to bacteriophage solution. Still, round structures were observed on the surface of these fabrics, with the same appearance as the ones shown in Figure 5.10, where fabrics had been incubated with phage. For example, the silk fabric shown in Figure 5.9.F seems to be the most densely covered with these round units, which appear clustered together, in comparison to the other

images, although this cloth did not come in contact with T4 at all. Therefore, it is arguable whether these structures actually represent phage particles or just nodules made of thin fibres.

A more precise diagnostic of the binding pattern of phage to the dyed and undyed cloths could be performed if samples were examined after each incubation. Here, the samples took 1 to 3 days to be analysed, after being exposed to the phage solution. However, preparation of samples for SEM is very time consuming and requires many preliminary steps. In addition, processing fabric samples was quite inconvenient, as access to the electron microscope was restricted, the equipment being located in a different laboratory than the one where the study was conducted.

In order to confirm the present results, a more powerful electron microscope should be employed. The microscope used here could magnify images up to 800 \times . However, despite being a large bacteriophage, T4's size is too small to be imaged using such a low magnification. Its head measures 120 nm in length and 86 nm in width, whilst the tail is approximately 92.5 nm long (Rao and Black, 2010; Yap *et al.*, 2016). For example, Ackermann's (2009) EM images of bacteriophages are magnified 92,400 \times and 3,297,000 \times , to produce a clear representation of the viral particles.

In conclusion, it is unclear whether T4 bacteriophage particles bind to the selection of five Procion dyes used in this study, or if the binding is significantly different from undyed silk and cotton. Although the use of an SEM could provide the most accurate method for validating this theory, the microscope must be more powerful and fabric samples must be imaged before and after exposure to phage. In addition, much larger sample sizes should be used and both small-scale and large-scale studies should be conducted, using greater volumes of phage solution and larger pieces of fabrics.

6. General discussion and future recommendations

The present study provides a basis for further investigations in the potential use of Procion dyes for binding nucleic acids and viruses. To date, considerable research has been performed in the field of dye-ligand chromatography for protein purification using reactive Procion dyes. Here, it was demonstrated that a large variety of bacterial proteins bind to these compounds by conduction of SDS-PAGE electrophoresis. Also, various binding patterns of five bacterial proteins were observed between the five dyes used. However, the list of proteins showing a significant level of interaction with the dyes is by no means extensive. Further work could focus on analysing the binding of more proteins. In addition, it would be interesting to compare the binding of protein extracts sourced from distinct species, like yeast, mammal tissue etc. Moreover, identification of proteins showing high degree of binding could be performed by Western Blotting.

In terms of nucleic acids, it is rather unclear if more binding was observed in case of RNA or DNA. Additionally, elution of RNA from dye-tagged resin was not performed here, due to time restrictions. It is also unknown if RNA has higher affinity to RB4 only, in comparison to DNA, or if this behaviour can be expected in the case of other dyes. Larger sample sizes, as well as repeating the same experiments multiple times are necessary to confirm the present results. Moreover, DNA chromatography fractions should undergo electrophoresis on agarose gels, to verify the elution pattern illustrated by DNA concentration data. It is also not known whether temperature could have had an effect on the binding of both proteins and nucleic acids to the clear and dyed beads. In this study, experiments were carried out at room temperature, which fluctuated around 5-6 degrees Celsius throughout the 10 months period in which they were conducted. Furthermore, pH of the Sephadex beads, protein, nucleic acid and T4 samples was not recorded in the present study. While buffers are utilised to maintain relatively constant pH conditions, it is advisable to routinely monitor and confirm pH stability. It is known that in the case of proteins pH and temperature influence their interaction with ligands bound to chromatography matrices (Lowe, 1979). Therefore, it would be interesting to assess the binding of proteins, nucleic acids and even bacteriophage to the dyes, to verify if dyes' binding capacity is temperature dependent.

Experiments testing the binding of phage to clear and RB4-tagged resin in tubes should be repeated multiple times, with a number of replicates high enough to increase results' validity. Additionally, matrices dyed with the rest of the dyes, or even other Procion dyes, could be used. Generally, the higher the number of replicates, the greater the statistical power. A better approach could have been repeating the experiment three times, and using three replicates per sample each time, like in previous experiments of the present study. Alternatively, an online statistical power calculator could be employed, which estimates the required sample size for determining a

meaningful effect with a desired level of confidence, based on data obtained from a previously conducted pilot study. Also, the experiment involving binding of T4 to the Sephadex matrices could be improved by diluting the phage solution to a concentration of approximately 10^1 . This would allow easy detection of any potential binding by the phage assay.

Operational errors might have arisen from many sources in the case of T4-related experiments. Firstly, phage solution has to be perfectly homogenous to minimise replication variability. Secondly, if phage particles bind to the plastic pipette tips, they cannot be pipetted out; in addition, some phage might end up on the outside surface of the pipette tip during pipetting. Thirdly, the suspension of *E. coli* and phage was mixed with soft agar, vortexed and poured on an agar plate, but a small amount of mixture could always remain at the bottom of the test tube after pouring it into Petri dishes. This was difficult to control, as the procedure needs to be carried out rapidly, to prevent the premature setting of the soft agar. It was not feasible to use a pipette to remove residual soft agar from the tube's base due to having to process so many samples and replicates in a short time. Thus, such experiments should be carried out by more individuals, in order to minimise procedural errors.

Despite their ample use in the life sciences and textile industries, reactive dyes represent a major concern for the environment. Around 100,000 tonnes of various commercially available synthetic dyes are produced every year, and once used, they are often disposed into water bodies and onto land, contaminating the natural environment and many habitats. In time, chemical decomposition, including oxidation and hydrolysis, generates toxic metabolites, which negatively influence animal and human health (Katheresan *et al.*, 2018; Han *et al.*, 2009). Toxicity of reactive dyes has been attributed to generation of aromatic amines during dye degradation (Leme *et al.*, 2015). The specific five Procion dyes used in this study are not known to demonstrate any harmful effects in particular, but are nevertheless hazardous. Considering some positive outcome in the experiments involving phage binding to dyed fabrics, it would be interesting to exploit these properties in other areas. If Procion dyes have an ability to capture viruses or if the latter get inactivated as a result of binding to these dyes, they could potentially be used in dyeing clothes or protective masks, as well as other types of medical PPE, to limit the transmission of infection to some extent. However, implementing a system for dyeing PPE for such purposes, performed at industrial scale, may cause additional environmental pollution. Therefore, alongside with the production of such protective items, methods for decontaminating wastewaters should be considered. Harmful effects on skin and respiratory system are known to occur in the case of textile industry workers, who expose themselves to dye powders and solutions. However, these are not known to be toxic after being bound to textile surfaces (Docker *et al.*, 1987; Maiphethlo, 2007). Yet, dye "bleeding" off fabrics may occur during extreme perspiration. Therefore, some treatments should be implemented to boost colour fastness during fabric dyeing, such as additional rinsing (Leme *et al.*, 2014). A less

environmentally harmful approach would involve natural dye extracts from plants, such as chlorophyll and carotenoids, to bind to polysaccharide matrices and eventually to fabrics. Eventually, naturally dyed resins could be tested in protein affinity chromatography. To date and to our knowledge, no such studies have been conducted yet.

There seems to be increasing interest for research on the use of nanomaterials for pathogen inactivation and capturing. Recently, a thin, flexible low-density polyethylene film impregnated with titanium dioxide was found to inactivate a variety of viruses, amongst which SARS2, in the presence of UV-light. The anti-viral properties exhibited by the nanomaterial work by targeting the viral lipid membrane and degrade its genetic material (Han *et al.*, 2022). Given these, an interesting approach would be combining technology aiming at both immobilising viruses on various surfaces and breaking down their nucleic acid content.

The present study provides a basis of results, open to further investigations, raising a set of questions that remain to be answered, such as: What is the exact effect of dyes on viral viability? Does viral inactivation occur as a result of dye-bacteriophage interaction? If so, does this inactivation take place due to dye toxicity or due to another phenomenon? A way to explore this possible “inactivation theory” would be designing an experiment in which to expose the bacteriophage to different concentrations of Procion dyes solution and then assess its infectability, by incubation with the *E. coli* host. Another method would involve a modified resazurin assay; first, the phage would be incubated with dye-conjugated chromatography resin; then, small volumes of the mixture would be placed in the wells of a 96 well-plate, to which *E. coli* would be added; afterwards, various doses of resazurin would be mixed into the wells and fluorescent signals would be determined using a plate reader. Thus, only active T4 would be able to infect and kill bacteria, impeding the conversion of resazurin to resorufin. Such outcome would indicate that the dyes possess a T4 inhibitory potential.

In view of the present results and the observed binding activity of phage to the fabrics (initial adsorption, followed by desorption, and final reabsorption), it could be stated that these dyes are not toxic for the phage. In fact, the observed pattern could be due to temporary virus inhibition. This could result from the formation of chemical linkages between viral tail pins and dyes' molecules, in the same fashion that bacteriophages recognise and bind host cells (Arya *et al.*, 2011). However, if detachment of phage from the dyed fabrics does occur after 60 minutes of incubation, it should be examined to what extent it does so i.e. how many viral particles are released back and why, and how efficient such system would be for capturing viruses. Nevertheless, if dyes' ability to attract or repel viruses is not sufficiently strong, these synthetic dyes could possibly be used in conjunction with other compounds (such as herbal dyes) to produce the intended effect.

The medicinal potential of some plants has been explored in the past. Several studies have tested the antimicrobial activity of coloured extracts, especially due to the antibiotics crisis, resulting from the emergence of multidrug resistant bacteria. Plants themselves produce secondary antimicrobial metabolites and store them into their tissues, in order to confer them protection against pathogenic agents. Such substances are able to eliminate infectious microorganisms, without having any toxic effect on the host's cells and their potential could be investigated for therapeutic use (Gupta *et al.*, 2004). *Punica granatum* for example, commonly known as pomegranate, represents a natural dye originating from the fruit of the same name (Wells, 2013). This dye is recognised as a strong antimicrobial, owing to the high tannins content. Tannins represent a class of compounds known for their antimicrobial effectiveness. Naphthoquinone pigments found in lawsone from the henna plant, juglone from walnuts and lapachol from alkanet, also known as bugloss, have shown remarkable anti-fungal, anti-bacterial and anti-viral properties (Gupta *et al.*, 2004; Wells, 2013). *In vitro* studies on lapachol have proved its anti-viral attributes against the activation of Epstein-Barr's virus early antigen and enterovirus. Lapachol derivatives have been shown to be able to interact with Nsp9 in SARS-CoV-19 *in silico*. Nsp9 is a non-structural protein involved in replication of coronaviruses, and lapachol could represent an ideal potential ligand to bind to it and inhibit its activity (Sacau *et al.*, 2003; Ventura Pinto, 1987; Junior *et al.*, 2022).

Given these premises, medicinal plants able to produce natural dyestuffs which exhibit antimicrobial properties may be potentially used in dyeing clothes and other textiles, to limit the spread of disease. Therefore, it could be assumed that such products would have the potential to reduce the spread of some transmissible diseases. In addition, these dyes are naturally sourced, therefore their use could present many advantages. To name a few, they could limit the number of allergies arising from close contact with synthetic compounds in clothes, in contrast to allergy-producing synthetic dyes, the dyeing process would be more ecologically efficient, as natural dyes are biodegradable. Such approach could help limit the industrial wastewater issue. In addition, it is known that some dyes sourced from plants, such as harda and indigo, are natural fertilisers, thus wastewater resulting from dyeing processes could be safely disposed onto fields to aid agriculture. Unfortunately, the production costs of such fabrics would be higher, as extraction procedures require technical knowledge and time, as opposed to rapid industrialised production of synthetic dyes (Verma and Gupta, 2017; Samanta and Konar, 2011).

The Procion dyes used in the present experiment demonstrated different binding behaviour to proteins, nucleic acids, and viral particles. Protein 3 appeared to bind best to Red H-3BN, Orange MX-G and Red MX-5B. Proteins 1, 2 and 4 indicated strong binding affinity to Orange MX-G. Also, proteins 1 and 2 bound superiorly to Red H-3BN. Bacterial DNA proved high affinity to the Blue MX-R dye and Orange MX-G. In the case of T4, the dyes producing the most dramatic reduction in titre were Red MX-5B and Yellow MX-4R. However, the experiments should be

repeated using an inert chromatographic support, like Sepharose CL-2B, to rule out any potential binding owing to the nature of used resin. Additionally, bioinformatics analyses could provide more insights in the binding of macromolecules to these dyes, via a visual computational approach.

7. Conclusions

In conclusion, the present study lays the foundations for research in the potential use of Procion dyes to bind biomolecules. Bacterial proteins, nucleic acids and T4 bacteriophage bound differentially to the selection of five Procion dyes. The selection of five proteins were found to preferentially bind either Red H-3BN, Orange MX-G, Red MX-5B or RB4. RNA was found to bind better to the RB4 dye in comparison to DNA. Clear slurry appeared to be less efficient in binding DNA than dye-tagged slurry, when flowing through a traditional chromatography column. A reduced T4 titre was observed upon incubation with RB4-tagged DEAE Sephadex A-50, in comparison to undyed resin. Incubation of phage sample with cotton dyed with Red MX-5B and Yellow MX-R was found to decrease phage titre substantially. Nevertheless, magnification levels of the SEM used here were not powerful enough to confirm that the drop in phage concentration was due to phage binding to these dyes. Therefore, it is still unclear whether Procion dyes could have the potential to limit the spread of viral diseases. Future work should focus on validating the present results.

8. Funding

The present study was funded and coordinated by Comax Life Sciences Co. Ltd and Canterbury Christ Church University.

9. References

- Acikara, Ö.B. (2013) "Ion exchange chromatography and its applications", *Column chromatography*, 10, p.55744.
- Ackermann, H.W. (2009) "Basic phage electron microscopy", *Bacteriophages* (pp. 113-126), Humana press.
- Ades, S.E. and Sauer, R.T. (1995) "Specificity of minor-groove and major-groove interactions in a homeodomain-DNA complex", *Biochemistry*, 34(44), pp.14601-14608.
- Agrawal, B.B. and Goldstein, I.J. (1965) "Specific binding of concanavalin A to cross-linked dextran gels", *Biochemical Journal*, 96(3), p.23contd.
- Ahmed, N.S. (2005) "The use of sodium edate in the dyeing of cotton with reactive dyes", *Dyes and Pigments*, 65(3), pp.221-225.
- Alberts, B., Johnson, A., Lewis, J., Raff, M., Roberts, K. and Walter, P. (2002) "The RNA world and the origins of life", *Molecular Biology of the Cell. 4th edition*, Garland Science.
- Ali, N., Rampazzo, R.D.C.P., Costa, A.D.T. and Krieger, M.A. (2017) "Current nucleic acid extraction methods and their implications to point-of-care diagnostics", *BioMed research international*, 2017.
- Almeida, E.J.R. and Corso, C.R. (2014) "Comparative study of toxicity of azo dye Procion Red MX-5B following biosorption and biodegradation treatments with the fungi *Aspergillus niger* and *Aspergillus terreus*", *Chemosphere*, 112, pp.317-322.
- Andac, C.A., Andac, M. and Denizli, A. (2007) "Predicting the binding properties of cibacron blue F3GA in affinity separation systems", *International journal of biological macromolecules*, 41(4), pp.430-438.
- Anser, M.K., Islam, T., Khan, M.A., Zaman, K., Nassani, A.A., Askar, S.E., Abro, M.M.Q. and Kabbani, A. (2020) "Identifying the potential causes, consequences, and prevention of communicable diseases (including COVID-19)", *BioMed Research International*, 2020.

- Ardila-Leal, L.D., Poutou-Piñales, R.A., Pedroza-Rodríguez, A.M. and Quevedo-Hidalgo, B.E. (2021) “A brief history of colour, the environmental impact of synthetic dyes and removal by using laccases”, *Molecules*, 26(13), p.3813.
- Arya, S.K., Singh, A., Naidoo, R., Wu, P., McDermott, M.T. and Evoy, S. (2011) “Chemically immobilized T4-bacteriophage for specific *Escherichia coli* detection using surface plasmon resonance”, *Analyst*, 136(3), pp.486-492.
- Atkinson, T., Hammond, P.M., Hartwell, R.D., Hughes, P., Scawen, M.D., Sherwood, R.F., Small, D.A., Bruton, C.J., Harvey, M.J. and Lowe, C.R. (1981) “Triazine-dye affinity chromatography”, *Biochemical Society Transactions*, pp.290-293.
- Azmi, W., Sani, R.K. and Banerjee, U.C. (1998) “Biodegradation of triphenylmethane dyes”, *Enzyme and microbial technology*, 22(3), pp.185-191.
- Bafana, A., Devi, S.S. and Chakrabarti, T. (2011) “Azo dyes: past, present and the future”, *Environmental Reviews*, 19(NA), pp.350-371.
- Baird, J.K., Sherwood, R.F., Carr, R.J.G. and Atkinson, A. (1976) “Enzyme purification by substrate elution chromatography from procion dye—polysaccharide matrices”, *FEBS letters*, 70(1-2), pp.61-66.
- Balloux, F. and van Dorp, L. (2017) “Q&A: What are pathogens, and what have they done to and for us?”, *BMC biology*, 15(1), pp.1-6.
- Bautz, E.K.F. and Hall, B.D. (1962) “The isolation of T4-specific RNA on a DNA-cellulose column”, *Proceedings of the National Academy of Sciences*, 48(3), pp.400-408.
- Boone, S.A. and Gerba, C.P. (2007) “Significance of fomites in the spread of respiratory and enteric viral disease”, *Applied and environmental microbiology*, 73(6), pp.1687-1696.
- Boyer, P.M. and Hsu, J.T. (1993) “Protein purification by dye-ligand chromatography”, *Chromatography*, pp.1-44.

- Buchanan, R.L., Whiting, R.C. and Damert, W.C. (1997) “When is simple good enough: a comparison of the Gompertz, Baranyi, and three-phase linear models for fitting bacterial growth curves”, *Food microbiology*, 14(4), pp.313-326.
- Budin, G., Chung, H.J., Lee, H. and Weissleder, R. (2012) “A magnetic Gram stain for bacterial detection”, *Angewandte Chemie*, 124(31), pp.7872-7875.
- Bulut, C. and Kato, Y. (2020) “Epidemiology of COVID-19”, *Turkish journal of medical sciences*, 50(SI-1), pp.563-570.
- Burge, S., Parkinson, G.N., Hazel, P., Todd, A.K. and Neidle, S. (2006) “Quadruplex DNA: sequence, topology and structure”, *Nucleic acids research*, 34(19), pp.5402-5415.
- Castaño, N., Cordts, S.C., Kurosu Jalil, M., Zhang, K.S., Koppaka, S., Bick, A.D., Paul, R. and Tang, S.K., (2021) “Fomite transmission, physicochemical origin of virus–surface interactions, and disinfection strategies for enveloped viruses with applications to SARS-CoV-2”, *ACS omega*, 6(10), pp.6509-6527.
- Ceelen, M. (2019) *Phage stock preparation* Available at: <<https://dx.doi.org/10.17504/protocols.io.7kthkwn>> (Accessed 15 July 2022).
- Chandra, G., Patel, P., Kost, T.A. and Gray, J.G. (1992) “Large-scale purification of plasmid DNA by fast protein liquid chromatography using a Hi-Load Q Sepharose column”, *Analytical biochemistry*, 203(1), pp.169-172.
- Charlton, A. and Zachariou, M. (2008) “Affinity Chromatography. In *Molecular Biomethods Handbook*”, Humana Press, pp. 741-765.
- Clark, M. (2011) *Handbook of textile and industrial dyeing: principles, processes and types of dyes*. Elsevier.
- Cole, E.C. and Cook, C.E. (1998) “Characterization of infectious aerosols in health care facilities: an aid to effective engineering controls and preventive strategies”, *American journal of infection control*, 26(4), pp.453-464.
- Cone, A.J. (2015) “Zymoclean™ Gel DNA Recovery Kit”

- Coskun, O. (2016) "Separation techniques: chromatography", *Northern clinics of Istanbul*, 3(2), p.156.
- Curtius, J., Granzin, M. and Schrod, J. (2021) "Testing mobile air purifiers in a school classroom: Reducing the airborne transmission risk for SARS-CoV-2", *Aerosol Science and Technology*, 55(5), pp.586-599.
- Cytiva (n.d.) *DEAE Sephadex A-50* – Cytiva. Available at: <<https://www.cytivalifesciences.com/en/us/shop/chromatography/resins/ion-exchange/deae-sephadex-a-50-p-00796>> (Accessed 23 September 2022).
- Cytiva life sciences (n.d.) *AKTA Start Maintenance Manual*. Available at: <<https://cdn.cytivalifesciences.com/api/public/content/digi-16611-original#>> (Accessed 1 October 2022).
- de Azeredo, H.M. (2013) "Antimicrobial nanostructures in food packaging", *Trends in food science & technology*, 30(1), pp.56-69.
- Dehasque, M., Pečnerová, P., Kempe Lagerholm, V., Ersmark, E., Danilov, G.K., Mortensen, P., Vartanyan, S. and Dalén, L. (2022) "Development and optimization of a silica column-based extraction protocol for ancient DNA", *Genes*, 13(4), p.687.
- Deng, Y., Xu, S., Webb, K., Wright, H., Dimick, P.S., Cremaschi, S. and Eden, M.R. (2020) "Sensitivity Analysis of Desulfurization Costs for Small-Scale Natural Gas Sweetening Units", *Computer Aided Chemical Engineering*, 48, pp. 973-978, Elsevier.
- Denizli, A. and Pişkin, E. (2001) "Dye-ligand affinity systems. Journal of Biochemical and Biophysical Methods", 49(1-3), pp.391-416.
- Docker, A., Wattie, J.M., Topping, M.D., Luczynska, C.M., Taylor, A.N., Pickering, C.A., Thomas, P. and Gompertz, D. (1987) "Clinical and immunological investigations of respiratory disease in workers using reactive dyes", *Occupational and Environmental Medicine*, 44(8), pp.534-541.
- Draz, M.S. and Shafiee, H. (2018) "Applications of gold nanoparticles in virus detection", *Theranostics*, 8(7), p.1985.

- Drexler, M. (2010) *What you need to know about Infectious Disease*. Washington, D.C.: National Academy of Sciences.
- Drocourt, J.L., Thang, D.C. and Thang, M.N. (1978) “Blue-Dextran—Sephrose Affinity Chromatography: Recognition of a Polynucleotide Binding Site of a Protein”, *European Journal of Biochemistry*, 82(2), pp.355-362.
- Dudman, W.F. and Bishop, C.T. (1968) “Electrophoresis of dyed polysaccharides on cellulose acetate”, *Canadian Journal of Chemistry*, 46(19), pp.3079-3084.
- Duranti, C., Lastraioli, E., Iorio, J., Capitani, C., Carraresi, L., Gonnelli, L. and Arcangeli, A. (2021) “Expression and purification of a novel single-chain diabody (scDb-hERG1/β1) from *Pichia pastoris* transformants”, *Protein Expression and Purification*, 184, p.105879.
- Easton, L.E., Shibata, Y. and Lukavsky, P.J. (2010) “Rapid, nondenaturing RNA purification using weak anion-exchange fast performance liquid chromatography”, *RNA*, 16(3), pp.647-653.
- Elbing, K.L. and Brent, R. (2018) “Recipes and tools for culture of *Escherichia coli*”, *Current protocols in molecular biology*, 125(1), p.e83.
- Emlen, W. and Burdick, G. (1983) “Purification of DNA antibodies using cibacron blue F3GA affinity chromatography”, *Journal of immunological methods*, 62(2), pp.205-215.
- Epolito, W.J., Lee, Y.H., Bottomley, L.A. and Pavlostathis, S.G. (2005) “Characterization of the textile anthraquinone dye Reactive Blue 4”, *Dyes and Pigments*, 67(1), pp.35-46.
- Ersson, B., Rydén, L. and Janson, J.C. (2011) “Introduction to protein purification”, *Protein Purification: Principles, High Resolution Methods, and Applications*, pp.1-22.
- Farag, A.M. and Hassan, M.A. (2004) “Purification, characterization and immobilization of a keratinase from *Aspergillus oryzae*”, *Enzyme and Microbial Technology*, 34(2), pp.85-93.
- Fastcolours.com (n.d.) *FastColours LLP How to dye silk with Procion MX Dyes*. Available at: <<https://www.fastcolours.com/how-to-dye-silk-with-procion-mx-dyes-66-w.asp?fbclid=IwAR3a07owZLCd99wVrAUxcszaUblI--utEYedg4kKaO3VGu8Ygn->

- Hamlin, J.D., Phillips, D.A.S. and Whiting, A. (1999) "UV/Visible spectroscopic studies of the effects of common salt and urea upon reactive dye solutions", *Dyes and Pigments*, 41(1-2), pp.137-142.
- Han, F., Kambala, V.S.R., Srinivasan, M., Rajarathnam, D. and Naidu, R. (2009) "Tailored titanium dioxide photocatalysts for the degradation of organic dyes in wastewater treatment: a review", *Applied Catalysis A: General*, 359(1-2), pp.25-40.
- Han, R., Coey, J.D., O'Rourke, C., Bamford, C.G. and Mills, A. (2022) "Flexible, disposable photocatalytic plastic films for the destruction of viruses", *Journal of Photochemistry and Photobiology B: Biology*, p.112551.
- Hariani, P.L., Faizal, M., Ridwan, R., Marsi, M. and Setiabudidaya, D. (2013) "Synthesis and properties of Fe₃O₄ nanoparticles by co-precipitation method to removal procion dye", *International Journal of Environmental Science and Development*, 4(3), pp.336-340.
- Hayden, O., Lieberzeit, P.A., Blaas, D. and Dickert, F.L. (2006) "Artificial antibodies for bioanalyte detection—Sensing viruses and proteins", *Advanced Functional Materials*, 16(10), pp.1269-1278.
- Hodgskiss, T. and Wadley, L. (2017) "How people used ochre at Rose Cottage Cave, South Africa: Sixty thousand years of evidence from the Middle Stone Age", *PloS one*, 12(4), p.e0176317.
- Holland, A. (2015) *Procion MX Fibre Reactive Dyes*. Georgeweil.com. Available at: <https://www.georgeweil.com/blog/procion-mx-fibre-reactive-dyes/?fbclid=IwAR1iU1m2JXKNZ11TdpeQM9UQe2WgOycv00tel5EB8H9QH2_P5nrApw6fZA0> (Accessed 15 July 2022).
- Holmes, W.M., Hurd, R.E., Reid, B.R., Rimerman, R.A. and Hatfield, G.W. (1975) "Separation of transfer ribonucleic acid by Sepharose chromatography using reverse salt gradients", *Proceedings of the National Academy of Sciences*, 72(3), pp.1068-1071.
- Jensen, L.B. (1963) "Royal purple of Tyre", *Journal of Near Eastern Studies*, 22(2), pp.104-118.
- Jungbauer, A. and Hahn, R. (2009) "Ion-exchange chromatography", *Methods in enzymology*, 463, pp.349-371.

- Junior, N.N., Santos, I.A., Meireles, B.A., Nicolau, M.S.A.P., Lapa, I.R., Aguiar, R.S., Jardim, A.C.G. and José, D.P. (2022) “In silico evaluation of lapachol derivatives binding to the Nsp9 of SARS-CoV-2”, *Journal of Biomolecular Structure and Dynamics*, 40(13), pp.5917-5931.
- Kanetkar, V.R. (2010) “Colour: History and advancements”, *Resonance*, 15(9), pp.794-803.
- Katheresan, V., Kandedo, J. and Lau, S.Y. (2018) “Efficiency of various recent wastewater dye removal methods: A review”, *Journal of environmental chemical engineering*, 6(4), pp.4676-4697.
- Klecker, C. and Nair, L.S. (2017) “Matrix Chemistry Controlling Stem Cell Behavior”, *Biology and Engineering of Stem Cell Niches* (pp. 195-213). Academic Press.
- Koch, C., Borg, L., Skjødt, K. and Houen, G. (1998) “Affinity chromatography of serine proteases on the triazine dye ligand Cibacron Blue F3G-A”, *Journal of Chromatography B: Biomedical Sciences and Applications*, 718(1), pp.41-46.
- Kumar, S., Dalvi, D.B., Moorthy, M., Korde, S.S., Fondekar, K.P., Sahasrabudhe, S.D., Schacht, H.T., Ekkundi, V.S., Halik, C., Choudhury, R. and Kumar, A. (2009) “Discriminatory protein binding by a library of 96 new affinity resins: A novel dye-affinity chromatography tool-kit”, *Journal of Chromatography B*, 877(29), pp.3610-3618.
- Kumeria, T. and Santos, A. (2015) “Nanoporous alumina membranes for chromatography and molecular transporting”, *Nanoporous Alumina* (pp. 293-318). Springer, Cham.
- Labrou, N.E. (2014) “Protein purification: an overview”, *Protein Downstream Processing*, pp.3-10.
- Lednicky, J.A., Lauzardo, M., Fan, Z.H., Jutla, A., Tilly, T.B., Gangwar, M., Usmani, M., Shankar, S.N., Mohamed, K., Eiguren-Fernandez, A. and Stephenson, C.J. (2020) “Viable SARS-CoV-2 in the air of a hospital room with COVID-19 patients”, *International Journal of Infectious Diseases*, 100, pp.476-482.
- Leibo, S.P. and Mazur, P. (1966) “Effect of osmotic shock and low salt concentration on survival and density of bacteriophages T4B and T4Bo1”, *Biophysical Journal*, 6(6), pp.747-772.

- Leiman, P.G., Kanamaru, S., Mesyanzhinov, V.V., Arisaka, F. and Rossmann, M.G. (2003) "Structure and morphogenesis of bacteriophage T4", *Cellular and Molecular Life Sciences CMLS*, 60(11), pp.2356-2370.
- Leme, D.M., de Oliveira, G.A.R., Meireles, G., dos Santos, T.C., Zanoni, M.V.B. and de Oliveira, D.P. (2014). "Genotoxicological assessment of two reactive dyes extracted from cotton fibres using artificial sweat", *Toxicology in Vitro*, 28(1), pp.31-38.
- Leme, D.M., de Oliveira, G.A.R., Meireles, G., Brito, L.B., Rodrigues, L.D.B. and Palma de Oliveira, D. (2015) "Eco-and genotoxicological assessments of two reactive textile dyes", *Journal of Toxicology and Environmental Health, Part A*, 78(5), pp.287-300.
- Lowe, C.R. (1979) "Immobilized nucleotides and coenzymes for affinity chromatography", *Pure and Applied Chemistry*, 51(7), pp.1429-1441.
- Lowe, C.R. (2001) "Combinatorial approaches to affinity chromatography", *Current Opinion in Chemical Biology*, 5(3), pp.248-256.
- Lowe, C.R., Hans, M., Spibey, N. and Drabble, W.T. (1980) "The purification of inosine 5'-monophosphate dehydrogenase from *Escherichia coli* by affinity chromatography on immobilized Procion dyes", *Analytical biochemistry*, 104(1), pp.23-28.
- Lowe, C.R., Small, D.A.P. and Atkinson, A. (1981) "Some preparative and analytical applications of triazine dyes", *International Journal of Biochemistry*, 13(1), pp.33-40.
- Maffeo, C., Yoo, J., Comer, J., Wells, D.B., Luan, B. and Aksimentiev, A. (2014) "Close encounters with DNA", *Journal of Physics: Condensed Matter*, 26(41), p.413101.
- Magdeldin, S. and Moser, A. (2012) *Affinity Chromatography: Principles and Applications*. INTECH Open Access Publisher.
- Maiphethlo, L. (2007) "Contact dermatitis in the textile industry: allergies in the workplace", *Current Allergy & Clinical Immunology*, 20(1), pp.28-35.
- McMichael, A.J. and Woodruff, R.E. (2008) "Climate change and infectious diseases", *The social ecology of infectious diseases*, pp. 378-407, Academic Press.

- Medical Advisory Secretariat Ontario (2005) “Air cleaning technologies: an evidence-based analysis”, *Ontario health technology assessment series*, 5(17), p.1.
- Meng, M. and Ducho, C. (2018) “Oligonucleotide analogues with cationic backbone linkages”, *Beilstein Journal of Organic Chemistry*, 14(1), pp.1293-1308.
- Miranda, F., Kupeyan, C., Rochat, H., Rochat, C. and Lissitzky, S. (1970) “Purification of animal neurotoxins: isolation and characterization of eleven neurotoxins from the venoms of the scorpions *Androctonus australis Hector*, *Buthus occitanus tunetanus* and *Leiurus quinquestriatus quinquestriatus*”, *European Journal of Biochemistry*, 16(3), pp.514-523.
- Mohanraj, V.J. and Chen, Y. (2006) “Nanoparticles-a review”, *Tropical journal of pharmaceutical research*, 5(1), pp.561-573.
- Mustafa, F., Hassan, R.Y. and Andreescu, S. (2017) “Multifunctional nanotechnology-enabled sensors for rapid capture and detection of pathogens”, *Sensors*, 17(9), p.2121.
- Nakamura, W., Hosoda, S. and Hayashi, K. (1974) “Purification and properties of rat liver glutathione peroxidase”, *Biochimica et Biophysica Acta (BBA)-Enzymology*, 358(2), pp.251-261.
- Novick, D. and Rubinstein, M. (2012) “Ligand affinity chromatography, an indispensable method for the purification of soluble cytokine receptors and binding proteins”, *Cytokine Protocols* (pp. 195-214). Humana Press, Totowa, NJ.
- Platto, S., Xue, T. and Carafoli, E. (2020) “COVID19: an announced pandemic”, *Cell Death & Disease*, 11(9), pp.1-13.
- Priyadarshini, R., Raj, G. and Shewade, D. (2016) “Chromatography—The essence of bioanalysis”, *European Journal of Biomedical Pharmaceutics Science*, 3(1), pp.366-377.
- Pubchem.ncbi.nlm.nih.gov (n.d.) *Bromophenol blue*. Available at: <<https://pubchem.ncbi.nlm.nih.gov/compound/8272>> (Accessed 10 August 2022).
- Rahman, A., Urabe, T. and Kishimoto, N. (2013) “Color removal of reactive Procion dyes by clay adsorbents”, *Procedia Environmental Sciences*, 17, pp.270-278.

- Rao, V.B. and Black, L.W. (2010) "Structure and assembly of bacteriophage T4 head", *Virology journal*, 7(1), pp.1-14.
- Ray, P.C., Khan, S.A., Singh, A.K., Senapati, D. and Fan, Z. (2012) "Nanomaterials for targeted detection and photothermal killing of bacteria", *Chemical Society Reviews*, 41(8), pp.3193-3209.
- Rodriguez, E.L., Poddar, S., Iftekhar, S., Suh, K., Woolfork, A.G., Ovbude, S., Pekarek, A., Walters, M., Lott, S. and Hage, D.S. (2020) "Affinity chromatography: A review of trends and developments over the past 50 years", *Journal of Chromatography B*, 1157, p.122332.
- Roelants, P., Boon, B. and Lhoest, W. (1968) "Evaluation of a Commercial Air Filter for Removal of Virus from the Air", *Applied Microbiology*, 16(10), pp.1465-1467.
- Roque, A.C.A. and Lowe, C.R. (2008) "Affinity chromatography", *Affinity chromatography*, pp.1-23.
- Sacau, E.P., Estévez-Braun, A., Ravelo, Á.G., Ferro, E.A., Tokuda, H., Mukainaka, T. and Nishino, H. (2003) "Inhibitory effects of lapachol derivatives on epstein-barr virus activation", *Bioorganic & medicinal chemistry*, 11(4), pp.483-488.
- Saker, L., Lee, K., Cannito, B., Gilmore, A. and Campbell-Lendrum, D.H. (2004) *Globalization and infectious diseases: a review of the linkages*. Geneva: World Health Organization.
- Samanta, A.K. and Konar, A. (2011) "Dyeing of textiles with natural dyes", *Natural dyes*, 3(30-56).
- Sander, E.G., McCormick, D.B. and Wright, L.D. (1966) "Column chromatography of nucleotides over thymidylate-cellulose", *Journal of Chromatography*, 21, pp.419-423.
- Sari, M.I., Agustina, T.E., Melwita, E. and Aprianti, T. (2017) "Color and COD degradation in photocatalytic process of procion red by using TiO₂ catalyst under solar irradiation", *AIP Conference Proceedings* (Vol. 1903, No. 1). AIP Publishing.
- Scawen, M.D., Hammond, P.M., Comer, M.J. and Atkinson, T. (1983) "The application of triazine dye affinity chromatography to the large-scale purification of glycerokinase from *Bacillus stearothermophilus*", *Analytical biochemistry*, 132(2), pp.413-417.

- Schasfoort, R.B., Bergveld, P., Kooyman, R.P.H. and Greve, J. (1990) "Possibilities and limitations of direct detection of protein charges by means of an immunological field-effect transistor", *Analytica chimica acta*, 238, pp.323-329.
- Scribner, E.J. and Krueger, A.P. (1937) "The effect of NaCl on the phage-bacterium reaction", *The Journal of General Physiology*, 21(1), p.1.
- Sedgwick, P. (2015) "A comparison of parametric and non-parametric statistical tests", *BMJ*, 350.
- Simonetti, O., Martini, M. and Armocida, E. (2021) "COVID-19 and Spanish flu-18: review of medical and social parallelisms between two global pandemics", *Journal of preventive medicine and hygiene*, 62(3), p.E613.
- Siva, R. (2007) "Status of natural dyes and dye-yielding plants in India", *Current science*, pp.916-925.
- Slezak, T. and Kossiakoff, A.A. (2021) "Engineered ultra-high affinity synthetic antibodies for SARS-CoV-2 neutralization and detection", *Journal of Molecular Biology*, 433(10), 166956.
- Srivastava, A.K., Yadev, R., Rai, V.N., Ganguly, T. and Deb, S.K. (2012) "Surface plasmon resonance in gold nanoparticles", *AIP Conference Proceedings*, 1447(1), pp. 305-306, American Institute of Physics.
- Stachurska, X., Roszak, M., Jabłońska, J., Mizielińska, M. and Nawrotek, P. (2021) "Double-Layer Agar (DLA) Modifications for the First Step of the Phage-Antibiotic Synergy (PAS) Identification", *Antibiotics*, 10(11), p.1306.
- Stellwagen, E. (1993) "Affinity chromatography with immobilized dyes", *Molecular interactions in Bioseparations*, pp. 247-255, Springer, Boston, MA.
- Stellwagen, E. (1995) "Dye affinity chromatography", *Current Protocols in Protein Science*, (1), p.92.
- Straif-Bourgeois, S. and Ratard, R. (2005) "Infectious disease epidemiology", *Handbook of Epidemiology*, pp. 1327-1362, Springer, Berlin, Heidelberg.
- Sulakvelidze, A., Alavidze, Z. and Morris Jr, J.G. (2001) "Bacteriophage therapy", *Antimicrobial agents and chemotherapy*, 45(3), pp.649-659.

- Tappe, H., Helmling, W., Mischke, P., Rebsamen, K., Reiher, U., Russ, W., Schläfer, L. and Vermehren, P. (2000) "Reactive dyes", *Ullmann's Encyclopedia of Industrial Chemistry*.
- Teng, J., Yuan, F., Ye, Y., Zheng, L., Yao, L., Xue, F., Chen, W. and Li, B. (2016) "Aptamer-based technologies in foodborne pathogen detection", *Frontiers in Microbiology*, 7, p.1426.
- Thompson, S.T., Cass, K.H. and Stellwagen, E. (1975) "Blue dextran-sepharose: an affinity column for the dinucleotide fold in proteins", *Proceedings of the National Academy of Sciences*, 72(2), pp.669-672.
- Thorat, A.A. and Suryanarayanan, R. (2019) "Characterization of phosphate buffered saline (PBS) in frozen state and after freeze-drying", *Pharmaceutical research*, 36(7), pp.1-11.
- van Doremalen, N., Bushmaker, T., Morris, D.H., Holbrook, M.G., Gamble, A., Williamson, B.N., Tamin, A., Harcourt, J.L., Thornburg, N.J., Gerber, S.I. and Lloyd-Smith, J.O. (2020) "Aerosol and surface stability of SARS-CoV-2 as compared with SARS-CoV-1", *New England journal of medicine*, 382(16), pp.1564-1567.
- Velavan, T.P. and Meyer, C.G. (2020) "The COVID-19 epidemic", *Tropical medicine & international health*, 25(3), p.278.
- Ventura Pinto, A., Pinto, M.D.C.F., Lagrota, M.H., Wigg, M.D. and Aguiar, A.N.S. (1987) "Antiviral activity of naphthoquinones: I. Lapachol derivatives against enteroviruses", *Revista latinoamericana de microbiologia*, pp.15-20.
- Verma, M.S., Rogowski, J.L., Jones, L. and Gu, F.X. (2015) "Colorimetric biosensing of pathogens using gold nanoparticles", *Biotechnology advances*, 33(6), pp.666-680.
- Verma, S. and Gupta, G. (2017) "Natural dyes and its applications: A brief review", *International Journal of Research and Analytical Reviews*, 4(4), pp.57-60.
- Vijayan, V.K., Paramesh, H., Salvi, S.S. and Dalal, A.A.K. (2015) "Enhancing indoor air quality—The air filter advantage", *Lung India: Official Organ of Indian Chest Society*, 32(5), p.473.
- Villarreal, L.P. (2004) "Are viruses alive?", *Scientific American*, 291(6), pp.100-105.

- Walker, J.M. (1994) “Nondenaturing polyacrylamide gel electrophoresis of proteins”, *Basic protein and peptide protocols*, pp.17-22.
- Wang, C.C., Prather, K.A., Sznitman, J., Jimenez, J.L., Lakdawala, S.S., Tufekci, Z. and Marr, L.C. (2021) “Airborne transmission of respiratory viruses”, *Science*, 373(6558), p.eabd9149.
- Weaver, G.H. (1919) “Droplet infection and its prevention by the face mask”, *The Journal of Infectious Diseases*, pp.218-230.
- Wells, K. (2013) “Colour, health and wellbeing: The hidden qualities and properties of natural dyes”, *Journal of the International Colour Association*, 11, pp.28-36.
- WHO.int (2020) *The top 10 causes of death* Available at: <<https://www.who.int/news-room/fact-sheets/detail/the-top-10-causes-of-death>> (Accessed 18 March 2022).
- Wilson, J.E. (1976) “Applications of blue dextran and Cibacron Blue F3GA in purification and structural studies of nucleotide-requiring enzymes”, *Biochemical and Biophysical Research Communications*, 72(3), pp.816-823.
- World Health Organization (2000) *The world health report 2000: health systems: improving performance*, World Health Organization.
- World Health Organization (2014) “Antimicrobial resistance: global report on surveillance”, World Health Organization.
- Yamasaki, Y., Teramoto, Y. and Yoshikawa, K. (2001) “Disappearance of the Negative Charge in Giant DNA with a Folding Transition”, *Biophysical Journal*, 80(6), pp.2823-2832.
- Yan, Z. (2019) *Western blot quantification by ImageJ*. Available at: <<https://training.cvr.virginia.edu/Yan/Protocols/Western%20blot%20quantification%20by%20Image%20J.pdf>> (Accessed 7 September 2022).
- Yap, M.L., Klose, T., Arisaka, F., Speir, J.A., Veessler, D., Fokine, A. and Rossmann, M.G. (2016) “Role of bacteriophage T4 baseplate in regulating assembly and infection”, *Proceedings of the National Academy of Sciences*, 113(10), pp.2654-2659.

Yewdall, N.A., Mason, A.F. and Van Hest, J.C. (2018) “The hallmarks of living systems: towards creating artificial cells”, *Interface Focus*, 8(5), p.20180023.

Yoo, D., Provchy, J., Park, C., Schulz, C. and Walker, K. (2014) “Automated high-throughput protein purification using an ÄKTA purifier and a CETAC autosampler”, *Journal of chromatography A*, 1344, pp.23-30.

Zacharias, N., Haag, A., Brang-Lamprecht, R., Gebel, J., Essert, S.M., Kistemann, T., Exner, M., Mutters, N.T. and Engelhart, S. (2021) “Air filtration as a tool for the reduction of viral aerosols”, *Science of The Total Environment*, 772, p.144956.

Zeugin, J.A. and Hartley, J.L. (1985) “Ethanol precipitation of DNA”, *Focus*, 7(4), pp.1-2.

10. Appendix

10.1 Results of statistical analyses

10.1.1 Testing the affinity of bacterial proteins for the Reactive Blue 4 dye

Table 10.1. P-value results of Ryan-Joiner analyses, testing the normal distribution of the concentration of unbound protein, where protein has been incubated with clear Sephadex and RB4-dyed resin. Each data set consists of three replicates (for each incubation time and for the stock). Interpretation of results is indicated between brackets, where n = normally distributed data; nn = not normally distributed data; Seph = Sephadex; RB4-Seph = RB4-tagged slurry. Stock = protein concentration in the initial stock.

Time	Protein data normality	
	Seph	RB4-Seph
1 min	> 0.100 (n)	> 0.100 (n)
5 min	> 0.100 (n)	> 0.100 (n)
10 min	0.025 (nn)	> 0.100 (n)
30 min	> 0.100 (n)	> 0.100 (n)
60 min	> 0.100 (n)	> 0.100 (n)
Stock	0.058 (n)	

Table 10.2. Results of comparisons of unbound protein concentration in tubes where the protein mixture has been incubated with clear slurry and RB4-tagged Sephadex A-50. Names of performed post-hoc tests, P-values outcome and their significance are indicated. For One-Way ANOVA results: means that do not share a letter are significantly different from one another. s = significantly different; ns = not significantly different. Seph = Sephadex; RB4-Seph = RB4-tagged Sephadex; Stock = protein concentration in the initial stock.

Compared tubes	Test	Time	P-value	Post-hoc test	Observed difference with post-hoc test	Interpretation
Stock/Seph/RB4-Seph	One-Way ANOVA	1 min	0.000	Tukey	Stock (A); Seph (B); RB4 (C)	s
	One-Way ANOVA	5 min	0.000	Tukey	Stock (A); Seph (B); RB4 (C)	s
	Kruskal-Wallis	10 min	0.027	Mann-Whitney	0.081	ns (due to post-hoc test)
	One-Way ANOVA	30 min	0.000	Tukey	Stock (A); Seph (B); RB4 (B)	s
	One-Way ANOVA	60 min	0.000	Tukey	Stock (A); Seph (B); RB4 (B)	s

Table 10.3. Results of comparisons between incubation times of the concentration of unbound protein, in tubes where the protein mixture has been incubated with clear and RB4-tagged resin. Name of performed tests, P-values results, and their significance are indicated. s = significantly different; ns = not significantly different. Seph = Sephadex; RB4-Seph = RB4-tagged Sephadex.

		Comparison 1/5/10/30/60 min	
	Test	P-value	Observed difference with post-hoc test
Seph	Kruskall-Wallis	0.159 (ns)	-
RB4-Seph	One-Way ANOVA	0.000 (s)	60 (A); 10 (B); 30 (B); 5 (B); 1 (B)

10.1.2 *Testing the affinity of bacterial proteins for the Procion dyes by SDS-PAGE gel electrophoresis*

Table 10.4. P-value results of Ryan-Joiner analyses, testing the normal distribution of mean bacterial protein concentration of samples ready to run on SDS-PAGE gels. Each data set tested for normality consists of three replicates (three measurements of protein concentration in each sample). Collected = collected protein; w1 = protein concentration in the first wash; w2 = protein concentration in the second wash; w3 = protein concentration in the third wash; elution = protein concentration after elution; n = normally distributed data.

Slurry	Protein control	Sample				Elution
		Collected	W1	W2	W3	
Sephadex	> 0.100 (n)	> 0.100 (n)	> 0.100 (n)	> 0.100 (n)	> 0.100 (n)	> 0.100 (n)
RB4		> 0.100 (n)				
Red MX-5B		> 0.100 (n)				
Orange MX-G		> 0.100 (n)	> 0.100 (n)	> 0.100 (n)	> 0.100 (n)	0.084 (n)
Red H-3BN		0.055 (n)	> 0.100 (n)	> 0.100 (n)	> 0.100 (n)	> 0.100 (n)
Yellow MX-4R		> 0.100 (n)				

Table 10.5. One-Way ANOVA results of comparisons between protein concentration in samples ready to run on SDS-PAGE gels. Comparisons are performed between samples washed/eluted from various matrices. Corresponding P-values and their interpretations are indicated. Results of Tukey's post-hoc tests are shown, where means that do not share a letter are significantly different. S = significantly different means; ns = not significantly different means.

One-Way ANOVA results and interpretation									
	Seph/RB4/Red MX/ Orange/Red H/Yellow	Observed difference with post-hoc test							
Collected	0.000 (s)	Red MX (A); Orange (B); Yellow (B); Red H (B) RB4 (B); Seph (C)							
W1	0.000 (s)	Red H (A); Yellow (A); Orange (A); RB4 (A); Red MX (A); Seph (B)							
W2	0.432 (ns)	-							
W3	0.002 (s)	Red H (A); Red MX (A); Orange (A, B); RB4 (A, B); Yellow (A, B); Seph (B)							
Elution	0.001 (s)	Orange (A); RB4 (A, B); Seph (A, B, C); Red MX (B, C); Yellow (C); Red H (C)							

Table 10.6. One-Way ANOVA results of comparisons between protein concentration in samples ready to run on SDS-PAGE gels. Comparisons are performed between samples washed/eluted from the same matrix. Corresponding P-values and their interpretations are indicated. Results of Tukey’s post-hoc tests are shown, where means that do not share a letter are significantly different. Samples in the “Observed difference” column indicates the highest protein concentrations from left to right (left to right = highest to lowest protein concentration means). S = significantly different means; initial = protein concentration in the initial aliquot (before exposure to the matrices).

One-Way ANOVA results and interpretation		
Slurry	Comparison Initial/Col/W1/W2/W3/El	Observed difference with post-hoc test
Seph	0.000 (s)	Initial (A); El (B); Col (B); W1 (C); W2 (C, D); W3 (D)
RB4	0.000 (s)	Initial (A); El (B); Col (B); W1 (C); W2 (C, D); W3 (D)
Red MX	0.000 (s)	Initial (A); Col (B); El (C); W1 (D); W2 (D, E); W3 (E)
Orange	0.000 (s)	Initial (A); El (B); Col (B); W1 (C); W2 (C, D); W3 (D)
Red H	0.000 (s)	Initial (A); Col (B); El (C); W1 (C); W2 (D); W3 (D)
Yellow	0.000 (s)	Initial (A); Col (B); El (C); W1 (C); W2 (D); W3 (E)

Table 10.7. P-value results of Ryan-Joiner analyses, testing the normal distribution of mean band intensity data on SDS-PAGE gels (data generated using ImageJ). Each data set tested for normality consists of two replicates (measurements of band intensity performed on two replicate gels). Collected = intensity of bands produced by “collected protein” protein sample; w1 = intensity of bands produced by “wash 1” protein sample; w2 = intensity of bands produced by “wash 2” protein sample; w3 = intensity of bands produced by “wash 3” protein sample; elution = intensity of bands produced by “elution” protein sample; n = normally distributed data.

Slurry	Protein control	Sample				
		Collected	W1	W2	W3	Elution
Sephadex	> 0.100 (n)	> 0.100 (n)	> 0.100 (n)	> 0.100 (n)	> 0.100 (n)	> 0.100 (n)
RB4		> 0.100 (n)				
Red MX-5B		> 0.100 (n)				
Orange MX-G		> 0.100 (n)				
Red H-3BN		0.055 (n)	> 0.100 (n)	> 0.100 (n)	> 0.100 (n)	> 0.100 (n)
Yellow MX-4R		> 0.100 (n)				

Grouping Information Using the Tukey Method and 95% Confidence

Factor	N	Mean	Grouping
Coll. Yellow	2	0.544	A
Coll. seph	2	0.525	A
Coll. RB4	2	0.9676	A
Coll. Red MX	2	0.29271	A
Coll. Orange	2	0.2885	A
Coll. Red H	2	0.25120	A

Means that do not share a letter are significantly different.

Analysis of Variance

Source	DF	Adj SS	Adj MS	F-Value	P-Value
Factor	5	0.1640	0.03280	1.63	0.282
Error	6	0.1205	0.02008		
Total	11	0.2845			

Grouping Information Using the Tukey Method and 95% Confidence

Factor	N	Mean	Grouping
W1 Seph	2	0.467	A
W1 RB4	2	0.2982	A
W1 Red MX	2	0.19096	A
W1 Orange	2	0.1594	A
W1 Yellow	2	0.1550	A
W1 Red H	2	0.134808	A

Means that do not share a letter are significantly different.

Analysis of Variance

Source	DF	Adj SS	Adj MS	F-Value	P-Value
Factor	5	0.1640	0.03280	1.63	0.282
Error	6	0.1205	0.02008		
Total	11	0.2845			

Grouping Information Using the Tukey Method and 95% Confidence

Factor	N	Mean	Grouping
W2 Seph	2	0.506	A
W2 RB4	2	0.246	A
W2 Red MX	2	0.16526	A
W2 Yellow	2	0.1607	A
W2 Red H	2	0.12721	A
W2 Orange	2	0.1268	A

Means that do not share a letter are significantly different.

Analysis of Variance

Source	DF	Adj SS	Adj MS	F-Value	P-Value
Factor	5	0.21227	0.04245	2.95	0.110
Error	6	0.08644	0.01441		
Total	11	0.29871			

Grouping Information Using the Tukey Method and 95% Confidence

Factor	N	Mean	Grouping
W3 Seph	2	0.477	A
W3 RB4	2	0.275	A
W3 Red MX	2	0.17188	A
W3 Yellow	2	0.1637	A
W3 Orange	2	0.1488	A
W3 Red H	2	0.11177	A

Means that do not share a letter are significantly different.

Analysis of Variance

Source	DF	Adj SS	Adj MS	F-Value	P-Value
Factor	5	0.18235	0.03647	3.05	0.104
Error	6	0.07186	0.01198		
Total	11	0.25420			

Grouping Information Using the Tukey Method and 95% Confidence

Factor	N	Mean	Grouping
El. RB4	2	0.63551	A
El. Red MX	2	0.5644	A
El. Seph	2	0.56355	A
El. Orange	2	0.5908	A
El. Red H	2	0.4488	A
El. Yellow	2	0.4258	A

Means that do not share a letter are significantly different.

Analysis of Variance

Source	DF	Adj SS	Adj MS	F-Value	P-Value
Factor	5	0.06261	0.01252	4.19	0.055
Error	6	0.01795	0.002992		
Total	11	0.08056			

Figure 10.1. Minitab results output of the One-Way ANOVA tests, conducted using the Tukey method, for comparing the intensity of bands produced by Protein 1. Coll. = collected protein; W1 = wash 1; W2 = wash 2; W3 = wash 3; El. = eluted protein; Seph = clear Sephadex A-50; RB4 = resin tagged with Reactive Blue 4; Red H = resin tagged with Red H-3BN' Red MX- resin tagged with Red MX-5B; Yellow = resin tagged with Yellow MX-4R; Orange = resin tagged with Orange MX-G.

Grouping Information Using the Tukey Method and 95% Confidence

Factor	N	Mean	Grouping
Coll. seph	2	0.445	A
Coll. Yellow	2	0.384	A
Coll. RB4	2	0.331	A
Coll. Red MX	2	0.31478	A
Coll. Orange	2	0.2871	A
Coll. Red H	2	0.1614	A

Means that do not share a letter are significantly different.

Analysis of Variance

Source	DF	Adj SS	Adj MS	F-Value	P-Value
Factor	5	0.09238	0.01848	0.54	0.740
Error	6	0.20379	0.03397		
Total	11	0.29618			

Grouping Information Using the Tukey Method and 95% Confidence

Factor	N	Mean	Grouping
W1 Seph	2	0.483	A
W1 RB4	2	0.372	A
W1 Yellow	2	0.264	A
W1 Red MX	2	0.1669	A
W1 Orange	2	0.1517	A
W1 Red H	2	0.0774	A

Means that do not share a letter are significantly different.

Analysis of Variance

Source	DF	Adj SS	Adj MS	F-Value	P-Value
Factor	5	0.2313	0.04625	1.17	0.422
Error	6	0.2382	0.03969		
Total	11	0.4694			

Grouping Information Using the Tukey Method and 95% Confidence

Factor	N	Mean	Grouping
W2 Seph	2	0.548	A
W2 RB4	2	0.325	A
W2 Yellow	2	0.306	A
W2 Red MX	2	0.1378	A
W2 Orange	2	0.1257	A
W2 Red H	2	0.0975	A

Means that do not share a letter are significantly different.

Analysis of Variance

Source	DF	Adj SS	Adj MS	F-Value	P-Value
Factor	5	0.2975	0.05951	1.76	0.256
Error	6	0.2032	0.03386		
Total	11	0.5007			

Grouping Information Using the Tukey Method and 95% Confidence

Factor	N	Mean	Grouping
W3 Seph	2	0.5332	A
W3 Yellow	2	0.326	A
W3 RB4	2	0.318	A
W3 Orange	2	0.1912	A
W3 Red MX	2	0.1866	A
W3 Red H	2	0.1111	A

Means that do not share a letter are significantly different.

Analysis of Variance

Source	DF	Adj SS	Adj MS	F-Value	P-Value
Factor	5	0.2255	0.04510	1.72	0.264
Error	6	0.1575	0.02625		
Total	11	0.3830			

Grouping Information Using the Tukey Method and 95% Confidence

Factor	N	Mean	Grouping
El. Yellow	2	0.775	A
El. RB4	2	0.682860	A
El. Seph	2	0.6345	A
El. Red MX	2	0.5067	A
El. Red H	2	0.5053	A
El. Orange	2	0.4949	A

Means that do not share a letter are significantly different.

Analysis of Variance

Source	DF	Adj SS	Adj MS	F-Value	P-Value
Factor	5	0.1349	0.02697	0.60	0.707
Error	6	0.2718	0.04530		
Total	11	0.4067			

Figure 10.2. Minitab results output of the One-Way ANOVA tests, conducted using the Tukey method, for comparing the intensity of bands produced by Protein 2. Coll. = collected protein; W1 = wash 1; W2 = wash 2; W3 = wash 3; El. = eluted protein; Seph = clear Sephadex A-50; RB4 = resin tagged with Reactive Blue 4; Red H = resin tagged with Red H-3BN' Red MX- resin tagged with Red MX-5B; Yellow = resin tagged with Yellow MX-4R; Orange = resin tagged with Orange MX-G.

Grouping Information Using the Tukey Method and 95% Confidence

Factor	N	Mean	Grouping
Coll. Yellow	2	0.415	A
Coll. seph	2	0.407	A
Coll. RB4	2	0.27659	A
Coll. Red MX	2	0.2407	A
Coll. Orange	2	0.1550	A
Coll. Red H	2	0.1397	A

Means that do not share a letter are significantly different.

Analysis of Variance

Source	DF	Adj SS	Adj MS	F-Value	P-Value
Factor	5	0.1420	0.02840	1.00	0.491
Error	6	0.1710	0.02849		
Total	11	0.3130			

Grouping Information Using the Tukey Method and 95% Confidence

Factor	N	Mean	Grouping
W1 Seph	2	0.411	A
W1 Yellow	2	0.288	A
W1 RB4	2	0.1812	A
W1 Red MX	2	0.149890	A
W1 Red H	2	0.0996	A
W1 Orange	2	0.0668	A

Means that do not share a letter are significantly different.

Analysis of Variance

Source	DF	Adj SS	Adj MS	F-Value	P-Value
Factor	5	0.1656	0.03311	0.91	0.530
Error	6	0.2176	0.03627		
Total	11	0.3832			

Grouping Information Using the Tukey Method and 95% Confidence

Factor	N	Mean	Grouping
W2 Seph	2	0.446	A
W2 Yellow	2	0.302	A
W2 Red MX	2	0.141591	A
W2 RB4	2	0.1336	A
W2 Red H	2	0.09148	A
W2 Orange	2	0.0790	A

Means that do not share a letter are significantly different.

Analysis of Variance

Source	DF	Adj SS	Adj MS	F-Value	P-Value
Factor	5	0.2099	0.04198	1.71	0.266
Error	6	0.1474	0.02456		
Total	11	0.3573			

Grouping Information Using the Tukey Method and 95% Confidence

Factor	N	Mean	Grouping
W3 Seph	2	0.419	A
W3 Yellow	2	0.317	A
W3 RB4	2	0.2017	A
W3 Red MX	2	0.165555	A
W3 Red H	2	0.10241	A
W3 Orange	2	0.1012	A

Means that do not share a letter are significantly different.

Analysis of Variance

Source	DF	Adj SS	Adj MS	F-Value	P-Value
Factor	5	0.1602	0.03205	1.38	0.351
Error	6	0.1397	0.02328		
Total	11	0.2999			

Grouping Information Using the Tukey Method and 95% Confidence

Factor	N	Mean	Grouping
El. Yellow	2	0.797	A
El. RB4	2	0.7455	A
El. Red MX	2	0.5711	A
El. Seph	2	0.51249	A
El. Orange	2	0.4466	A
El. Red H	2	0.4098	A

Means that do not share a letter are significantly different.

Analysis of Variance

Source	DF	Adj SS	Adj MS	F-Value	P-Value
Factor	5	0.2519	0.05038	0.84	0.566
Error	6	0.3593	0.05989		
Total	11	0.6112			

Figure 10.3. Minitab results output of the One-Way ANOVA tests, conducted using the Tukey method, for comparing the intensity of bands produced by Protein 3. Coll. = collected protein; W1 = wash 1; W2 = wash 2; W3 = wash 3; El. = eluted protein; Seph = clear Sephadex A-50; RB4 = resin tagged with Reactive Blue 4; Red H = resin tagged with Red H-3BN' Red MX- resin tagged with Red MX-5B; Yellow = resin tagged with Yellow MX-4R; Orange = resin tagged with Orange MX-G.

Grouping Information Using the Tukey Method and 95% Confidence

Factor	N	Mean	Grouping
Coll. Yellow	2	0.774	A
Coll. seph	2	0.574	A
Coll. RB4	2	0.402	A
Coll. Red MX	2	0.2849	A
Coll. Red H	2	0.20468	A
Coll. Orange	2	0.17264	A

Means that do not share a letter are significantly different.

Analysis of Variance

Source	DF	Adj SS	Adj MS	F-Value	P-Value
Factor	5	0.5460	0.10919	1.22	0.403
Error	6	0.5383	0.08971		
Total	11	1.0842			

Grouping Information Using the Tukey Method and 95% Confidence

Factor	N	Mean	Grouping
W1 Yellow	2	0.555	A
W1 Seph	2	0.544	A
W1 RB4	2	0.3278	A
W1 Red MX	2	0.2388	A
W1 Red H	2	0.13523	A
W1 Orange	2	0.130141	A

Means that do not share a letter are significantly different.

Analysis of Variance

Source	DF	Adj SS	Adj MS	F-Value	P-Value
Factor	5	0.3647	0.07294	0.78	0.598
Error	6	0.5603	0.09338		
Total	11	0.9250			

Grouping Information Using the Tukey Method and 95% Confidence

Factor	N	Mean	Grouping
W2 Seph	2	0.624	A
W2 Yellow	2	0.540	A
W2 RB4	2	0.265	A
W2 Red MX	2	0.1881	A
W2 Orange	2	0.129369	A
W2 Red H	2	0.0808	A

Means that do not share a letter are significantly different.

Analysis of Variance

Source	DF	Adj SS	Adj MS	F-Value	P-Value
Factor	5	0.5065	0.10131	1.06	0.462
Error	6	0.5717	0.09528		
Total	11	1.0782			

Grouping Information Using the Tukey Method and 95% Confidence

Factor	N	Mean	Grouping
W3 Yellow	2	0.571	A
W3 Seph	2	0.556	A
W3 RB4	2	0.279	A
W3 Red MX	2	0.1523	A
W3 Red H	2	0.1082	A
W3 Orange	2	0.09070	A

Means that do not share a letter are significantly different.

Analysis of Variance

Source	DF	Adj SS	Adj MS	F-Value	P-Value
Factor	5	0.4837	0.09675	1.18	0.417
Error	6	0.4927	0.08211		
Total	11	0.9764			

Grouping Information Using the Tukey Method and 95% Confidence

Factor	N	Mean	Grouping
El. Yellow	2	1.087	A
El. Seph	2	0.6537	A
El. RB4	2	0.652	A
El. Red MX	2	0.4713	A
El. Orange	2	0.34215	A
El. Red H	2	0.2066	A

Means that do not share a letter are significantly different.

Analysis of Variance

Source	DF	Adj SS	Adj MS	F-Value	P-Value
Factor	5	0.9503	0.1901	0.91	0.531
Error	6	1.2520	0.2087		
Total	11	2.2023			

Figure 10.4. Minitab results output of the One-Way ANOVA tests, conducted using the Tukey method, for comparing the intensity of bands produced by Protein 4. Coll. = collected protein; W1 = wash 1; W2 = wash 2; W3 = wash 3; El. = eluted protein; Seph = clear Sephadex A-50; RB4 = resin tagged with Reactive Blue 4; Red H = resin tagged with Red H-3BN' Red MX- resin tagged with Red MX-5B; Yellow = resin tagged with Yellow MX-4R; Orange = resin tagged with Orange MX-G.

Grouping Information Using the Tukey Method and 95% Confidence

Factor	N	Mean	Grouping
Coll. seph	2	1.106	A
Coll. RB4	2	0.645	A
Coll. Red MX	2	0.4550	A
Coll. Yellow	2	0.3897	A
Coll. Orange	2	0.29675	A
Coll. Red H	2	0.2497	A

Means that do not share a letter are significantly different.

Analysis of Variance

Source	DF	Adj SS	Adj MS	F-Value	P-Value
Factor	5	1.0065	0.20130	2.14	0.191
Error	6	0.5652	0.09419		
Total	11	1.5717			

Grouping Information Using the Tukey Method and 95% Confidence

Factor	N	Mean	Grouping
W1 Seph	2	1.262	A
W1 RB4	2	0.5972	A
W1 Red MX	2	0.4524	A
W1 Yellow	2	0.3024	A
W1 Orange	2	0.257413	A
W1 Red H	2	0.2078	A

Means that do not share a letter are significantly different.

Analysis of Variance

Source	DF	Adj SS	Adj MS	F-Value	P-Value
Factor	5	1.5504	0.3101	2.40	0.158
Error	6	0.7748	0.1291		
Total	11	2.3252			

Grouping Information Using the Tukey Method and 95% Confidence

Factor	N	Mean	Grouping
W2 Seph	2	1.338	A
W2 RB4	2	0.5606	A
W2 Red MX	2	0.3992	A
W2 Yellow	2	0.312	A
W2 Orange	2	0.25033	A
W2 Red H	2	0.1629	A

Means that do not share a letter are significantly different.

Analysis of Variance

Source	DF	Adj SS	Adj MS	F-Value	P-Value
Factor	5	1.8536	0.3707	2.62	0.136
Error	6	0.8491	0.1415		
Total	11	2.7027			

Grouping Information Using the Tukey Method and 95% Confidence

Factor	N	Mean	Grouping
W3 Seph	2	1.270	A
W3 RB4	2	0.5603	A
W3 Red MX	2	0.3732	A
W3 Yellow	2	0.263	A
W3 Orange	2	0.2150	A
W3 Red H	2	0.13430	A

Means that do not share a letter are significantly different.

Analysis of Variance

Source	DF	Adj SS	Adj MS	F-Value	P-Value
Factor	5	1.7576	0.3515	3.50	0.079
Error	6	0.6020	0.1003		
Total	11	2.3596			

Grouping Information Using the Tukey Method and 95% Confidence

Factor	N	Mean	Grouping
El. Seph	2	1.266	A
El. RB4	2	0.7225	A B
El. Red MX	2	0.6144	A B
El. Yellow	2	0.413	A B
El. Orange	2	0.39382	A B
El. Red H	2	0.2805	B

Means that do not share a letter are significantly different.

Analysis of Variance

Source	DF	Adj SS	Adj MS	F-Value	P-Value
Factor	5	1.2726	0.25452	4.37	0.050
Error	6	0.3497	0.05828		
Total	11	1.6223			

Figure 10.5. Minitab results output of the One-Way ANOVA tests, conducted using the Tukey method, for comparing the intensity of bands produced by Protein 5. Coll. = collected protein; W1 = wash 1; W2 = wash 2; W3 = wash 3; El. = eluted protein; Seph = clear Sephadex A-50; RB4 = resin tagged with Reactive Blue 4; Red H = resin tagged with Red H-3BN' Red MX- resin tagged with Red MX-5B; Yellow = resin tagged with Yellow MX-4R; Orange = resin tagged with Orange MX-G.

Grouping Information Using the Tukey Method and 95% Confidence

Factor	N	Mean	Grouping
Protein ctrl Seph	2	1.000	A
El. Seph	2	0.9659	A B
W2 Seph	2	0.95058	A B
W1 Seph	2	0.9434	B C
W3 Seph	2	0.94178	B C
Coll. seph	2	0.93674	B C
PBS Seph	2	0.8950	C

Means that do not share a letter are significantly different.

Analysis of Variance

Source	DF	Adj SS	Adj MS	F-Value	P-Value
Factor	6	0.012047	0.002008	11.35	0.003
Error	7	0.001238	0.000177		
Total	13	0.013286			

Grouping Information Using the Tukey Method and 95% Confidence

Factor	N	Mean	Grouping
Ctrl RB4	2	1.000	A
El. RB4	2	0.9685	A
Coll. RB4	2	0.9201	A
W1 RB4	2	0.9175	A
W3 RB4	2	0.9160	A
W2 RB4	2	0.9122	A
PBS RB4	2	0.8855	A

Means that do not share a letter are significantly different.

Analysis of Variance

Source	DF	Adj SS	Adj MS	F-Value	P-Value
Factor	6	0.018235	0.003039	2.97	0.090
Error	7	0.007153	0.001022		
Total	13	0.025388			

Grouping Information Using the Tukey Method and 95% Confidence

Factor	N	Mean	Grouping
Ctrl Red H	2	1.000	A
El. Red H	2	0.8256	B
Coll. Red H	2	0.7805	B C
W3 Red H	2	0.7663	B C
W1 Red H	2	0.7645	B C
W2 Red H	2	0.7622	B C
PBS Red H	2	0.7377	C

Means that do not share a letter are significantly different.

Analysis of Variance

Source	DF	Adj SS	Adj MS	F-Value	P-Value
Factor	6	0.097093	0.016182	42.19	0.000
Error	7	0.002685	0.000384		
Total	13	0.099778			

Grouping Information Using the Tukey Method and 95% Confidence

Factor	N	Mean	Grouping
Ctrl Yellow	2	1.000	A
El. Yellow	2	0.9162	A
Coll. Yellow	2	0.8676	A
W3 Yellow	2	0.8575	A
W2 Yellow	2	0.854	A
W1 Yellow	2	0.851	A
PBS Yellow	2	0.842	A

Means that do not share a letter are significantly different.

Analysis of Variance

Source	DF	Adj SS	Adj MS	F-Value	P-Value
Factor	6	0.03843	0.006405	0.39	0.866
Error	7	0.11603	0.016576		
Total	13	0.15446			

Grouping Information Using the Tukey Method and 95% Confidence

Factor	N	Mean	Grouping
Ctrl Orange	2	1.000	A
El. Orange	2	0.84256	B
Coll. Orange	2	0.7801	B C
W1 Orange	2	0.7535	B C
W3 Orange	2	0.7505	B C
W2 Orange	2	0.7498	B C
PBS Orange	2	0.7164	C

Means that do not share a letter are significantly different.

Analysis of Variance

Source	DF	Adj SS	Adj MS	F-Value	P-Value
Factor	6	0.112620	0.018770	18.67	0.001
Error	7	0.007038	0.001005		
Total	13	0.119658			

Grouping Information Using the Tukey Method and 95% Confidence

Factor	N	Mean	Grouping
Ctrl Red MX	2	1.000	A
El. Red MX	2	0.843229	B
Coll. Red MX	2	0.77179	C
W1 Red MX	2	0.74746	C
W3 Red MX	2	0.7421	C
W2 Red MX	2	0.73767	C D
PBS Red MX	2	0.6946	D

Means that do not share a letter are significantly different.

Analysis of Variance

Source	DF	Adj SS	Adj MS	F-Value	P-Value
Factor	6	0.126376	0.021063	152.54	0.000
Error	7	0.000967	0.000138		
Total	13	0.127343			

Figure 10.6. Minitab results output of the One-Way ANOVA tests, conducted using the Tukey method, for comparing the intensity of whole protein lanes (comparisons of corresponding protein lanes are made within the same gels).

Grouping Information Using the Tukey Method and 95% Confidence

Factor	N	Mean	Grouping
Coll. seph	2	0.93674	A
Coll. RB4	2	0.9201	A
Coll. Yellow	2	0.8676	A
Coll. Red H	2	0.7805	A
Coll. Orange	2	0.7801	A
Coll. Red MX	2	0.77179	A

Means that do not share a letter are significantly different.

Analysis of Variance

Source	DF	Adj SS	Adj MS	F-Value	P-Value
Factor	5	0.05652	0.011303	3.71	0.071
Error	6	0.01829	0.003048		
Total	11	0.07480			

Grouping Information Using the Tukey Method and 95% Confidence

Factor	N	Mean	Grouping
W1 Seph	2	0.9434	A
W1 RB4	2	0.9175	A
W1 Yellow	2	0.851	A
W1 Red H	2	0.7645	A
W1 Orange	2	0.7535	A
W1 Red MX	2	0.74746	A

Means that do not share a letter are significantly different.

Analysis of Variance

Source	DF	Adj SS	Adj MS	F-Value	P-Value
Factor	5	0.07580	0.015160	3.89	0.064
Error	6	0.02336	0.003894		
Total	11	0.09916			

Grouping Information Using the Tukey Method and 95% Confidence

Factor	N	Mean	Grouping
W2 Seph	2	0.95058	A
W2 RB4	2	0.9122	A
W2 Yellow	2	0.854	A
W2 Red H	2	0.7622	A
W2 Orange	2	0.7498	A
W2 Red MX	2	0.73767	A

Means that do not share a letter are significantly different.

Analysis of Variance

Source	DF	Adj SS	Adj MS	F-Value	P-Value
Factor	5	0.08273	0.016546	4.14	0.057
Error	6	0.02400	0.003999		
Total	11	0.10673			

Grouping Information Using the Tukey Method and 95% Confidence

Factor	N	Mean	Grouping
W3 Seph	2	0.94178	A
W3 RB4	2	0.9160	A
W3 Yellow	2	0.8575	A
W3 Red H	2	0.7663	A
W3 Orange	2	0.7505	A
W3 Red MX	2	0.7421	A

Means that do not share a letter are significantly different.

Analysis of Variance

Source	DF	Adj SS	Adj MS	F-Value	P-Value
Factor	5	0.07747	0.015495	3.91	0.063
Error	6	0.02375	0.003958		
Total	11	0.10122			

Grouping Information Using the Tukey Method and 95% Confidence

Factor	N	Mean	Grouping
EI. RB4	2	0.9685	A
EI. Seph	2	0.9659	A
EI. Yellow	2	0.9162	A
EI. Red MX	2	0.843229	A
EI. Orange	2	0.84256	A
EI. Red H	2	0.8256	A

Means that do not share a letter are significantly different.

Analysis of Variance

Source	DF	Adj SS	Adj MS	F-Value	P-Value
Factor	5	0.04225	0.008450	2.54	0.144
Error	6	0.01995	0.003325		
Total	11	0.06220			

Figure 10.7. Minitab results output of the One-Way ANOVA tests, conducted using the Tukey method, for comparing the intensity of whole protein gel lanes (comparisons of corresponding protein lanes are made between various gels).

Table 10.8. One-Way ANOVA results of comparisons between the intensity of bands produced by Proteins 1 – 5 within the same gel. Corresponding P-values and their meaning are indicated, where s = significantly different; ns = not significantly different.

Proteins 1-5 differences within same gel						
Sample	Slurry					
	Seph	RB4	Red H	Yellow	Orange	Red MX
Coll.	0.730 (ns)	0.323 (ns)	0.031 (s)	0.204 (ns)	0.101 (ns)	0.078 (ns)
W1	0.955 (ns)	0.290 (ns)	0.023 (s)	0.585 (ns)	0.006 (s)	0.017 (s)
W2	0.931 (ns)	0.262 (ns)	0.076 (ns)	0.782 (ns)	0.006 (s)	0.006 (s)
W3	0.562 (ns)	0.378 (ns)	0.498 (ns)	0.917 (ns)	0.099 (ns)	0.028 (s)
El.	0.049 (s)	0.680 (ns)	0.092 (ns)	0.695 (ns)	0.127 (ns)	0.342 (ns)

Table 10.9. Significant P-values resulting from tests comparing the intensity of bands produced by Proteins 1 – 5 amongst all SDS-PAGE gels, performed after obtaining significant One-Way ANOVA associated P-values. The associated ANOVA P-value and the type of post-hoc tests are indicated. Conduction of a Fisher’s test was necessary due to insignificant P-values resulting from Tukey’s method for proteins eluted from clear Sephadex slurry. Numbers appearing in front of the sample type represent the protein indices. For example, 5 W2 = Protein 5 band intensity in the second PBS wash. Means listed first in the cells under “Different pairs of means” (left side) indicate the most significant bands’ intensities, whilst the last proteins listed (right side) show the faintest bands.

Significantly different means paired with post-hoc tests			
Slurry	ANOVA P-value	Post-hoc test	Different pairs of means
Seph	0.049	Fisher LSD	5 El. (A); 4 El. (A, B); 2 El. (A, B); 1 El. (B, C); 3 El. (C)
Red H	0.031	Tukey	1 Coll. (A); 5 Coll. (A, B); 4 Coll. (A, B); 2 Coll. (A, B); 3 Coll. (B)
Red H	0.023	Tukey	5 W1 (A); 4 W1 (A, B); 1 W1 (A, B); 3 W1 (B); 2 W1 (B)
Orange	0.006	Tukey	5 W1 (A); 1 W1 (B); 2 W1 (B); 4 W1 (B); 3 W1 (B)
Orange	0.006	Tukey	5 W2 (A); 4 W2 (B); 1 W2 (B); 2 W2 (B); 3 W2 (B)
Red MX	0.017	Tukey	5 W1 (A); 4 W1 (A, B); 1 W1 (B); 2 W1 (B); 3 W1 (B)
Red MX	0.006	Tukey	5 W2 (A); 4 W2 (B); 1 W2 (B); 3 W2 (B); 2 W2 (B)
Red MX	0.028	Tukey	5 W3 (A); 2 W3 (A, B); 3 W3 (A, B); 1 W3 (B); 4 W3 (B)

10.1.3 *Testing the binding of bacterial nucleic acids to the Reactive Blue 4 dye*

Table 10.10. P-value results of Ryan-Joiner analyses, testing the normal distribution of unbound DNA or RNA concentration, where nucleic acids have been incubated with clear Sephadex and RB4-dyed resin. Each data set consists of three replicates (for each incubation time and for each stock). Interpretation of results is indicated between brackets, where n = normally distributed data; nn = not normally distributed data; Seph = Sephadex; RB4-Seph = RB4-tagged slurry. Stock = nucleic acid concentration in the initial stock.

Time	Data normality			
	RNA		DNA	
	Seph	RB4-Seph	Seph	RB4-Seph
1 min	> 0.100 (n)	> 0.100 (n)	0.033 (nn)	> 0.100 (n)
5 min	> 0.100 (n)	> 0.100 (n)	> 0.100 (n)	> 0.100 (n)
10 min	> 0.100 (n)	> 0.100 (n)	> 0.100 (n)	> 0.100 (n)
30 min	> 0.100 (n)	> 0.100 (n)	> 0.100 (n)	> 0.100 (n)
60 min	0.017 (nn)	> 0.100 (n)	> 0.100 (n)	> 0.100 (n)
	RNA		DNA	
Stock	0.012 (nn)		> 0.100 (n)	

Table 10.11. Results of comparisons between concentration of DNA or RNA (in the supernatant), upon incubation with clear slurry and RB4-tagged Sephadex A-50. Names of performed post-hoc tests, P-values results, and their significance are indicated. For One-Way ANOVA results: means that do not share a letter are significantly different from one another. s = significantly different; ns = not significantly different. Seph = Sephadex; RB4-Seph = RB4-tagged Sephadex; Stock = nucleic acid concentration in the initial stock

Compared tubes	Test	Time	P-value	Post hoc test	Observed difference with post-hoc test	Interpretation
Stock DNA/Seph DNA/RB4-Seph DNA	Kruskall-Wallis	1 min	0.061	-	-	ns
	One-Way ANOVA	5 min	0.000	Tukey	DNA stock (A); DNA RB4 (B); DNA seph (C)	s
	One-Way ANOVA	10 min	0.000	Tukey	DNA stock (A); DNA RB4 (B); DNA seph (C)	s
	One-Way ANOVA	30 min	0.000	Tukey	DNA stock (A); DNA RB4 (B); DNA seph (B)	s
	One-Way ANOVA	60 min	0.000	Tukey	DNA stock (A); DNA RB4 (B); DNA seph (B)	s
	Kruskall-Wallis	1 min	0.066	-	-	ns
Stock RNA/Seph RNA/RB4-Seph RNA	Kruskall-Wallis	5 min	0.027	Mann-Whitney U	P = 0.081	ns (due to post-hoc test)
	Kruskall-Wallis	10 min	0.061	-	-	ns
	Kruskall-Wallis	30 min	0.027	Mann-Whitney U	P = 0.081	ns (due to post-hoc test)
	Kruskall-Wallis	60 min	0.051	-	-	ns
	Kruskall-Wallis	1 min	0.066	-	-	ns

Table 10.12. Results of comparisons between incubation times of the concentration of unbound DNA or RNA, in tubes containing clear and RB4-tagged resin. Name of performed tests, P-values results, and their significance are indicated. s = significantly different; ns = not significantly different. Seph = Sephadex; RB4-Seph = RB4-tagged Sephadex.

		Comparison 1/5/10/30/60 min	
		Test	P-value
DNA	Seph	Kruskall-Wallis	0.483 (ns)
	RB4-Seph	One-Way ANOVA	0.087 (ns)
RNA	Seph	Kruskall-Wallis	0.199 (ns)
	RB4-Seph	One-Way ANOVA	0.463 (ns)

10.1.4 *DNA binding to clear and dye-tagged DEAE-Sephadex A-50 in columns*

Table 10.13. Results of Ryan-Joiner analyses testing the normal distribution of DNA concentration data, in fraction samples washed and eluted from clear and dye-tagged DEAE Sephadex A-50. Corresponding P-values and significance are indicated. “Resin type” column specified the type of slurry DNA was eluted from. n = normally distributed data; Seph = Sephadex.

	Data normality	
	Resin type	P - value
Fractions 1-30	Clear Seph	> 0.100 (n)
	RB4	> 0.100 (n)
	Orange MX-G	> 0.100 (n)
	Yellow MX-4R	> 0.100 (n)
	Red MX-5B	> 0.100 (n)
Fractions 1-40	Red H-3BN	> 0.100 (n)

Table 10.14. Absolute values representing mean DNA concentration in fractions eluted from clear and Procion dye-tagged slurry, using traditional chromatography columns.

Fraction number	Procion dye names and associated DNA concentration					
	Red H-3BN	No dye (clear slurry/control)	Reactive Blue 4	Orange MX-G	Red MX-5B	Yellow MX-4R
1	1.144	0.000	0.000	0.000	0.000	0.000
2	1.517	0.000	0.000	0.000	0.000	0.000
3	0.862	0.364	0.000	0.000	0.011	0.000
4	0.830	0.364	0.000	0.356	0.000	0.000
5	1.016	1.756	1.553	0.780	0.072	0.095
6	1.352	2.532	1.404	1.419	0.257	1.210
7	0.769	2.481	2.959	1.695	0.684	1.169
8	2.355	3.333	2.284	1.545	0.566	2.954
9	2.553	3.638	2.572	1.449	0.595	3.595
10	3.238	4.142	3.878	1.736	1.195	2.150
11	4.048	4.313	3.448	2.229	2.192	3.218
12	4.230	3.788	3.559	2.705	3.128	3.555
13	6.059	3.423	8.630	3.131	3.083	1.911
14	2.328	3.892	4.450	3.549	2.892	2.962
15	3.815	2.907	2.637	3.223	2.793	2.281
16	3.012	2.474	4.748	2.528	1.637	6.420
17	2.396	2.534	4.275	2.219	1.122	3.194
18	1.935	2.412	2.051	2.355	1.079	2.055
19	1.551	2.242	4.000	2.125	1.047	0.952
20	1.928	2.093	3.719	2.099	1.143	0.853
21	1.707	1.651	3.166	1.400	0.714	1.490
22	1.421	1.943	1.421	4.027	2.154	4.778
23	1.819	2.716	2.788	10.894	6.564	8.704
24	3.063	9.065	3.358	4.488	9.129	10.988
25	4.694	21.767	23.918	28.276	20.131	34.512
26	7.751	45.779	33.861	32.989	83.410	46.580
27	11.960	53.573	57.062	35.679	66.771	75.975
28	17.084	44.146	21.143	11.452	18.819	32.349
29	17.226	12.209	2.940	4.609	4.047	8.191
30	17.976	4.073	1.667	1.611	0.436	2.956
31	26.737	-	-	-	-	-
32	23.673	-	-	-	-	-
33	15.019	-	-	-	-	-
34	17.306	-	-	-	-	-
35	7.899	-	-	-	-	-
36	5.726	-	-	-	-	-
37	5.640	-	-	-	-	-
38	4.376	-	-	-	-	-
39	3.298	-	-	-	-	-
40	1.852	-	-	-	-	-

Table 10.15. Results of One-Way ANOVA tests assessing the difference between the mean bacterial DNA concentration present in chromatography fractions, eluted off clear and Procion dye-tagged resin. The amount of bacterial DNA in each fraction is expressed as a percentage value from the initial DNA concentration in the aliquot run on the column. Each percentage value represents the mean of three spectrophotometer readings. Results of Tukey’s post-hoc tests are shown in the column on the right-hand side, where means that did not share a letter were significantly different from one another. s = significantly different.

Fraction	Slurry						ANOVA P-Value	Interpretation	Observed difference with post-hoc test
	Red H-3BN Sephadex	Clear Sephadex	Orange MX-G Sephadex	Red MX-5B Sephadex	Yellow MX-4R Sephadex	RB4 Sephadex			
1	0.360	0.000	0.000	0.000	0.000	0.000	0.000	s	RedH (A); RB4 (B); Yellow (B); RedMX (B); Orange (B); Seph (B)
2	0.477	0.000	0.000	0.000	0.000	0.000	0.000	s	RedH (A); RB4 (B); Yellow (B); RedMX (B); Orange (B); Seph (B)
3	0.271	0.141	0.000	0.005	0.000	0.000	0.000	s	RedH (A); RB4 (B); Yellow (B); RedMX (B); Orange (B); Seph (B)
4	0.830	0.141	0.114	0.000	0.000	0.000	0.000	s	RedH (A); Seph (A, B); Orange (B); RB4 (B); Yellow (B); RedMX (B)
5	0.320	0.682	0.251	0.030	0.038	0.444	0.000	s	Seph (A); RB4 (B); RedH (B); Orange (B); Yellow (C); RedMX (C)
6	0.425	0.984	0.456	0.106	0.484	0.401	0.000	s	Seph (A); Yellow (B); Orange (B); RedH (B); RB4 (B); RedMX (C)
7	0.242	0.964	0.545	0.282	0.468	0.846	0.000	s	Seph (A); RB4 (A, B); Orange (B, C); Yellow (C); RedMX (C); RedH (C)
8	0.741	1.294	0.496	0.233	1.183	0.653	0.001	s	Seph (A); Yellow (A, B); RedH (A, B, C); RB4 (B, C); Orange (C); RedMX (C)
9	0.803	1.413	0.466	0.245	1.439	0.735	0.000	s	Yellow (A); Seph (A); RedH (B); RB4 (B, C); Orange (C, D); RedMX (D)
10	1.019	1.609	0.558	0.493	0.861	1.109	0.000	s	Seph (A); RB4 (B); RedH (B, C); Yellow (C); Orange (D); RedMX (D)
11	1.274	1.675	0.716	0.904	1.288	0.986	0.000	s	Seph (A); Yellow (B); RedH (B); RB4 (C); RedMX (C, D); Orange (D)
12	1.331	1.471	0.869	1.289	1.423	1.017	0.000	s	Seph (A); Yellow (A); RedH (A); RedMX (A); RB4 (B); Orange (B)
13	1.906	1.329	1.006	1.271	0.765	2.467	0.000	s	RB4 (A); RedH (B); Seph (C); RedMX (C); Orange (D); Yellow (B)
14	0.732	1.512	1.141	1.192	1.186	1.272	0.000	s	Seph (A); RB4 (B); RedMX (B); Yellow (B); Orange (B); RedH (C)
15	1.200	1.129	1.036	1.151	0.913	0.754	0.001	s	RedH (A); RedMX (A, B); Seph (A, B); Orange (A, B); Yellow (B, C); RB4 (C)
16	0.948	0.961	0.813	0.675	2.570	1.357	0.000	s	Yellow (A); RB4 (B); Seph (C); RedH (C); Orange (C); RedMX (C)
17	0.754	0.984	0.713	0.462	1.279	1.222	0.000	s	Yellow (A); RB4 (A); Seph (B); RedH (C); Orange (C); RedMX (D)
18	0.609	0.937	0.757	0.445	0.823	0.586	0.018	s	Seph (A); Yellow (A, B); Orange (A, B); RedH (A, B); RB4 (A, B); RedMX (B)
19	0.488	0.871	0.683	0.432	0.381	1.143	0.000	s	RB4 (A); Seph (B); Orange (C); RedH (D); RedMX (D); Yellow (D)
20	0.607	0.813	0.675	0.471	0.341	1.063	0.000	s	RB4 (A); Seph (A, B); Orange (NC); RedH (D); RedMX (D); Yellow (C)
21	0.537	0.641	0.450	0.294	0.596	0.905	0.001	s	RB4 (A); Seph (A, B); Yellow (B, C); RedH (B, C); Orange (B, C); RedMX (C)
22	0.447	0.755	1.294	0.888	1.913	0.406	0.000	s	Yellow (A); Orange (B); RedMX (C); Seph (C); RedH (D); RB4 (D)
23	0.572	1.055	3.501	2.706	3.484	0.797	0.000	s	Orange (A); Yellow (A); RedMX (B); Seph (C); RB4 (C); RedH (C)
24	0.964	3.521	1.443	3.762	4.399	0.960	0.000	s	Yellow (A); RedMX (A, B); Seph (B); Orange (C); RedH (C); RB4 (C)
25	1.477	8.454	9.088	8.297	13.816	6.836	0.000	s	Yellow (A); Orange (B); Seph (B); RedMX (C); RB4 (D); RedH (D)
26	2.439	17.780	10.603	34.378	18.647	9.678	0.000	s	RedMX (A); Yellow (B); Seph (B); Orange (C); RB4 (C); RedH (D)
27	3.763	20.807	11.468	27.520	30.415	16.310	0.000	s	Yellow (A); RedMX (B); Seph (C); RB4 (D); Orange (E); RedH (F)
28	5.376	17.145	3.681	7.756	12.950	6.043	0.000	s	Seph (A); Yellow (B); RedMX (C); RB4 (D); RedH (D); Orange (E)
29	5.420	4.742	1.482	1.668	3.279	0.840	0.000	s	RedH (A); Seph (B); Yellow (C); RedMX (D); Orange (D); RB4 (E)
30	5.656	1.582	0.518	0.180	1.184	0.476	0.000	s	RedH (A); Seph (B); Yellow (C); Orange (D); RB4 (D, E); RedMX (E)

31	8.413	-	-	-	-	-	-	-	-	-
32	7.449	-	-	-	-	-	-	-	-	-
33	4.726	-	-	-	-	-	-	-	-	-
34	5.446	-	-	-	-	-	-	-	-	-
35	2.486	-	-	-	-	-	-	-	-	-
36	1.802	-	-	-	-	-	-	-	-	-
37	1.775	-	-	-	-	-	-	-	-	-
38	1.377	-	-	-	-	-	-	-	-	-
39	1.038	-	-	-	-	-	-	-	-	-
40	0.583	-	-	-	-	-	-	-	-	-
Total percentage recovered	77.084	95.390	54.824	97.134	106.125	59.306	-	-	-	-

10.1.5 *Testing the effect of sodium chloride on phage survival*

Table 10.16. P-value results of Ryan-Joiner analyses, testing the normal distribution of mean PFU/mL in tubes where phage was exposed to 0.1, 0.2, 0.3, 0.4 and 1 M NaCl solutions and in the control phage solution. n = normally distributed data.

NaCl concentration	P-value of the distribution of PFU/mL
Control (no salt)	> 0.100 (n)
0.1 M	> 0.100 (n)
0.2 M	> 0.100 (n)
0.3 M	> 0.100 (n)
0.4 M	> 0.100 (n)
1 M	> 0.100 (n)

Table 10.17. Result of One-Way ANOVA testing the difference between the mean phage concentration in the control phage tube and in tubes where the T4 solution was exposed to 0.1, 0.2, 0.3, 0.4 and 1 M NaCl solutions. Corresponding P-value and its significance are indicated. ns = not significantly different means.

One-Way ANOVA results and interpretation	
Control/ 0.1 M/ 0.2 M/ 0.3 M/ 0.4 M/ 1 M NaCl	0.262 (ns)

10.1.6 *Testing the binding of phage to polysaccharide matrices*

Table 10.18. P-value results of Ryan-Joiner analyses, testing the normal distribution of PFU/mL in the tube containing T4 bacteriophage, and in the supernatant of tubes where phage was incubated with clear and RB4-tagged resin. Each data set consists of two replicates (for each incubation time and for each tube). Interpretation of results is indicated between brackets, where n = normally distributed data; Phage = phage concentration in the T4 stock, un-exposed to slurry; Phage + slurry = phage concentration in tubes containing clear slurry; Phage + RB4-slurry = phage concentration in tubes containing RB4-tagged slurry.

Time	Data normality		
	Phage	Phage + slurry	Phage + RB4-slurry
1 min	> 0.100 (n)	> 0.100 (n)	> 0.100 (n)
30 min	> 0.100 (n)	> 0.100 (n)	> 0.100 (n)
60 min	> 0.100 (n)	> 0.100 (n)	> 0.100 (n)

Table 10.19. Results of One-Way ANOVA testing the difference between the mean phage concentration in the control tube and in tubes where the T4 solution was exposed to un-dyed and RB4-dyed slurry. Corresponding P-values and their significance are indicated. Results of Tukey’s post-hoc test is shown, where means that do not share a letter are significantly different. Phage = phage concentration in the T4 stock, un-exposed to slurry; Phage + slurry = phage concentration in tubes containing clear slurry; Phage + RB4-slurry = phage concentration in tubes containing RB4-tagged slurry; ns = not significantly different means; s = significantly different means.

Time	One-Way ANOVA results and interpretation	Observed difference with post-hoc test
	Phage/ Phage + slurry/ Phage + RB4-slurry	
1 min	0.051 (ns)	-
30 min	0.057 (ns)	-
60 min	0.028 (s)	Phage (A); Phage + slurry (B); Phage + RB4-slurry (B)

Table 10.20. One-way ANOVA results of comparisons between incubation times of tubes containing control T4 stock and in tubes where the T4 solution was exposed to un-dyed and RB4-dyed slurry. Name of performed tests, P-value results and their significance are indicated. Phage = phage concentration in the T4 stock, un-exposed to slurry; Phage + slurry = phage concentration in tubes containing clear slurry; Phage + RB4-slurry = phage concentration in tubes containing RB4-tagged slurry; ns = not significantly different means.

	1/ 30/ 60 minutes
Phage	0.424 (ns)
Phage + slurry	0.408 (ns)
Phage + RB4-slurry	0.580 (ns)

10.1.7 Testing the binding of phage to natural fabrics

Table 10.21. P-values resulting from Ryan-Joiner tests for normality and their significance. Tested data represents the phage titre in tubes exposed to dyed and un-dyed fabrics. Stock control = phage concentration in the initial stock; Control = undyed fabric; Red H = Red H-3BN; Red MX = Red MX-5B; Yellow = Yellow MX-4R; Orange = Orange MX-G; RB4 = Blue MX-R; n = normally distributed data.

		Cotton					
Time	Stock control	Control	Red MX	Yellow	Orange	Red H	RB4
1 min	> 0.100 (n)	> 0.100 (n)	> 0.100 (n)	> 0.100 (n)	> 0.100 (n)	> 0.100 (n)	> 0.100 (n)
30 min	> 0.100 (n)	> 0.100 (n)	> 0.100 (n)	> 0.100 (n)	> 0.100 (n)	> 0.100 (n)	> 0.100 (n)
60 min	> 0.100 (n)	> 0.100 (n)	> 0.100 (n)	> 0.100 (n)	> 0.100 (n)	> 0.100 (n)	> 0.100 (n)
		Silk					
Time	Stock control	Control	Red MX	Yellow	Orange	Red H	RB4
1 min	> 0.100 (n)	> 0.100 (n)	> 0.100 (n)	> 0.100 (n)	> 0.100 (n)	> 0.100 (n)	> 0.100 (n)
30 min	> 0.100 (n)	> 0.100 (n)	> 0.100 (n)	> 0.100 (n)	> 0.100 (n)	> 0.100 (n)	> 0.100 (n)
60 min	> 0.100 (n)	> 0.100 (n)	> 0.100 (n)	> 0.100 (n)	> 0.100 (n)	> 0.100 (n)	> 0.100 (n)

Table 10.22. P-values of One-Way ANOVA and their significance. The tests compared phage titres in phage solution exposed to dyed and un-dyed cotton and silk. Stock = phage concentration in the initial stock; s = significant P-value.

	Cotton	Silk
Time	Stock/Control/Red MX/Yellow/Red H/Orange/RB4	Stock/Control/Red MX/Yellow/Red H/Orange/RB4
1 min	0.000 (s)	0.000 (s)
30 min	0.001 (s)	0.034 (s)
60 min	0.000 (s)	0.001 (s)

Table 10.23. Significant P-values resulting from tests performed after obtaining significant One-Way ANOVA associated P-values. The incubation time and type of post-hoc tests are indicated. Conduction of a Fisher’s test was necessary due to insignificant P-values resulting from Tukey’s method for silk, after 30 minutes of incubation. C = cotton; S = silk; Control = un-dyed fabric.

1 min			
Tukey Simultaneous Tests for Differences of Means			
Cotton		Silk	
Difference of Levels	Adjusted P Value	Difference of Levels	Adjusted P Value
C Control - Stock	0.001	S Control - Stock	0
C Red MX - Stock	0.015	S Red MX - Stock	0
C Red H - C Control	0.035	S Yellow - S Control	0.023
C Orange - C Control	0.02	S Red H - S Control	0.008
C RB4 - C Control	0.001	S Orange - S Control	0.007
C RB4 - C Red MX	0.008	S RB4 - S Control	0.023
		S Yellow - S Red MX	0.039
		S Red H - S Red MX	0.014
		S Orange - S Red MX	0.012
		S RB4 - S Red MX	0.039
30 min			
Tukey Simultaneous Tests for Differences of Means		Fisher Individual Tests for Differences of Means	
Cotton		Silk	
Difference of Levels	Adjusted P Value	Difference of Levels	Adjusted P Value
C Yellow - Stock	0.01	S Red MX - Stock	0.007
C RB4 - C Control	0.037	S Yellow - Stock	0.01
C RB4 - C Red MX	0.006	S Orange - S Red MX	0.014
C Orange - C Yellow	0.022	S RB4 - S Red MX	0.018
C RB4 - C Yellow	0.001	S Orange - S Yellow	0.02
		S RB4 - S Yellow	0.025
60 min			
Tukey Simultaneous Tests for Differences of Means			
Cotton		Silk	
Difference of Levels	Adjusted P Value	Difference of Levels	Adjusted P Value
C Red MX - Stock	0	S Control - Stock	0.032
C Yellow - Stock	0	S Red MX - Stock	0.002
C Red MX - C Control	0	S RB4 - S Control	0.032
C Yellow - C Control	0	S Red H - S Red MX	0.04
C Red H - C Red MX	0	S Orange - S Red MX	0.032
C Orange - C Red MX	0	S RB4 - S Red MX	0.002
C RB4 - C Red MX	0		
C Red H - C Yellow	0		
C Orange - C Yellow	0		
C RB4 - C Yellow	0		

Table 10.24. P-values of One-Way ANOVA tests and their significance. The tests represent a comparison between various incubation times of phage solution with dyed and undyed cotton and silk. Stock = phage concentration in the initial stock; s = significantly different means: ns = not significantly different means.

	Cotton					
Time	Control	Red MX	Yellow	Orange	Red H	RB4
1/30/60 min	0.018 (s)	0.000 (s)	0.000 (s)	0.540 (ns)	0.230 (ns)	0.581 (ns)
	Silk					
Time	Control	Red MX	Yellow	Orange	Red H	RB4
1/30/60 min	0.000 (s)	0.328 (ns)	0.225 (ns)	0.181 (ns)	0.357 (ns)	0.336 (ns)

Table 10.25. Significant P-values resulting from Tukey's post-hoc test, performed after obtaining significant One-Way ANOVA associated P-values. 1 = 1 minute; 30 = 30 minutes; 60 = 60 minutes; 1/30/60 min = comparison between 1, 30 and 60 minutes.

1/30/60 min	
Cotton	
Tukey Simultaneous Tests for Differences of Means	
Cotton contr 1- Cotton contr 30	0.034
Cotton contr 1 - Cotton contr 60	0.024
Red MX 60 - Red MX 1	0
Red MX 60 - Red MX 30	0
Yellow 60 - Yellow 1	0
Yellow 60 - Yellow 30	0
Silk	
Silk control 30- Silk control 1	0
Silk control 60- Silk control 1	0.005
Silk control 60- Silk control 30	0.043

10.1.8 *Testing the binding of phage to pre-wetted silk and cotton and dry dark-RB4 silk*

Table 10.26. P-value results of Ryan-Joiner analyses, testing the normal distribution of mean PFU/mL in the stock control tube and in tubes where phage was exposed to wet un-dyed cotton, wet un-dyed silk and deeply dyed (dark) RB4 silk. C = cotton; S = silk; n = normally distributed data.

Data normality				
Time	Stock control	C wet	S wet	S dark RB4
1 min	> 0.100 (n)	> 0.100 (n)	> 0.100 (n)	> 0.100 (n)
30 min	> 0.100 (n)	> 0.100 (n)	> 0.100 (n)	> 0.100 (n)
60 min	> 0.100 (n)	> 0.100 (n)	> 0.100 (n)	> 0.100 (n)

Table 10.27. Results of One-Way ANOVA testing the difference between the phage concentration in tubes containing phage solution exposed to LB pre-wetted cotton, silk and dry dark (deeply dyed) RB4 silk. Corresponding P-values and their significance are indicated. Results of Tukey’s post-hoc tests are shown, where means that do not share a letter are significantly different. s = significantly different means; c = cotton; s = silk.

Time	One-Way ANOVA				P-value	Observed difference with post-hoc test
	Stock control	C wet	S wet	S dark RB4		
1 min	Stock control	C wet	S wet	S dark RB4	0.000 (s)	Stock ctrl (A); S wet (B); C wet (B); S dark RB4 (C)
30 min	Stock control	C wet	S wet	S dark RB4	0.037 (s)	Stock ctrl (A); S dark RB4 (A,B); S wet (A,B); C wet (B)
60 min	Stock control	C wet	S wet	S dark RB4	0.000 (s)	Stock ctrl (A); C wet (B); S dark RB4 (B); S wet (C)

Table 10.28. One-way ANOVA results of comparisons between incubation times of phage with pre-wetted cotton, pre-wetted silk and dark RB4-tagged silk. P-values, their interpretation and outcome of Tukey’s post-hoc analyses are indicated. s = significantly different means; ns = not significantly different means; C = cotton; S = silk; numbers in the “Observed difference” column indicate the incubation time.

Fabrics	One-Way ANOVA		Observed difference with post-hoc test
	Comparison 1/30/60 minutes		
C wet	0.174 (ns)		-
S wet	0.013 (s)		30 (A); 1 (A); 60 (B)
S dark RB4	0.000 (s)		30 (A); 60 (B); 1 (C)